AN ABSTRACT OF THE THESIS OF

Jeffrey L. Thielman for the degree of Master of Science in Mechanical Engineering presented on December 10, 2003.

Title: Evaluation and Optimization of Large-Scale Engineering System Modularity Using an Axiomatic Design Approach

Abstract approved:          Redacted for privacy

Ping  Ge

Large-scale engineering systems provide important functions and at the same time address serious concerns to human society. Because of the complexity and resources involved, the development of these systems is currently a challenging undertaking. In this work, an axiomatic design approach, based on Suh's axiomatic design theory, and combined with aspects of design of experiments, response surface modeling, and optimization techniques, is developed for the evaluation and improvement of large-scale engineering systems. Modularity is a key factor in producing simpler structures, more robust performance, and consuming fewer resources, and therefore, used as a consistent criteria to evaluate and improve an existing design. The mathematical representation of functional independence in Suh's axiomatic design theory is adopted to measure modularity at both conceptual and parametric levels. At a conceptual level, the approach organizes and decomposes multiple, competing functional requirements of a large-scale engineering system, and relates them to their associated physical embodiments based on axiom 1. The design matrix, Reangularity,

and Semiangularity, are used at a parametric level to evaluate the modularity of the system design. If the evaluation shows any areas for improvement, an optimization procedure is adopted to achieve a safer and more robust design by increasing the modularity. The Reactor Cavity Cooling System in General Atomics' Gas Turbine – Modular Helium Reactor is used to demonstrate the use of the axiomatic design approach in an industrial application. The results show that the axiomatic design approach provides a viable approach to systematically evaluate a large-scale engineering system against multiple, competing design objectives and help improve the quality of the current design.

Evaluation and Optimization of Large-Scale Engineering System Modularity Using an
Axiomatic Design Approach


by

Jeffrey L. Thielman




A THESIS

submitted to

Oregon State University




in partial fulfillment of

the requirements for the

degree of


Master of Science




Presented: December 10, 2003

Commencement: June, 2004

Master of Science thesis of <u>Jeffrey L. Thielman</u> presented on <u>December 10, 2003.</u>

APPROVED:  Redacted for privacy

_____          /        ✔          _____

Major Professor, representing Mechanical Engineering

Redacted for privacy

_____

Head of the Department of Mechanical Engineering

# Redacted for privacy

_____          //~~          _____

Dean of the Graduate School

I understand that my thesis will become part of the permanent collection of Oregon State University libraries. My signature below authorizes release of my thesis to any reader upon request.  Redacted for privacy

Jeffrey L. Thielman, Author

## ACKNOWLEDGEMENTS

TABLE OF CONTENTS

TABLE OF CONTENTS (Continued)

# LIST OF FIGURES

# LIST OF TABLES

# LIST OF APPENDIX FIGURES

# NOMENCLATURE

A – Area

$A_{out}$ – Outlet flow area

$C_p$ – specific heat

D – diameter

DM – Design Matrix

DP – Design Parameter

$\Delta p_o$ – Outlet pressure drop

$D_r$ – Riser depth

$\varepsilon$ – emmisivity

e – roughness

$f$ – friction factor

FR – Functional Requirement

$g_x$ – gravity in the x direction

h – heat transfer coefficient

$H_r$ – Riser height

k – form loss factor

$L_{in}$ – Inlet length

$L_{out}$ – Outlet length of cooling system

$\dot{m}$ – mass flow rate

MWe – Megawatts electrical

MWth – Megawatts thermal

$n_r$ – Number of risers

Nu – Nusselt number

P – Perimeter

Pr – Prandtl Number

$\dot{q}$ – heat transfer rate

$\rho$ – density

R – Reangularity

$Re_D$ – Reynolds number (Diameter)

S – Semiangularity

t – time

T – temperature

$T_{air,exit}$ – Maximum air temperature at riser exit

$T_{rx,max}$ – Maximum reactor vessel temperature

$T_{wall,max}$ – Max riser wall termperature (at top of riser)

u – velocity

$v_{air}$ – Air velocity at riser exit

$W_r$ – Riser width

$Z_{in}$ – Inlet delta z

$z_{in}$-$z_{out}$ – delta Z between inlet and outlet

# 1. INTRODUCTION

Large-scale engineering systems are characterized by a great number of functions and parts, which frequently result in large size. They play a very important role in facilitating, enhancing, or extending our life on the earth. For instance, cars and ships are an inseparable part of many people's daily life. Compared to Columbus' strenuous adventure, it only takes a Boeing-747 a day or so to take several hundred passengers from one side of the earth to the other. Nuclear power plants provide a tremendous amount of energy to support about one-sixth of the world's population. Rockets and space stations have made our dream of the life beyond the earth a partial reality. As many of these large-scale engineering systems have become routine functions upon which the modern human society depends, society is concerned with their safe use and environmental impact. As competition increases between the companies in a global market place, more and more attention is paid to enhancing robustness and long-term reliability while reducing cost and improving profit margin. This work includes the development and application of a systematic design methodology for delivering desirable large-scale engineering systems where these issues are considered.

## 1.1 THE PROBLEM AND TECHNICAL CHALLENGES

The development of a large-scale engineering system usually involves multiple, competing design objectives and constraints, and collaboration of multi-disciplinary working groups. Ideally, a design methodology would exist, which allows product designers to a) evaluate their design alternatives on a common basis with different stakeholders and across different design stages, b) generate high-quality product design

that best meets the multiple, competing design requirements, and c) use minimum resources and time.

Today, most design groups use local, segmented, highly heuristic approaches when developing large-scale engineering systems. When applied to the evaluation of competing design alternatives, the existing approaches cannot provide a shared evaluation basis among the working groups. A consistent design framework is also lacking across design stages. Qualitative methods, such as Quality Function Deployment (QFD) [1], work effectively for generating functional requirements and concepts at an abstract level. It is hard to use QFD to select and specify design alternatives at more detailed level in configuration and parametric stage. On the other hand, Taguchi's robust design principles have been widely used to produce high-quality design alternatives at a parametric level [2,3]. However, it is not clear how to apply Taguchi's principles to generate good concepts from qualitative functionality descriptions. Due to the inconsistent criteria adopted, estimations regarding product quality generated at conceptual stage may not be properly implemented at detailed or embodiment stage. Consequently, numerous iterations are often needed to search for a proper result, and this entails a large increase of cost. We argue that a consistent, robust, and efficient, design methodology is needed in order to deliver high-quality large-scale engineering systems.

## 1.2 RESEARCH GOAL AND OBJECTIVE

Modularity has been gradually accepted as a key concept in designing high-quality large-scale engineering systems due to its role in enhancing structural simplicity, ensuring robust performance, and reducing development cost. This work intends to use modularity as a main design objective in the design process through consistent,

quantifiable, measures. Suh's Axiomatic Design Theory [4] is adopted, and an axiomatic design approach for evaluating and optimizing the modularity of large-scale engineering systems is developed. The General Atomics nuclear gas turbine-modular helium reactor (GT-MHR) is used to demonstrate the use of the axiomatic design approach in industrial practice.

## 1.3 LARGE SCALE SYSTEM EVALUATION AND IMPROVEMENT USING AXIOMATIC DESIGN

The following method has been developed to evaluate and improve large scale system design. Based on Suh's Axiom 1, the functional requirements (FRs) and design parameters (DPs) of a large-scale engineering system are decomposed from a high, qualitative level to the lowest, quantitative level, where specific performance requirements and design variables can be used to represent the FRs and DPs. A design matrix that represents a mapping relationship between the FRs and DPs at each level of the decomposition is generated. A system model is built to capture the underlying relationships between the performance and design variables, and is then used to populate the design matrix between the performance and design variables. Reangularity (R) and Semangularity (S) can be calculated and used to evaluate the functional independence of the current design. Finally, an optimization design model is built and used to obtain an improved design with a higher degree of functional independence. The application results show that, compared to the current design, the optimized system may lead to a more robust and cost-effective core cooling functional unit for the nuclear reactor system.

## 1.4 OUTLINE DESCRIPTION

A review of literature, both used in this work and similar to this work, is included as Chapter 2. Chapter 3 contains a detailed description of the method proposed in this

work. Chapter 4 contains a case study based on a nuclear reactor cooling system using the proposed method. Finally, Chapter 5 contains conclusions and recommendations based on the case study.

# 2. LITERATURE REVIEW

## 2.1 GENERATION IV NUCLEAR REACTORS

Currently about 17% of the world's electrical power is created by nuclear power reactors. Most of the commercial power reactors in the world are pressurized water reactors (PWR) or boiling water reactors (BWR), and are classified as Generation II reactors. Currently several companies are developing a third generation of power reactors that are still based on using water to transfer energy from the reactor core to the electrical power generators. A group of government agencies, universities, and corporations from the United States and around the world have created the Generation IV International Forum (GIF) to guide the development of a new class reactors that use means other than water to transfer energy from the reactor core to the electrical power generators [6], with enhanced safety, sustainability, and proliferation resistance.

### 2.1.1 Generation IV Development Goals

To guide the various design groups working on Generation IV (Gen-IV) reactors, the Roadmap Committee of the GIF has developed a set of eight technology goals that are categorized by sustainability, safety & reliability, and economics [7].

The three sustainability goals are focused on resources (SU-1), waste (SU-2), and non-proliferation (SU-3):

- SU-1: Generation IV nuclear energy systems including fuel cycles will provide sustainable energy generation that meets clean air objectives and promotes long-term availability of systems and effective fuel utilization for worldwide energy production.

- SU-2: Generation IV systems will minimize and manage their nuclear waste and notably reduce the long term stewardship burden in the future, thereby improving protection for public health and the environment.

- SU-3: Generation IV nuclear energy systems including fuel cycles will increase the assurance that they are a very unattractive and least desirable route for diversion or theft of weapons-usable materials.

The three safety & reliability goals are focused on excellence (SR-1), minimizing possible core damage (SR-2), and emergency response (SR-3):

- SR-1: Generation IV nuclear energy systems operations will excel in safety and reliability.

- SR-2: Generation IV nuclear energy systems will have a very low likelihood and degree of reactor core damage.

- SR-3: Generation IV nuclear energy systems will eliminate the need for offsite emergency response.

The two economics goals are focused on life cycle cost (E-1) and risk to capital investment (E-2):

- EC-1: Generation IV nuclear energy systems will have a clear life-cycle cost advantage over other energy sources.

- EC-2: Generation IV nuclear energy systems will have a level of financial risk comparable to other energy projects.

## 2.1.2 Generation IV Concepts

Many different design concepts were proposed for potential Gen-IV reactors, including water, gas, and liquid metal cooled reactors. Currently, none of the water cooled reactors are under further consideration. The concepts were proposed by various universities and corporations, and are at various levels of development.

Twenty-one different gas cooled reactors were proposed and grouped into four distinct categories[8].

- Pebble bed reactor (PBR) systems

- Prismatic fuel modular reactor (PMR) systems

- Very High Temperature Reactor (VHTR) systems

- Gas-cooled Fast Reactor (GFR) systems

Thirty-three different liquid metal cooled reactors were proposed, of which twenty-seven were categorized in five groups [9].

- Medium-to-large sodium-cooled, mixed-oxide fueled reactors

- Medium-to-large sodium-cooled, metal-fueled (U-TRU-Zr metal) reactors

- Medium-sized Pb or Pb-Bi cooled; MOX or Th-U-TRU-Zr metal alloy fueled reactors

- Small, Pb or Pb-Bi cooled; metal or nitride fueled reactors

- Sodium-cooled concepts that eliminate the traditional secondary sodium loops by development of novel new steam generators.

## 2.1.3 General Atomics' GT-MHR Reactor

One of the most developed Generation IV concepts is the Gas Turbine-Modular Helium Reactor (GT-MHR) from General Atomics [10,11]. It is a PMR reactor which uses helium as the primary coolant, and has been under development for several decades with various names and configurations. The current GT-MHR module (Figure 1) is a 286MWe / 600MWth power system which couples a gas cooled reactor in one vessel with a high efficiency Brayton cycle gas turbine in an adjacent vessel.
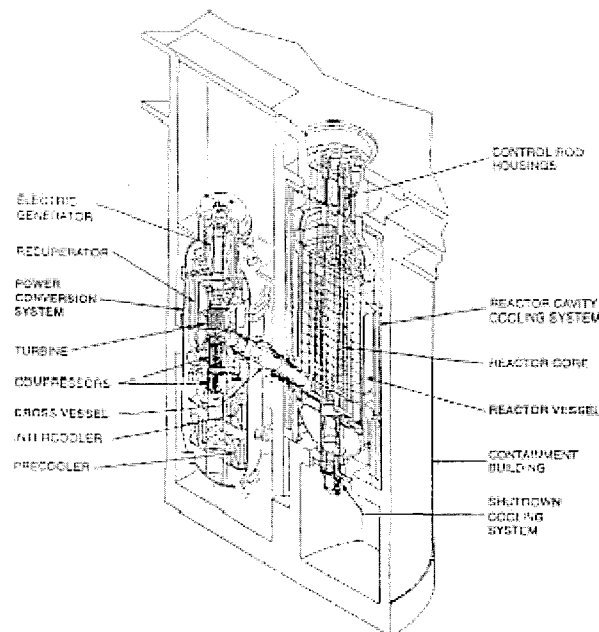


**Figure 1 - GT-MHR Reactor Concept [11]**

The GT-MHR attempts to achieve the various Gen-IV technology goals by several innovative means:

- Sustainability: The system operates on a special TRISO coated fuel pellet that is proliferation resistant because the uranium cannot be removed from it.

- Safety: The designers have created a system that is inherently safe, where temperature cannot not reach critical levels under typical worst case scenarios and radionuclides cannot escape the fuel pellets.

- Economics: To minimize waste and improve profitability, this reactor achieves one of the highest efficiencies (48%) of any power generation system ever proposed. This is largely due to Brayton cycle gas turbine, but is also due to reduced requirements for redundant safety systems.

Among these goals, safety is of special concern for the GT-MHR. It achieves part of its safety goals through an innovative approach to cooling. There are three systems which remove thermal energy from the core. The first is the power conversion system (PCS), which is the gas turbine. Under normal operation it is used to remove nearly all the energy produced by the reactor core. The second system is the shutdown cooling system (SCS), which is built into the bottom of the reactor core. It circulates helium throughout the core and across a heat exchanger. The secondary side of the heat exchanger is connected to a water coolant loop. This removes thermal energy during normal shutdown and refueling. The final cooling system is the reactor cavity cooling system (RCCS). This wholly passive system uses and radiation within the cavity to transfer thermal energy to the riser panels. The riser panels are connected to outside air, and remove the thermal energy by natural circulation. During normal operation and shutdown, the RCCS is used to maintain concrete temperatures within the reactor cavity.

During emergency shutdown, the system removes thermal energy from the vessel to prevent fuel meltdown or structural damage. Since the system is used during normal operation, no initiation is required during an emergency, and the system operates even if outside power is lost.

## 2.2 DESIGN APPROACHES

Many different approaches to solving engineering design problems have been developed over the past several decades. TRIZ is a qualitative method that attempts to aid the designer in developing solutions based on solutions from the past, such as those recorded in patent records. Robust Design provides principles and tools for the designer to find the parametric configuration that is most likely to work in all situations, considering variations from operating environment, normal wear and tear, and manufacturing variations. Axiomatic Design has both quantitative and qualitative measures to help the designer develop a solution that achieves a high degree of functional independence.

In the following sections, each of these approaches is reviewed and its use for large-scale system design problems, such as a nuclear reactor system, is discussed.

### 2.2.1 TRIZ

TRIZ, or the Theory of Inventive Problem Solving, was developed in the 1940's by Genrich S. Altshuller, a mechanical engineer working in the Soviet Navy patent office [12]. TRIZ is a qualitative problem solving method that is based on the fact most technical problems have already been solved elsewhere. Altshuller and others screened thousands of patents to determine how past problems were solved inventively. They found eight patterns of technical system evolution that form the foundation of TRIZ. They also identified 39 Engineering Parameters and 40 Inventive Principles to be used in

solving problems. The findings from their studies form the TRIZ knowledge base. Finally, they developed a number of tools to be used in problem solving.

Substance-Field Analysis is a tool for modeling problems related to new or existing problems. Each system has a function that represents an action towards another object, carried out using a field, which is typically some form of energy. Required Function Analysis takes the objective of a system and matches it with the most ideal method for carrying it out. The Algorithm for Inventive Problem Solving (ARIZ) is a set of procedures that transform real world problems into a form that can be solved using TRIZ. Anticipatory Failure Determination invents possible ways for a system to fail to perform its intended function, examines the possibility for failure to occur, and if necessary prevents it. Directed Product Evolution examines how designs have developed in the past and applies the results to current products to determine the next logical step in their evolution. All of these tools work together, and with the TRIZ knowledge base and theories provide a structured way to solve difficult problems inventively.

TRIZ has existed for 50 years, but until 10 years ago it was not well known outside of Russia. Since the breakup of the Soviet Union, it has gained popularity in many large companies in the United States and around the world due to its perceived benefit in solving otherwise difficult problems. Currently there are numerous resources in the U.S. for organizations that would like to implement TRIZ principles. There are many TRIZ consultants, such as Ideation International, Trizexperts, and Trisolver that can be brought in to solve problems that have proven unsolvable inside some companies. The consulting companies, along with others, also offer software that can be used to simplify TRIZ or speed up the process of applying it.

TRIZ has been used in solving numerous small design problems, such as a test probe for analog IC tests [13], an ATM paper handling mechanism [14], and a computer hard disk actuator arm[15]. In these case studies, as well as others, it has been documented to be very effective solving problems with individual parts or functions at a conceptual level. Unfortunately, some researchers have found it difficult to apply TRIZ to large-scale, or system, design problems [16]. Also, since it is entirely qualitative it does not provide a means to optimize a solution at the parametric level, determine how good a solution is, or compare competing solutions.

## 2.2.2 Robust Design

Dr. Genichi Taguchi began the development of what is now robust design in post-WWII Japan during the 1950's [2]. He worked for the Electrical Communication Laboratory (ECL), who was developing a new phone system for Japan. Since ECL outsourced their manufacturing, they needed to ensure that the products they designed were manufacturable and had high quality. This project provided the motivation to develop what have become Taguchi's Robust Design principles, which is the foundation of existing robust design approaches.

> *the state where the technology, product, or process performance is minimally sensitive to factors causing variability (either in the manufacturing or user's environment) and aging at the lowest unit manufacturing cost* [2].

While there are many different ways that robustness could be measured, Taguchi's Robust Design uses the Signal-to-Noise (S/N) Ratio. While there are numerous definitions for the S/N ratio, it serves as a measure of the effect of variation (noise) on a performance parameter (signal). The higher the S/N ratio, the more robust the system design. The Robust Design approach usually includes classical DOE or

orthogonal arrays, statistics based data analysis, response surface modeling, and optimization. Orthogonal arrays are used to map and simplify the design space [17]. Real or virtual experiments can be performed to determine the effect of individual sources of noise on a design. A two step optimization process is used with Robust Design. First, the variability of the system is reduced by attempting maximize the S/N ratio. Second, the system is adjusted to achieve a desired nominal target value.

Many researchers have taken the methods developed by Taguchi and expanded them for use in other fields. Robust Concept Exploration Method (RCEM) is one such method that is focused on product design. RCEM uses an S/N ratio, from Taguchi's Robust Design, as the objective function in a design optimization problem. It combines that with a system model and constraints to form the remainder of the problem, and finds the "best" design based on those inputs.

Once a design is developed, Robust Design provides a very effective set of tools for adjusting the parameters of a design into the most robust design. The processes used by Robust Design are very effective for both simple, small designs as well as large-scale systems, there is just much more work involved with a large-scale system. Robust Design has been applied to numerous designs, including an intercooler design by Nissan, fuel delivery system by Ford, and energy efficient compressors by Goldstar [2]. Since a numerical result is developed (S/N ratio) competing systems can be compared. Current robust design approaches are limited to situations where sufficient information about the target system is available. Moreover, it doesn't help designers generate innovative designs.

## 2.2.3 Suh's Axiomatic Design

In the late 1970's, Nam Suh of MIT began the development of what is now known as Axiomatic Design [4,5]. He had the desire to find a scientific basis for design and to provide the designer with a theoretical foundation based on logical and rational thought processes and tools. He found that good designers follow a few basic practices in creating good designs.

According to Webster's Dictionary, an axiom is "a self-evident principle or one that is accepted as true without proof as the basis for argument; a postulate." Axiomatic Design is based on two axioms.

> **Axiom 1 - The Independence Axiom:** In an acceptable design, the DPs and the FRs are related in such a way that specific DP can be adjusted to satisfy its corresponding FR without affecting other functional requirements.

> **Axiom 2 - The Information Axiom:** The best design is a functionally uncoupled design that has the minimum information content.

Axiomatic Design provides the designer a number of tools, which can be used to aid in the implementation of the first axiom. Some of the tools include, corollaries, theorems, zig-zag decomposition, and R/S analysis. Section 3.1 provides details on these tools and how they are used.

When several designs or design variations are created that meet the independence axiom, they can be evaluated by the information axiom to determine which is the 'best' design. Axiomatic Design defines the best design as the one with the highest probability of meeting the functional requirements.

To help designers implement Axiomatic Design, groups are available to teach AD and to consult on specific projects. The leading consultant for AD is Axiomatic Design Software, Inc. For mechanical system development they offer design review, design

completeness assessment, and project planning services. Additionally, they produce software to help implement Axiomatic Design during product development.

A number of successful applications of Axiomatic Design have been documented, including an ATM paper-handling mechanism [19], an inkjet printhead [20], and the design of a piece of clean-room production equipment [5]. The tools for decomposition can help guide a designer in finding a solution to a new design problem. They can be used to find solutions to both a general system level problem or to a specific part level problem. When several solutions are developed, there are tools that can be used to compare various designs and determine which is the best design. Axiomatic Design does not have the formal parametric tools for design evaluation and improvement like those of Robust Design. When applied to a specific design problem, extra effort is required:

      a)  to understand FRs/DPs of the targeted system;
      b)  to develop FR/DP relationships at both functional and parametric level;
      c)  to establish numerical strategy for calculating R and S;
      d)  to optimize R and S for design improvements.

## 2.3 SURROGATE MODELING METHODS

Surrogate models are used by designers as substitutes for highly accurate analytical, numerical, or computational models. They attempt to replace a more accurate, but computational complex model with a simpler model which has adequate accuracy. A number of various approaches have been developed to create and validate the accuracy of surrogate models.

### 2.3.1 Conventional Design of Experiment Techniques

Conventional design of experiments (DOE) is a statistics based experimentation method where purposeful changes in variables are made to determine the reasons for

change in one or more outputs [21]. Traditionally, people have approached this problem in one of two ways. First, they try to determine overall system behavior by testing each variable separately and then adding the effects. This works only if the variables do not interact with each other. Second, they attempt to test everything together, and develop an experimental plan that is too expensive to execute. DOE provides a method that overcomes both of these problems. The first is overcome because DOE varies the levels of multiple variables at the same time. The second is overcome by statistically selecting sample conditions, so that the necessary data is acquired while minimizing the number of tests performed.

A number of standard DOE methods exist which help the designer achieve desired results. Typically, a DOE requires the designer to select variables for the study, determine the number of levels for variables, and determine what fraction of the experiment to run. Ideally all variables are tested at once to fully understand the system. This often leads to an experiment that is too large and too expensive. One way to simplify a design is to select only the variables that will most reasonably affect the output variables or have interactions with each other.

Typical DOE experiments have two ($2^k$ design) or three ($3^k$ design) levels. For binary (on/off) variables, a two level design is the only option. For analog data, a two or three level design can be used. The advantage of a two level design is that there are fewer test conditions, while with a three level design a better understanding of linearity and interactions can be determined. The main exception is with discrete variables, which can have any number of levels, and all of the levels are used.

To get the most information about a design, all possible combinations (full-factorial design) of variables need to be tested. If very many variables are under consideration, the design also gets extremely large. For example if eight variables are

tested at two levels each, the experiment will require 256 individual tests. A partial factorial design, which statistically removes tests so only high order interactions are lost, can be used to reduce the number of tests required. In the above example, if a quarter factorial design is used, only 64 tests are required.

Frequently a sequential DOE process is also used to help minimize the resources required to characterize a system. In sequential DOE, the first step takes a rough look at the entire system. Usually a small fraction of a two level design is performed to identify key parameters which affect the output of the system. In the next step, variables are eliminated which do not affect the system, and more detailed tests are performed. The more detailed test might use a larger fraction or a three level design. Also, variables which do have interactions can be grouped and several smaller tests performed. This process can be repeated until enough understanding about the system is achieved.

DOE provides an excellent set of tools for creating experiments that maximize the statistical quality of data derived from a limited set of resources. Its techniques are well founded and accepted by numerous design communities. While it provides an excellent look at significance of different variables, it doesn't provide complete information needed to create a surrogate model.

## 2.3.2 Response Surface Modeling

A number of different tools exist to fit a model to a set of data. Regression is the simplest method for statistically fitting a model to data. Regression attempts to minimize the error between the data and the predictive model. Regression can be used to fit a polynomial model (linear, quadratic, etc) or a more complex function such as exponential or logarithmic. Response modeling is a statistical tool that combines tools from DOE and

regression, so that a statistically accurate model can be developed while a minimum of data is collected to form the model.

A number of tools exist for creating and analyzing response surface models, such a central composite and Box-Behnken designs [22]. In both of these, a small amount of data is collected, and then linear, linear interaction, and full quadratic models can be developed. Once a response model is developed, it is easy to create surface or contour plots of the model. From a surface or contour plot a specific operating point can be selected. Also, the response surface model can be combined with optimization, and a optimal point for a design selected which meets specified requirements [23].

Response surface models provide a nice addition to DOE, by allowing a user to develop a surrogate model from data. Also, the methods developed around response surface models are accepted by the statistics community.

## 2.3.3 Taguchi Orthogonal Arrays

Taguchi developed a method similar to DOE, known as orthogonal arrays, for identifying test conditions and analyzing the data that is collected. A number of standard designs have been developed by Taguchi which guide the designer in selecting test points. Various designs are available for different numbers of factors and different numbers of levels within each factor. The goal of the various designs is to maintain orthogonality between all test conditions.

Once data is collected, two methods exist for analyzing the data. First, ANalysis Of VAriance (ANOVA) can be used, which is the same as DOE uses for analysis. Also, Signal-to-Noise (S/N) ratios can be used for analysis. Once data is analyzed, various optimization models can be used to identify optimal operating points based on requirements for the design.

Taguchi methods are good at providing a consistent method for experiment design and analysis. Different designers can each develop a design for a system, and the resulting experiment will be much more similar than those developed by DOE or response surface methodology (RSM). Also, a number of tools exist for creating and analyzing Taguchi designs. Unfortunately, Taguchi Methods do not provide a good way for extracting a model that is usable in other applications. Also, Taguchi Methods are not statistically based, which has brought criticism from the statistics community.

## 2.4 OPTIMIZATION IN DESIGN

Optimization is a technique to help designers achieve desired objectives through a search for the optimum in a design space [24]. A single objective optimization is frequently expressed mathematically as a minimization problem, as follows:

$$minimize\ f(\mathbf{x}),\quad \mathbf{x} \in \Re^n$$

$$subject\ to: \mathbf{g}(\mathbf{x}) \le 0 \tag{2.1}$$

$$\mathbf{h}(\mathbf{x}) = 0$$

Where:

f(**x**) is objective function;

**x** are design variables, $\mathbf{x} = [x_1, x_2, ..., x_n]^T$, it is defined in a n-dimension real number space;

**g(x)** are inequality constraints, **h(x)** are equality constraints, they together define a feasible design space for the optimization

The goal of this minimization problem is to find x* that leads to the minimum value of the f(**x**), i.e., f(**x**\*) = minimum, in the feasible design space.

A wealth of different graphical, analytical, and numerical tools exist to solve this problem. Usually, the graphical and analytical tools are insufficient for complex

problems, such as the design of the GT-MHR. Numerical techniques are more applicable, including sequential linear programming (SLP), sequential quadratic programming (SQP), gradient methods, Newton methods, and others. Several software tools are also widely used in academia research and industrial practice; including Excel, MathCad, and Matlab.

## 2.5 SOFTWARE TOOLS

Countless software tools have been developed to aid designers including simple 2-d drawing programs, complex 3-d parametric solid modelers, basic spreadsheets, computational equation solvers, and process implementation tools. A variety of tools used for this research are described below.

### 2.5.1 Minitab

Minitab <http://www.minitab.com/> is one of the premier statistical software tools available today. It provides statisticians and engineers tools for the easy analysis of data, including basic statistics, regression analysis, analysis of variance, statistical process control, measurement system analysis, design of experiments (DOE), reliability analysis, as well as numerous others. It provides numerical and various graphical results for the analyses performed.

In this research, the DOE tools were primarily used. Factorial designs were used to determine which design parameters are significant and response surface models were used to create surrogate models (see sections 3.3 and 3.4).

As seen in Figure 2, Minitab uses a familiar spreadsheet layout for input.

MINITAB - RCCS Analysis.MPJ

File  Edit  Manip  Calc  Stat  Graph  Editor  Window  Help

Session

R denotes an observation with a large standardized residual.

**Normplot of Residuals for Triser,m**

**Residuals vs Fits for Triser,m**

——— 10/27/2003 7:23:10 PM ———

Welcome to Minitab, press F1 for help.
Retrieving project from file: C:\Documents and Settings\Owner\My Documents\School\Thesis\RCCS Analysis.MPJ

|  | C22 | C23 | C24 | C25 | C26 | C27 | C28 | C29 | C30 | C31 | C32 |
|---|---|---|---|---|---|---|---|---|---|---|---|
|  | CF Tair,exit | CF Triser,ave | CF Triser,max | CF Trx,max | CF sig Tair,exit | CF sig Pin | CF sig Pout | CF sig Vriser | CF sig Triser,max | CF sig Trx,max |  |
| 1 | 2.062E+03 | 1.809E+03 | 2.570E+03 | 2.319E+03 | 4.900E+01 | 9.999E-02 | 8.956E-02 | -2.348E+01 | 2.535E+03 | 2.346E+03 |  |
| 2 | -9.184E+01 | -7.604E+01 | -1.239E+02 | -1.075E+02 | 4.343E-14 | -6.676E-03 | -7.468E-03 | 3.812E+00 | -1.227E+02 | -1.093E+02 |  |
| 3 | 6.212E+00 | 3.980E+00 | 6.227E+00 | 5.300E+00 | -1.000E+00 | 3.026E-04 | 1.959E-04 | -7.466E-01 | 6.427E+00 | 4.967E+00 |  |
| 4 | -7.181E+02 | -4.810E+02 | -8.125E+02 | -6.089E+02 | -4.025E-13 | -4.412E-02 | -4.307E-02 | 4.620E+01 | -8.065E+02 | -6.154E+02 |  |
| 5 | -2.831E+00 | -2.344E+00 | -3.964E+00 | -3.440E+00 | 5.433E-17 | -2.278E-04 | -2.550E-04 | 1.027E-01 | -3.966E+00 | -3.371E+00 |  |
| 6 | -1.886E+00 | -1.380E+00 | -1.865E+00 | -1.877E+00 | 1.429E-15 | -2.766E-04 | -5.979E-04 | 1.768E-01 | -1.521E+00 | -1.805E+00 |  |
| 7 | 3.267E-02 | -1.091E-01 | 5.593E-03 | -1.091E-01 | 1.000E+00 | -2.615E-04 | 4.754E-04 | -3.008E-02 | -9.345E-01 | -9.379E-01 |  |
| 8 | -5.147E-01 | -7.031E-01 | -9.271E-01 | -4.115E-01 | 9.895E-15 | 3.221E-05 | 8.463E-05 | -6.810E-02 | 2.315E+00 | 2.169E+00 |  |

Current Worksheet: DOE Test 4     Editable     7:23 PM

**Figure 2 - Minitab Input Screen**

Once data is entered and analyzed, results can be viewed in the spreadsheet as well as interaction plots (Figure 3), residual plots (Figure 4), and 3-d surface plots (Figure 5).

Interaction Plot - Data Means for Triser,max
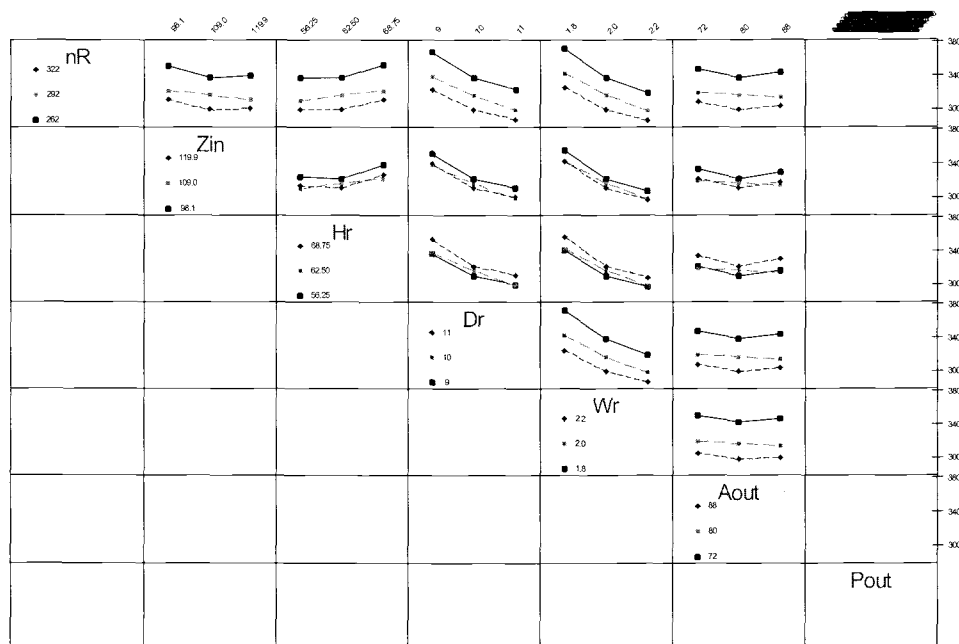


**Figure 3 - Sample Minitab Interaction Plot**

Normal Probability Plot of the Residuals

(response is Triser,m)
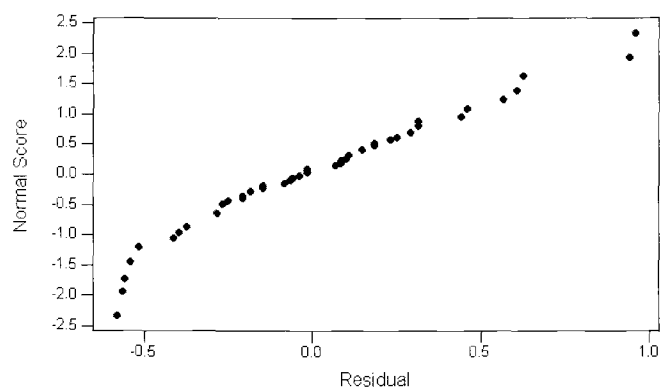


**Figure 4 - Example of Minitab residual plot**

Surface Plot of Vriser
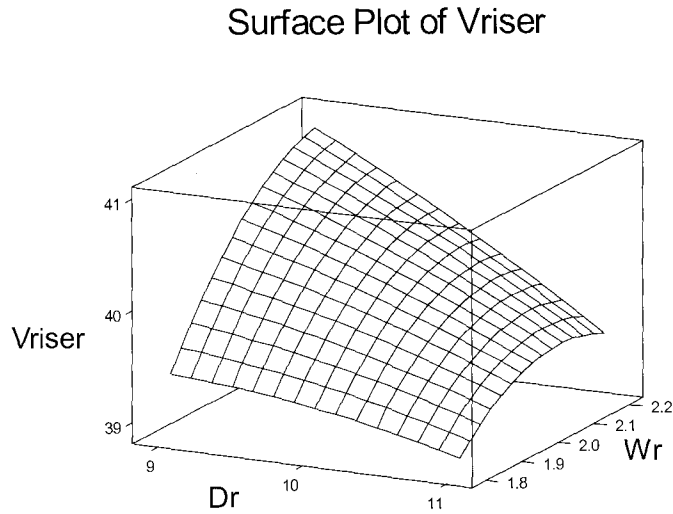


**Figure 5 - Sample Minitab Surface Plot**

## 2.5.2 Excel

Microsoft Excel <http://office.microsoft.com/excel> is the leading computer spreadsheet program. It is an extremely versatile software package which allows for analytical, numerical, and statistical analysis. In this study, the one-dimensional heat transfer model of the GT-MHR was created in Excel (section 4.3). Also, the system evaluation (section 4.5) and optimization routine (section 4.6) were developed in Excel.

Numerous add-ins have been developed for use with Microsoft Excel, including database access tools, the Analysis toolpak, and the Solver Add-In. The Solver Add-In (Figure 6) is primarily an optimization tool. It allows the user to minimize, maximize, or seek a target within a given cell. The goal is achieved by varying other cells, while maintaining a set of specified constraints.
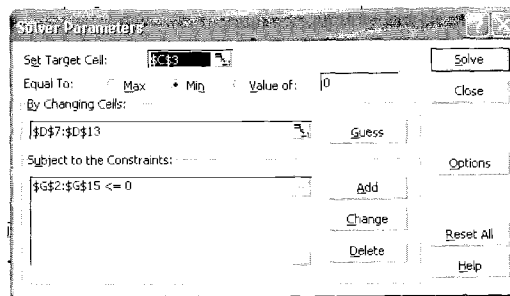
**Figure 6 - Sample of Excel Solver Dialog**

The solver tool has a number of different methods it can use to solve the optimization problem, including linear, Newton, and conjugate methods. The user can also specify what type of estimates to make and set iteration parameters.

### 2.5.3 Matlab

Matlab <http://www.mathworks.com/> is one of the most popular computational tools. It has tools for analysis of complex mathematical problems, visualization, control system design, digital signal processing, and image processing. One very common use is in performing very complex simulations of mathematically defined systems. One aspect that makes Matlab very powerful is its ability to execute C++ code. Even though entirely capable of handling the analysis required by this research, it was not utilized because of the complexity in performing the relatively simple calculations required.

### 2.5.4 MathCAD

MathCAD <http://www.mathcad.com/> is another popular computational tool. It has nearly identical capabilities to other packages, such as Matlab. One aspect that sets MathCAD apart is the visual interface for the user (Figure 7). The user creates equations so that they appear as they do when written out. Additionally, it allows symbolic evaluation of most problems, which is something most software packages do not offer. Many intermediate calculations were performed in MathCAD throughout the project.
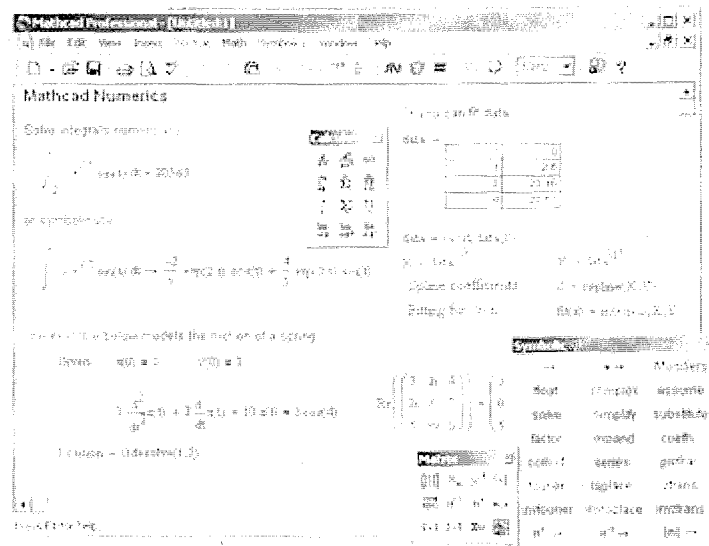
**Figure 7 - Sample of MathCAD Interface**

## 2.5.5 Acclaro Design Software

Acclaro Designer <http://www.axiomaticdesign.com/products/prod_designer.asp> from Axiomatic Design Software Inc. is software to help designers through the process of axiomatic design. It particularly focuses on the decomposition process (section 3.2) within Axiomatic Design. It allows users to map and decompose functional requirements, design variables, and process variables through various levels and then populate the design matrices (section 3.4). An example of the interface is shown in Figure 8. It also has tools for creating tree and flow chart diagrams once the system is established.

The tools provided by Acclaro Designer can help ease the implementation of Axiomatic Design in a product development atmosphere. The tools for mapping, decomposition, and creating design matrices work very well. Unfortunately, it does not allow for the design matrices to be populated quantitatively. As a result users cannot use this tool to perform a parametric analysis of a design or perform an R/S analysis. If these features were added, it would be an extremely useful tool.
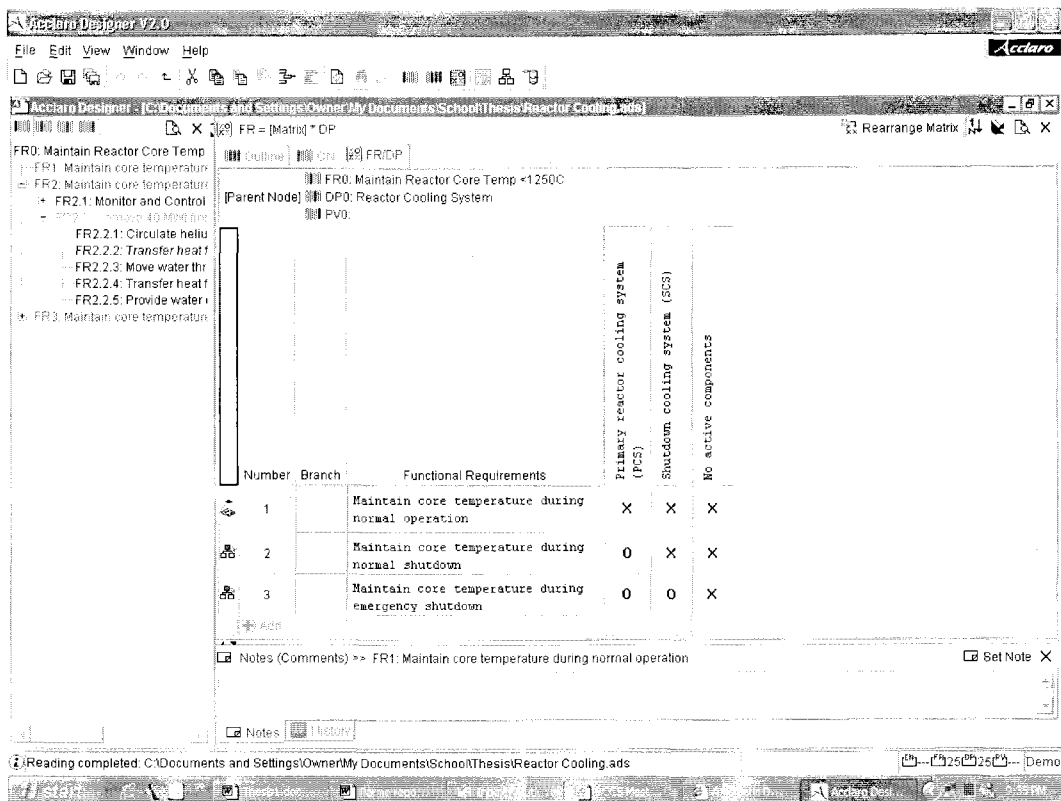
**Figure 8 - Acclaro Designer**

# 3. METHOD FOR EVALUATION AND OPTIMIZATION

A new, systematic approach was developed for evaluating and improving a large scale system design. This new approach is based on Suh's [4] Axiomatic Design Theory, Response Surface Modeling, and Design Optimization Theory [24]. The goal of the approach is to achieve functional independence throughout the entire system. This can also be viewed as limiting interactions between various parts of the system.
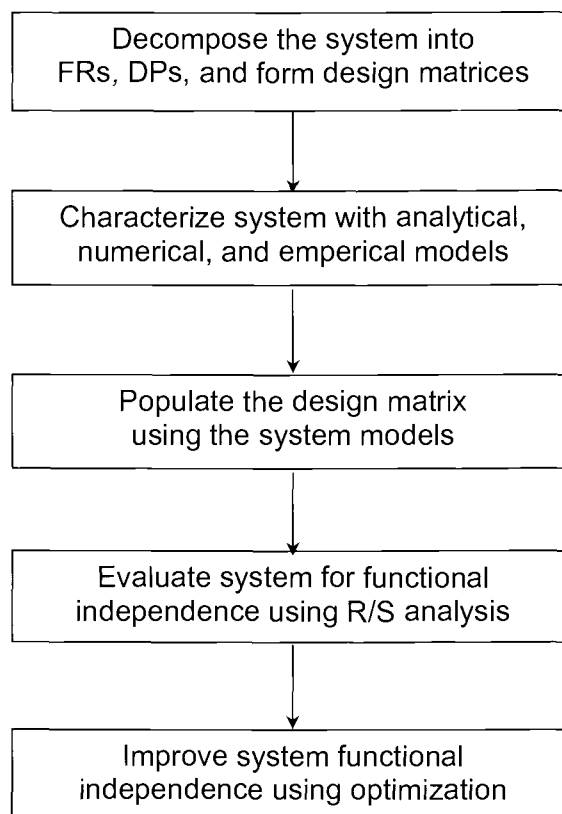


**Figure 9 - Proposed Approach for Evaluating and Improving a Large Scale System**

As shown in Figure 9, the approach has five basic steps. First, the system represented by functional requirements (FRs), design parameters (DPs), and their relations, in a design matrix form, using a decomposition and mapping process. At a low, parametric level, the functional requirements are performance parameters and the

design parameters are design variables. Second, a system model is developed which can be used to predict performance parameters from the design variables. Third, quantitative design matrices are created and populated with values derived from the system models. Next, an R/S analysis is performed on the quantitative design matrices to determine how good the design is by quantifying the functional independence of the design. Finally, an optimization design model is developed and resolved to minimize the functional coupling in the current design to get a better system.

## 3.1 IMPORTANT ASPECTS OF AXIOMATIC DESIGN

In the late 1970's, Nam P. Suh [4] began the development of what is known as Axiomatic Design Theory. The motivation was to establish a rigorous, scientific basis for successful product development. A typical large-scale engineering system, such as a nuclear reactor, airplane, automobile, or computer printer, is usually requires the satisfaction of multiple competing functionality requirements, such as performance, safety, economic concern, and environmental impact. Because of the complexity involved, the concepts generated often contain highly coupled functions. Such concepts lead to products that are redundant, costly, and difficult to manufacture. Functional independence is a core concept in Suh's axiomatic design theory, and can be used to develop products with decoupled or even uncoupled function structures, which are simpler, less expensive, and easier to make.

Suh's axiomatic design theory provides design researchers and practitioners with a consistent framework based on a logical thinking process, and techniques to carry out design activities in a well-organized manner. Four key elements of axiomatic design are used in the approach presented here. First, there are four primary design domains, described in section 3.1.1. Second, there are two design axioms, which provide

principles for decisions made during the design process, and are described in section 3.1.2. Third, the zig-zag design process, described in section 3.1.3, is used to realize the decomposition and mapping process. An R/S analysis is used to quantitatively evaluate the system for functional independence and is described in section 3.1.4.

## 3.1.1 Design World Domains

Suh modeled the design world into four different domains and their interactions, as shown in Figure 10. The customer domain consists of the specific attributes that customers desire for a system. The functional domain consists of the functional requirements (FRs) that are required for the system to meet the desired customer attributes (CA). The physical domain is made of the systems, sub-systems, components, and component properties (DPs) that satisfy the functional requirements. The process domain is the settings (PVs) which are required to manufacture the physical parts of the system. For the purpose of this work, the focus is on the functional domain, the physical domain, and the decomposition and mapping relations between them.
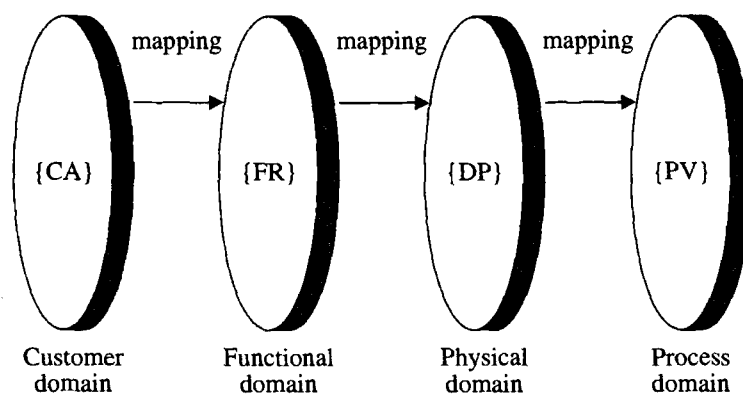


Figure 10 - Four domains of the design world [5]

## 3.1.2 Design Axioms

Axiomatic design provides two axioms to guide the zig-zag process and evaluate design alternatives. The two axioms are as follows:

**Axiom 1 - The Independence Axiom:** In an acceptable design, the DPs and the FRs are related in such a way that specific DP can be adjusted to satisfy its corresponding FR without affecting other functional requirements, i.e. functional independence.

**Axiom 2 - The Information Axiom:** The best design is a functionally uncoupled design that has the minimum information content.

Axiom 1 is used to select the qualified FR and DP sets, which represent good designs. Axiom 2 is used to pick out the best FR and DP setting(s) among them. In addition to the two axioms, eight corollaries, 26 general theorems, and 14 theorems, have been developed to guide and evaluate specific types of design.

## 3.1.3 Zig-Zag Design Process

The zig-zag design process is used to realize the system decomposition and mapping, and is illustrated in Figure 11. First, a top level set of FRs must be developed for the system that are both collectively exhaustive and mutually exclusive, meaning that a) they define the entire scope of requirements for the system, and b) there is not any overlap in the requirements which they define. Once the top level FRs are defined, they are mapped, or zigged, to DPs at the same level of detail. Then the top level FRs and DPs are both decomposed, or zagged, to lower level FRs and DPs. The zig-zag design process continues through a series of levels, from system, to sub-system, component, and function level. At each level, the mapping between FRs and DPs should obey Axiom

1. This process continues until a level is reached where the design may be described parametrically.
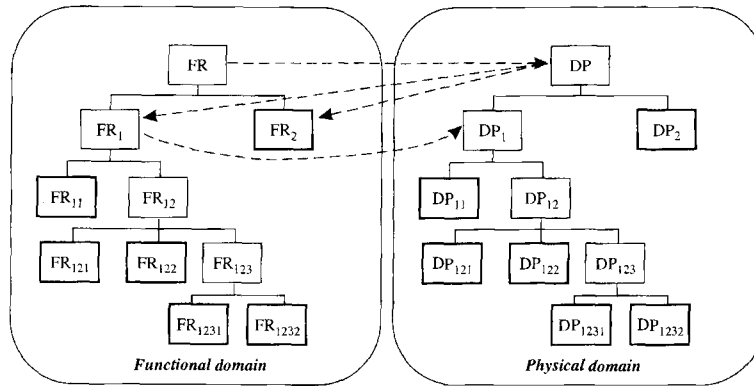


**Figure 11 - Zig-Zag Design Process [5]**

At each level of decomposition, a design matrix [**A**] is developed, which relates the FRs to their associated DPs at that level. When working at the top level design matrices, they can initially be populated with an X or O, respectively indicating a mapping relationship or lack of mapping relationship. Three different types of design matrices can result and are shown in Figure 12. From the left to the right, the first design matrix indicates a coupled design, the second a decoupled design, and the third an uncoupled design. An ideal design is one that can be represented by an uncoupled design matrix (each FR is controlled by only one DP and vise versa). Unfortunately, in the real world, most designs cannot be uncoupled, and a decoupled design is usually considered satisfactory. In any circumstance, a coupled design is to be avoided.

$$
\begin{Bmatrix} FR_1 \\ FR_2 \\ FR_3 \end{Bmatrix} = \begin{bmatrix} X & O & X \\ X & X & X \\ O & X & X \end{bmatrix} \begin{Bmatrix} DP_1 \\ DP_2 \\ DP_3 \end{Bmatrix}
\quad
\begin{Bmatrix} FR_1 \\ FR_2 \\ FR_3 \end{Bmatrix} = \begin{bmatrix} X & O & O \\ X & X & O \\ O & X & X \end{bmatrix} \begin{Bmatrix} DP_1 \\ DP_2 \\ DP_3 \end{Bmatrix}
\quad
\begin{Bmatrix} FR_1 \\ FR_2 \\ FR_3 \end{Bmatrix} = \begin{bmatrix} X & O & O \\ O & X & O \\ O & O & X \end{bmatrix} \begin{Bmatrix} DP_1 \\ DP_2 \\ DP_3 \end{Bmatrix}
$$

Coupled                Decoupled                Uncoupled

**Figure 12 - Design Matrix Types**

During the decomposition process, a design matrix may be developed which is not square, because there are different numbers of FRs and DPs at a certain level. A non-square design matrix indicates a possible redundant or over constrained design. Suh [5] has developed several corollaries to help designers improve these situations. For example, if there are more DPs than FRs, the design is redundant and a search for less redundant design is suggested. This can also be remedied by recognizing that some DPs are invariant, and thus allowing them to be considered as constraints, and changing the design to have the same number of DPs and FRs, which represents a desirable design based on Axiom 1.

## 3.1.4 Measurements of Functional Independence

A number of different measures of functional independence have been developed. The most common is reangularity (R) and semiangularity (S) [4]. R measures the angular relationship between the DP axes and S measures the magnitude of the diagonal elements of a normalized design matrix. R and S are further defined in section 3.5.

R and S only work where there are the same number of FRs and DPs (square design matrix). When the numbers of FRs and DPs differ, a different measure is required. One measure of functional independence that can be used in this situation is the orthogonality index ($\pi_o$) and alignment index ($\pi_a$) [4]. Orthogonality measures the independence of FRs and degree of coupling. The alignment index measures the axis alignments of DPs to FRs.

## 3.2 SYSTEM DECOMPOSITION

System decomposition is accomplished according to Axiom 1 and the guidelines of Axiomatic Design process, described in section 3.1.3. Typically a high level FR is

defined which relates directly to a customer requirement, and then a corresponding DP is defined. The decomposition progresses through the various levels until every FR/DP is described by a one or more performance variable/design variable.

Based on Axiom 1, it is desirable that the decomposition results in equal numbers of FRs and DPs at each level of decomposition. When they are not equal, either a different approach to the system definition needs to occur, or FRs and/or DPs need to either be added or removed. If there are more FRs than DPs, additional DPs must be developed or identified to achieve the various FRs. If there are fewer FRs than DPs, the number of DPs needs to be reduced.

A number of methods can be used to reduce the number of variables. An easy way is to remove those that you believe will have the least effect on the output, those which can be constrained by other variables, those which are not believed to vary across manufacturing, maintenance, or environment, or some other heuristic method. A good way to reduce the number of DPs is through a statistical t-test. Once a model is developed which characterizes the system, a two factor DOE can be performed using all of the DP variables. When analyzed, variables which do not have statistical significance can be constrained at a fixed value and removed from further analysis. If this is used, the designer can be ensured that significant variables are not removed.

## 3.3 SYSTEM CHARACTERIZATION

A number of techniques exist for characterizing a system, from back of the envelope estimations, to numerical simulations and sophisticated computational models built with tools such as FEA and CFD. Care must be taken to ensure that the model used has sufficient accuracy for the application.

Usually, a real world system simulation is extremely complex and requires extensive time from a person or computer to develop a set of results. For example, a CFD simulation for one set of initial conditions on a complex thermal system can take over one day. Quite often, these simulations are highly non-linear and non-polynomial, making manipulations, such as integrals and derivatives, extremely difficult or even impossible.

A common practice in design is to replace a complex system model with a quadratic surrogate model [18]. There are a number of ways the surrogate models can be obtained, such as a combination of DOE and response surface model building techniques [21]. In this work the following approach is taken: First, a 3-factor DOE can be performed using all DP variables and FR variables. When the DOE is analyzed it will identify which first order, second order, and interaction terms significantly affect each FR. A detailed response surface model can then be developed. For each FR, the significant DPs are modeled across three or more levels equally spaced throughout the design space for each variable. When analyzed, only the coefficients for the terms which the DOE identified as significant are calculated. The result is a statistically adequate quadratic surrogate model. It is important to test the accuracy of the model against the original data to ensure that sufficient accuracy is achieved. If the resulting surrogate models are not accurate enough, the process can be iterated for a higher order response model, with sequential DOE first determining the statistically significant elements, and then determining the model coefficients. Typically, over small regions represented by the design space for a given variable, a quadratic model can produce sufficient results.

## 3.4 POPULATE DESIGN MATRICES

Once the system is decomposed and models are developed for all relevant parts of the system, the design matrices can be populated with actual values. In the design matrix shown in Figure 12, the values of the individual elements are found by looking at the change in a functional requirement caused by a change in a design parameter, as shown in equation (3.1).

$$
\begin{Bmatrix} FR_1 \\ FR_2 \\ \vdots \\ FR_i \end{Bmatrix} = \begin{bmatrix} A_{11} & A_{12} & \cdots & A_{1j} \\ A_{21} & A_{22} & \cdots & A_{2j} \\ \vdots & \vdots & \ddots & \vdots \\ A_{i1} & A_{i2} & \cdots & A_{ij} \end{bmatrix} \cdot \begin{Bmatrix} DP_1 \\ DP_2 \\ \vdots \\ DP_j \end{Bmatrix} \quad where \quad A_{ij} = \frac{\partial FR_i}{\partial DP_j} \tag{3.1}
$$

In a system where there exist simple relationships, such as linear or polynomial, between the FRs and DPs, partial derivatives can be directly taken based on the relationships, and therefore, the design matrix can be easily populated. In many real world large-scale engineering systems the FR-DP relationships are highly nonlinear, and are impossible to be represented in a straightforward, closed, analytical, form. To populate a design matrix for such a system, sequential DOE and surrogate modeling processes are adopted to build differentiable functions for the underlying relationships between the FRs and DPs. Once the differentiable functions are obtained, the design matrix elements between the FRs and DPs can be instantiated with actual values ($A_{ij}$) using equation (3.1).

Once the design matrix is populated, it needs to be normalized and then configured into a matrix with the least coupling. The design matrix needs to be normalized so that the entire matrix is unitless. Prior to normalization, one cell might have relatively large values because it has units of °F/foot, while a nearby cell might have relatively small values because it has units of psi/foot. Many different normalization

techniques exist which could be used. The normalization in equation (3.2) was used in this work, which works to normalize rows and columns with their respective nominal values.

$$A_{i,j} \cdot \frac{\overline{DP_j}}{\overline{FR_i}} \quad where \ A_{i,j} = \frac{\partial FR_i}{\partial DP_j} \tag{3.2}$$

To reconfigure the design matrix, rows or columns can be switched with each other [4]. Columns and rows should be rearranged until the least coupling exists.

## 3.5 R/S ANALYSIS

Once the qualitative design matrix is populated with actual values ($A_{ij}$), an R/S analysis [5] can be performed to assess the functional coupling degree of a current design based on Axiom 1. Reangularity (R), shown in equation (3.3), measures the angular relationship between the DP axes. Semiangularity (S), shown in equation (3.4), measures the magnitude of the diagonal elements of a normalized design matrix.

$$R = \prod_{\substack{i=1 \\ j=1+i}}^{n-1} \left[ 1 - \frac{\left( \sum_{k=1}^{n} A_{ki} A_{kj} \right)^2}{\left( \sum_{k=1}^{n} A_{ki}^2 \right)\left( \sum_{k=1}^{n} A_{kj}^2 \right)} \right]^{1/2} \tag{3.3}$$

$$S = \prod_{j=1}^{n} \left[ \frac{|A_{jj}|}{\left( \sum_{k=1}^{n} A_{kj}^2 \right)^{1/2}} \right] \tag{3.4}$$

The result of the analysis helps identify how close the design matrix is to the ideal uncoupled matrix (see Figure 12). If the result is an uncoupled matrix, both R and S equal 1.0. When the matrix is decoupled, R and S are equal, but not 1.0, and when the

matrix is coupled, the values of R and S are different from each other and tend to approach zero. The closer the values of R and S, and the closer each is to a value of 1.0, the less functionally coupled the system. The closer the values are to 1.0, the larger the role of the diagonal element. The quantitative design matrix and R/S analysis can be used to determine where design changes are needed to improve the current system.

In arranging the matrix, as described in section 3.4, it can be difficult to identify which layout has the least coupling. Getting the best arrangement can be an iterative process, arranging the matrix and then looking at the results of R and S to see if the new arrangement is better.

## 3.6 OPTIMIZATION

An optimization design model contains three parts:

1. design variables [$\mathbf{x}$]
2. an objective function [f($\mathbf{x}$)]
3. design constraints [h($\mathbf{x}$) = 0 and g($\mathbf{x}$) ≤ 0]

The design variables here are the attributes of a system that can be specified by designers. Since the objective is to minimize functional independence, and the R/S analysis is a measure of functional independence, the objective function should be based on R and/or S. A number of possible functions, listed in Table 1, were proposed. For this problem, a good objective function will vary similarly for changes in either R or S. This can be measured by taking a partial derivative of the function with respect to both R and S. A good objective function will result in partial derivatives which are similar in both magnitude and tendency, or direction. Function (1) is not good because it doesn't take into account the effect of S. Likewise, a similar function built on S is also inadequate. Functions (3) and (4) are also not good objective functions, due to them

having an opposite direction. This means that an increase in R leads to an increase in the objective function while an increase in S leads to a decrease in the objective function, or vice versa.

| ID | Objective Function (f) | $\partial f/\partial R$ | $\partial f/\partial S$ | Goodness of function |
|----|------------------------|-----------|-----------|----------------------|
| 1 | $1/R$ | $-1/R^2$ | $0$ | Incomplete, no S |
| 2 | $1/(R+S)$ | $-1/(R+S)^2$ | $-1/(R+S)^2$ | Good |
| 3 | $R/(R+S)$ | $S/(R+S)^2$ | $-R/(R+S)^2$ | Bad, opposite direction |
| 4 | $R-S$ | $1$ | $-1$ | Bad, opposite direction |
| 5 | $(R+S)/(RS)$ | $-1/R^2$ | $-1/S^2$ | Good |

**Table 1- Possible objective functions**

Two of the functions were identified as good by the partial derivative measures. The one which converges faster is a relatively better objective function [24]. This can be identified by dividing the two functions and taking two limits. The first limit (R→S) addresses the system approaching a decoupled system and the second limit (R,S→1) addresses the system approaching an uncoupled system. If the limits are greater than 1, then the top function converges faster, and is the better function. If they are less than 1, then the bottom function is better.

$$\lim_{R\to S} \frac{\frac{R+S}{RS}}{\frac{1}{R+S}} = \lim_{R\to S} \frac{(R+S)^2}{RS} \Rightarrow \frac{(R+R)^2}{R^2} = \frac{4R^2}{R^2} = 4 \qquad (3.5)$$

$$\lim_{\substack{R\to 1 \\ S\to 1}} \frac{\frac{R+S}{RS}}{\frac{1}{R+S}} = \lim_{\substack{R\to 1 \\ S\to 1}} \frac{(R+S)^2}{RS} \Rightarrow \frac{(1+1)^2}{1^2} = 4 \qquad (3.6)$$

Since both limits (3.5 and 3.6) are greater than 1, the top function converges faster. Thus, the function in equation (3.7) is identified as the best proposed objective function, and is used as part of the optimization design model.

$$f(R,S) = \frac{R+S}{R \cdot S} \tag{3.7}$$

A series of equality constraints is defined by R, S, and the design matrix, in equations (3.1) to (3.4). If a surrogate model is used, an additional set of inequality constraints are defined by ranges of the design models over which the system models are built and validated, as shown in equation (3.8). Finally, additional requirements for the system may define additional inequality constraints.

$$\begin{aligned} x_{i,min} - x_i &\leq 0 \\ x_i - x_{i,max} &\leq 0 \end{aligned} \tag{3.8}$$

In summary, the optimization design model (3.9) is:

$$minimize \quad f(\mathbf{x}) \frac{R+S}{RS}, \quad \mathbf{x} \in \Re^n$$

$$subject\ to : R = f_R(\mathbf{x})$$

$$S = f_S(\mathbf{x})$$

$$\mathbf{x}_{min} - \mathbf{x} \leq 0 \tag{3.9}$$

$$\mathbf{x} - \mathbf{x}_{max} \leq 0$$

$$\mathbf{g}(\mathbf{x}) \leq 0$$

$$where$$

$$\mathbf{x} = \{x_1, x_2, \ldots x_n\}^T$$

Commercial optimization software is then used to obtain the design optimum, $\mathbf{x}^*$.

# 4. CASE STUDY WITH GT-MHR RCCS NUCLEAR REACTOR COOLING SYSTEM

In order to demonstrate the applicability of the method proposed in Section 3, General Atomics' GT-MHR Reactor Cavity Cooling System (RCCS) was selected as a case study for evaluation and identifying improvements. The case study focuses on the emergency operation of the RCCS only. The RCCS is used during normal operation, normal shutdown, and emergency shutdown. During normal operation and shutdown, the RCCS is used to remove about 3.3MW thermal energy from the cavity so the concrete walls of the cavity do not exceed a critical temperature of 120°F. During an emergency, the RCCS continues to operate and is the primary means for removing thermal energy from the reactor core. During emergency operation, the RCCS is to keep the core below 1450°F, the vessel below 900°F, and the concrete cavity below 120°F.

## 4.1 INTRODUCTION TO GT-MHR RCCS

The Reactor Cavity Cooling System of the GT-MHR introduces a somewhat unique paradigm for treating long-term decay heat removal after loss-of-coolant accidents (LOCAs). In general, power reactors today strive to achieve high values of thermal efficiency in an effort to maximize profitability. One way that designers do this is by insulating the system in an effort to reduce heat loss to the surroundings. This can have a measurable impact on the thermal efficiency, but can lead to trouble in the event of a LOCA. In this event, it is necessary to find a way to remove the decay heat from the reactor in order to prevent damage to the fuel assemblies or reactor vessel itself. Insulation works against this, causing the system to retain more heat. The result is that additional systems are needed to provide protection. These systems require additional design and capital expenditure, larger facilities to accommodate them, additional

periodic maintenance and testing to ensure operability, and still have the possibility of failure.

The GT-MHR designers have approached the problem of decay heat removal in a different way. The Reactor Cavity Cooling System (RCCS) is a natural circulation driven cooling system using air from the environment to remove heat from the reactor cavity. The reactor is not insulated, so whenever heat is generated within the vessel, a small portion of the heat escapes into the cavity. That heat is partially dissipated to the ground (as the reactor cavity is beneath ground level) and partially to the air that is being circulated through the RCCS cooling panel. The portion heat transferred to the air is the driving force for natural circulation. Since the RCCS operates continuously, it does not require initiation in the event of a casualty; it merely continues operating, and as the temperature in the reactor cavity increases, natural circulation increases and additional heat is removed.

The RCCS operation is relatively simple, requires no moving parts, and no initiation for it to operate. While sacrificing some thermal efficiency, the simplicity of the system is expected to maintain economic competitiveness due to reduced capital, manpower, maintenance, and operation costs. A major limitation is that, to ensure acceptable vessel and fuel temperatures during accident conditions, reactor power must be limited so that the shutdown (decay) heat levels are within the heat removal capability of the RCCS. Thus, the RCCS performance limits place significant limitations on the reactor design.

Immediately following a reactor shutdown, the decay heat produced exceeds the normal heat removal capability of the RCCS, resulting in rising reactor vessel and fuel temperatures. However, the GT-MHR has a large volume of graphite, which has a high heat capacity, and a large vessel mass, that together act to slow the heat-up rate during

the time when the decay heat generation exceeds the RCCS heat removal capability. In time, the decay power decreases and finally falls within the range of the RCCS's heat removal capability; this is approximately the point at which the fuel temperature will be at its peak value. Due to the high-temperature capability of reactor core and coated fuels adopted in GT-MHR design, given maximum decay power and likely worst case scenarios, this peak temperature will still be within the safe temperature range.

## 4.1.1 System requirements

The primary requirement of the RCCS is to maintain safe temperatures within all components at all times. In order to achieve this requirement, a number of quantifiable requirements were identified for the system, including:

- Fuel temperature below 3000°F
- Structural components below 900°F
- Concrete temperature below 120°F
- Run autonomously during an emergency
- Allow operation when partially blocked
- Operation be insensitive to wind direction or speed
- Maintain safe conditions with ambient temperature -45°F to 110°F
- Operate without outside power
- Remove 4MW thermal power from core cavity

## 4.1.2 System design issues

Current design practice for the GT-MHR and RCCS has been to specify the desired performance and other design constraints and then develop a suitable engineering solution to fulfill the requirements. Heuristics based judgment, refined sizing calculations, directed trade-off studies, and parametric analyses are all employed to help ensure an optimized design. Never the less, each functional requirement is optimized independently without considering its interdependence with other functions. The

selective attention to a limited subset of design parameters and requirements can lead to sub-optimal results. Furthermore, the approach aims at finding a workable solution but not necessarily an absolute optimum.

The RCCS design is in its preliminary stage. Areas requiring further development include:

- validation of integrated system performance;
- validation of major thermal properties (e.g., emissivity) over life;
- optimization of system performances for
- acceptable concrete temperature;
- minimum insulation in wall.
- Reduced cost through modular construction
- Detailed design considering vessel supports' effects on thermal performances
- Quantified uncertainty

## 4.2 SYSTEM DECOMPOSITION

The first step in evaluating the RCCS is to decompose the system until a parametric level is reached. One of the most important functions in a nuclear reactor is the ability for it to remove thermal energy and control temperature under all conditions. For the GT-MHR, this can be expressed as:

$FR_0$: Maintain reactor in safe operating condition with regard to temperature by $DP_0$: Reactor Cooling Systems

The high level FRs and DPs are decomposed into lower level FRs and DPs. Their mapping relationship is expressed by:

$$\begin{Bmatrix} FR_1 \\ FR_2 \\ FR_3 \end{Bmatrix} = \begin{bmatrix} X & X & X \\ O & X & X \\ O & O & X \end{bmatrix} \begin{Bmatrix} DP_1 \\ DP_2 \\ DP_3 \end{Bmatrix} \qquad \text{(Level 0)}$$

where  $FR_1$: Maintain safe reactor temperatures during normal operation
           $FR_2$: Maintain safe reactor temperatures during normal shutdown
           $FR_3$: Maintain safe reactor temperatures during emergency shutdown
by      $DP_1$: Power Conversion System (Helium Turbine)
           $DP_2$: Shutdown Cooling System (SCS)
           $DP_3$: Reactor Cavity Cooling System (RCCS)

The design matrix shows that the current RCCS design maintains relatively good functional independence at a high, abstract level.

## 4.2.1 Qualitative Decomposition

Since the purpose of this study is to evaluate the ability of the system to remain cool during emergency operations, the focus will be on the decomposition of $FR_3$ and $DP_3$, as follows:

$$\begin{Bmatrix} FR_{31} \\ FR_{32} \end{Bmatrix} = \begin{bmatrix} X & 0 \\ 0 & X \end{bmatrix} \begin{Bmatrix} DP_{31} \\ DP_{32} \end{Bmatrix} \qquad \text{(Level 3)}$$

where  $FR_{31}$: Run autonomously during an emergency
           $FR_{32}$: Keep core component temperatures below critical values
by      $DP_{31}$: Passive, redundant system
           $DP_{32}$: Air circulation through reactor cavity

Decomposing $FR_{31}$, we find:

$$\begin{Bmatrix} FR_{311} \\ FR_{312} \\ FR_{313} \end{Bmatrix} = \begin{bmatrix} X & 0 & 0 \\ 0 & X & 0 \\ 0 & 0 & X \end{bmatrix} \begin{Bmatrix} DP_{311} \\ DP_{312} \\ DP_{313} \end{Bmatrix} \qquad \text{(Level 3.1)}$$

where  $FR_{311}$: Allow operation when partially blocked
           $FR_{312}$: Insensitive to wind direction
           $FR_{313}$: Work without outside power
by      $DP_{311}$: Four inlets and outlets for natural circulation
           $DP_{312}$: Orientation of inlets and outlets
           $DP_{313}$: Completely passive system

Decomposing $FR_{32}$, we find:

$$\begin{Bmatrix} FR_{321} \\ FR_{322} \end{Bmatrix} = \begin{bmatrix} X & \sim 0 \\ 0 & X \end{bmatrix} \begin{Bmatrix} DP_{321} \\ DP_{322} \end{Bmatrix}$$   (Level 3.2)

where  $FR_{321}$: Keep fuel temperature below 1450C
       $FR_{322}$: Keep structural components below critical values
by     $DP_{321}$: Conductive heat transfer through core
       $DP_{322}$: Convective heat transfer through RCCS

The temperature of the fuel is largely a function of the core size and the decay power curve, rather than the RCCS. Since the analysis is more focused on the RCCS, we will continue by decomposing $FR_{322}$, as follows:

$$\begin{Bmatrix} FR_{3221} \\ FR_{3222} \\ FR_{3223} \\ FR_{3224} \\ FR_{3225} \\ FR_{3226} \\ FR_{3227} \end{Bmatrix} = \begin{bmatrix} A_{1,1} & A_{1,2} & A_{1,3} & A_{1,4} & A_{1,5} & A_{1,6} & A_{1,7} \\ A_{2,1} & A_{2,2} & A_{2,3} & A_{2,4} & A_{2,5} & A_{2,6} & A_{2,7} \\ A_{3,1} & A_{3,2} & A_{3,3} & A_{3,4} & A_{3,5} & A_{3,6} & A_{3,7} \\ A_{4,1} & A_{4,2} & A_{4,3} & A_{4,4} & A_{4,5} & A_{4,6} & A_{4,7} \\ A_{5,1} & A_{5,2} & A_{5,3} & A_{5,4} & A_{5,5} & A_{5,6} & A_{5,7} \\ A_{6,1} & A_{6,2} & A_{6,3} & A_{6,4} & A_{6,5} & A_{6,6} & A_{6,7} \\ A_{7,1} & A_{7,2} & A_{7,3} & A_{7,4} & A_{7,5} & A_{7,6} & A_{7,7} \end{bmatrix} \cdot \begin{Bmatrix} DP_{3221} \\ DP_{3222} \\ DP_{3223} \\ DP_{3224} \\ DP_{3225} \\ DP_{3226} \\ DP_{3227} \end{Bmatrix}$$   (Level 3.2.2)

where  $FR_{3221}$: Max air temperature (at riser exit) ($T_{air,exit}$)
       $FR_{3222}$: Max reactor vessel temperature ($T_{rx,max}$)
       $FR_{3223}$: Outlet pressure drop ($\Delta p_o$)
       $FR_{3224}$: Air velocity at riser exit ($v_{air}$)
       $FR_{3225}$: delta Z between inlet and outlet ($z_{in}$-$z_{out}$)
       $FR_{3226}$: Max riser wall termperature (at top of riser) ($T_{wall,max}$)
       $FR_{3227}$: Outlet length of cooling system ($L_{out}$)
by     $DP_{3221}$: Riser width ($W_r$)
       $DP_{3222}$: Riser depth ($D_r$)
       $DP_{3223}$: Number of risers ($n_r$)
       $DP_{3224}$: Riser height ($H_r$)
       $DP_{3225}$: Inlet delta z ($Z_{in}$)
       $DP_{3226}$: Oulet flow area ($A_{out}$)
       $DP_{3227}$: Inlet length ($L_{in}$)

At this point, the decomposition is at a point where we can begin to populate the matrix with actual numbers, rather than just X's. A system model is required to complete

the population of the design matrix. Refer to section 4.3 for the details on the populated matrix.

A breakdown of $FR_{321}$ was not performed due to a lack of information on what happens within the reactor core during an emergency shutdown. It is understood that the reactor core power has a decay profile, the power mostly heats the surrounding core for several days, and the RCCS continues to remove a relatively consistent amount of thermal energy during the shutdown. The temperature within the core rises until the decay power drops below the heat removal capability of the RCCS. The core is mostly made of solid graphite, which has a very high heat capacity.

## 4.2.2 Qualitative design matrix results

A final step in the decomposition of the RCCS is the development of a master matrix, which allows the user to identify interactions between FR's and DP's that exist at different levels of the decomposition (Figure 13). The master matrix shows that except for the coupling that may exist within the cooling system at level 3.2.2, there is no additional coupling. This is a result of the system having a very modular design, and indicates that at a high level the system maintains good functional independence, according to Axiom 1.

It is not necessary to further decompose $FR_{311}$, $FR_{312}$, $FR_{313}$, or their corresponding DPs, because each FR is completely satisfied by its corresponding DP. Each of these could be written as a true/false statement, where true=1 and false=0, and all of the X's on the diagonals would be replaced by a 1.

| | | | DP3: Reactor cavity cooling system | | | | | | | | | | |
| | | | DP3.1 | | | DP3.2 | | | | | | | |
| | | | | | | | DP3.2.2 | | | | | | |
| | | | Four inlets and oulets for natural circulation | Orientation of inlets and outlets | Completely passive system | Conductive Hx through core | Riser Width | Riser Depth | Number of Risers | Riser Height | Inlet Delta z | Outlet Area | Inlet Length |
| FR3: Maintain temp during emergency | FR3.1 | Allow operation when inlets or oulets are partially blocked | 1 | 0 | 0 | 0 | 0 | 0 | 0 | 0 | 0 | 0 | 0 |
| | | Insensitive to wind direction | 0 | 1 | 0 | 0 | 0 | 0 | 0 | 0 | 0 | 0 | 0 |
| | | Work without outside power | 0 | 0 | 1 | 0 | 0 | 0 | 0 | 0 | 0 | 0 | 0 |
| | FR3.2 / FR3.2.2 | Maximum Fuel temperature < 1450C | 0 | 0 | 0 | X | 0 | 0 | 0 | 0 | 0 | 0 | 0 |
| | | Air exit temperature | 0 | X | 0 | 0 | $A_{1,1}$ | $A_{1,2}$ | $A_{1,3}$ | $A_{1,4}$ | $A_{1,5}$ | $A_{1,6}$ | $A_{1,7}$ |
| | | Maximum Reactor Temperature | 0 | X | 0 | 0 | $A_{2,1}$ | $A_{2,2}$ | $A_{2,3}$ | $A_{2,4}$ | $A_{2,5}$ | $A_{2,6}$ | $A_{2,7}$ |
| | | Outlet pressure drop | 0 | X | 0 | 0 | $A_{3,1}$ | $A_{3,2}$ | $A_{3,3}$ | $A_{3,4}$ | $A_{3,5}$ | $A_{3,6}$ | $A_{3,7}$ |
| | | Air velocity in riser | 0 | X | 0 | 0 | $A_{4,1}$ | $A_{4,2}$ | $A_{4,3}$ | $A_{4,4}$ | $A_{4,5}$ | $A_{4,6}$ | $A_{4,7}$ |
| | | Delta z between inlet and outlet | 0 | 0 | 0 | 0 | $A_{5,1}$ | $A_{5,2}$ | $A_{5,3}$ | $A_{5,4}$ | $A_{5,5}$ | $A_{5,6}$ | $A_{5,7}$ |
| | | Maximum riser wall temperature | 0 | X | 0 | 0 | $A_{6,1}$ | $A_{6,2}$ | $A_{6,3}$ | $A_{6,4}$ | $A_{6,5}$ | $A_{6,6}$ | $A_{6,7}$ |
| | | Outlet Length | 0 | 0 | 0 | 0 | $A_{7,1}$ | $A_{7,2}$ | $A_{7,3}$ | $A_{7,4}$ | $A_{7,5}$ | $A_{7,6}$ | $A_{7,7}$ |

**Figure 13 - RCCS Master Matrix**

## 4.3 SYSTEM CHARACTERIZATION

There are numerous ways to characterize the GT-MHR RCCS, from simple heat transfer approximations to complex CFD simulations. For this work, a one-dimensional heat transfer model was developed to predict temperatures, air velocity, and pressure drops [25-27].

In order to conduct the analysis the following assumptions were made

- One dimensional flow
- Boussinesq approximation is valid
- System operating at steady state
- Both inlet and outlet are at atmospheric pressure
- Constant wall flux over entire area of risers
- Inlet and outlet height were same for buoyancy purposes
- Inlet and outlet length were different for friction purposes
- Inlet and outlet's were considered from and into very large areas
- No intermixing of outlet air and inlet air (implies constraint that the difference in height be sufficient to allow for such)
- Axial heating and heat losses assumed to be zero

## 4.3.1 Governing Equations

### 4.3.1.1 Control Volume Equations

For a control volume that encompasses the entire RCCS, the governing equations are the one-dimensional continuity equation (4.1), momentum conservation (4.2), and the energy equation (4.3).

$$\frac{\partial \rho}{\partial t} + \frac{\partial \rho u}{ds} = 0 \qquad (4.1)$$

$$\frac{\partial \rho u}{\partial t} + \frac{\partial \rho u^2}{\partial x} = \frac{-\partial P}{\partial x} + \rho g_x - \tau_w \frac{P_w}{A} \qquad (4.2)$$

$$\rho c_p \left( \frac{dT}{dt} + u \frac{dT}{ds} \right) = q_w'' \left( \frac{P_h}{A} \right) \qquad (4.3)$$

After applying the assumptions listed above and integrating over a loop, equation (4.4) is developed:

$$\oint \rho g_x \, dx = \oint \tau_w \frac{P_w}{A} \, dx \qquad (4.4)$$

The left side of the equation represents the buoyancy force due that will drive the natural circulation. The right side of the equation is the frictional losses that occur throughout the loop. The loop is divided into regions, shown in Figure 14.
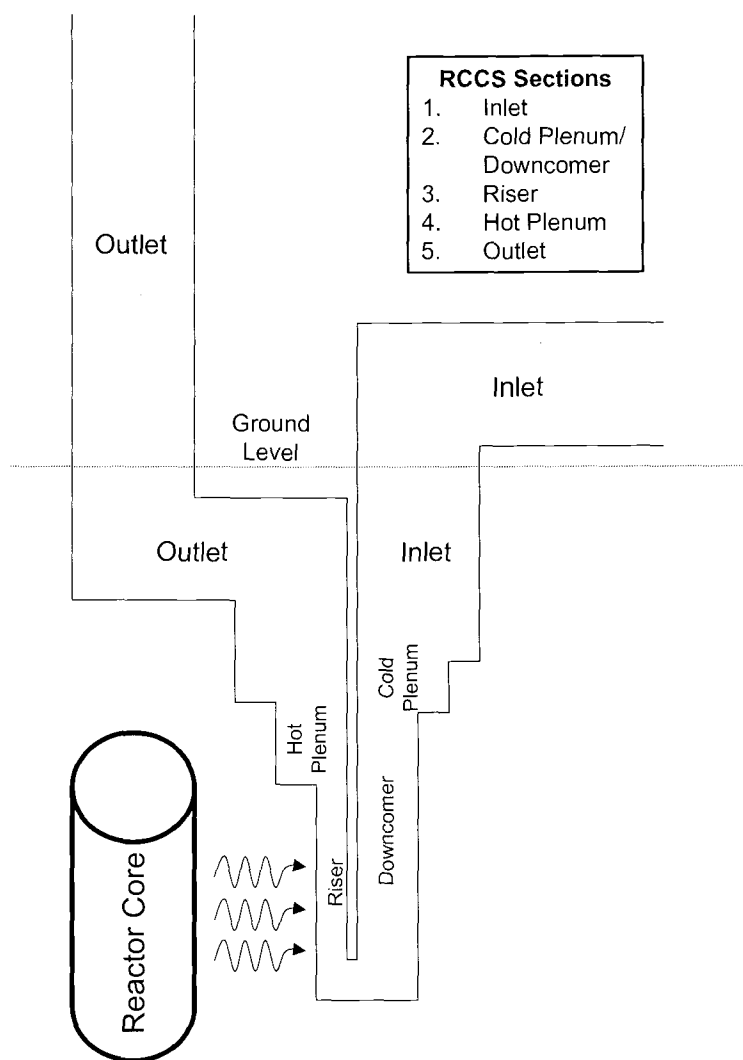


**Figure 14 - RCCS Schematic**

## 4.3.2 Derivation of Velocity Equation

### 4.3.2.1 Energy Equation

To solve the loop integral, additional equations are required. Applying the energy equation to the entire loop [Equation (4.5)], shows that heat only increases in the riser section.

$$\rho\, c_p\left(\frac{dT}{dt}+u\frac{dT}{ds}\right)=\begin{cases} q''_w\left(\dfrac{P_h}{A}\right) & \text{Riser Section} \\ 0 & \text{Downcomer Section} \\ 0 & \text{Exaust Section} \\ 0 & \text{Plenum Section} \end{cases} \tag{4.5}$$

### 4.3.2.2 Frictional Losses

For each section there are both frictional losses due to the shear stress with the wall and form losses. The form losses are due to the gas changing direction, and can be approximated as frictional losses if an equivalent length of pipe is used. Total friction loss per unit area is found by summing losses through all sections (4.6).

$$\rho u_{hot}^2 \sum_i \left(k+\frac{f_D L}{D}\right)\left(\frac{A_{riser}}{A_i}\right)^2 \tag{4.6}$$

Equation (4.7) is a correlation applicable for all frictional losses:

$$\frac{1}{\sqrt{f}}=-3.6\log_{10}\left[\frac{6.9}{Re}+\left(\frac{e}{3.7*D}\right)^{10/9}\right] \tag{4.7}$$

and is accurate to $\pm 1.5\%$ when:

- $10^8 \geq Re \geq 4 \cong 10^4$
- $e/D \# 0.05$ (relative roughness)

The ratio of areas is from the continuity equation, and is valid when there is no change in mass through the system. Also, incompressible flow is assumed for the purpose of mass flow rate balance. Therefore the mass flow rate is constant and the loss equation is simplified allowing relation of all losses to a reference value. Since air velocity in the riser is of primary interest, area and velocity of the riser will be used as reference values.

### 4.3.2.3 Geometry Losses

In equation (4.7), k represents any geometry loss. This model includes any transitions in size or flow direction.

For expansions:

$$k = 0.5\left(1 - \frac{A_{small}}{A_{large}}\right)^{3/4} \tag{4.8a}$$

For contractions:

$$k = \left(1 - \frac{A_{small}}{A_{large}}\right)^{2} \tag{4.8b}$$

The only significant changes in direction are the 10 inlet bends and the 9 exit bends. The number of bends are constraints to plant layout. Equation (4.9) is for square ductwork that undergoes a number (n) of 90E bends:

$$k = 0.99 \cdot n \tag{4.9}$$

As long as the flow area remains constant, it is not necessary to consider each bend as an independent region. All bends within a section may be included within a single term. For this system, the bends were identified as the primary area of energy loss outside of the riser section.

### 4.3.2.4 Buoyancy Forces

To calculate the buoyancy force, the Boussinesq approximation for density as a function of temperature is assumed (4.10). The thermal expansion coefficient is required to account for expansion in the buoyancy terms of the equations.

$$\beta \approx \frac{1}{v_\infty}\left(\frac{v - v_o}{T - T_o}\right) = \rho_o\left(\frac{\dfrac{1}{\rho} - \dfrac{1}{\rho_o}}{T - T_o}\right)$$
$$\rho_o - \rho \approx \rho\beta(T - To)$$
$$\rho = \rho_o(1 - \beta(T - T_o)) \tag{4.10}$$

For steady state conditions, the energy equation becomes:

$$\rho C_p\left(+u\frac{dT}{ds}\right) = q_w^{"}\left(\frac{P_h}{A}\right) \qquad riser\ section \tag{4.11}$$

Applying the Boussinesq approximation (4.10) to the riser section energy equation (4.11) gives:

$$\frac{bouyancy\ force}{area} = \rho_o\beta g H_{center}(T_H - T_o) \tag{4.12}$$

Solving the riser section energy equation (4.11) for $(T_h - T_o)$ and knowing that

$$(q^{"}\xi_r H_{riser}) = \dot{Q} \tag{4.13}$$

allows the buoyancy force to equal frictional losses. This results in the velocity equation (4.14). Unfortunately, velocity and friction loss are functions of each other, cannot be solved in a closed form, and require a numerical method to find a solution.

$$U_o = \left[\frac{\dot{Q} \cdot L_{TH}}{\dfrac{\rho_o A_o C_p}{2 \cdot \beta \cdot g}\displaystyle\sum_{i=1}^{N}\left[\left(\frac{f \cdot L}{D_H}\right) + k\right]\left(\frac{A_o}{A_i}\right)^2}\right]^{1/3} \tag{4.14}$$

## 4.3.3 Derivation of Temperature Equations

### 4.3.3.1  Heat transfer Equation

The energy equation (4.15) for heat transfer to air is:

$$\dot{q} = \dot{m} C_p \Delta T \tag{4.15}$$

where the change in temperature represents the temperature rise along the riser. The mass flow rate is constant throughout, and is easiest calculated with the reference values.

Specific heat, evaluated at the average temperature of maximum temperature and reference temperature will change with changes in velocity. An approximation, derived by regression of table values [27], and valid from 80°F through 1000°F is:

$$C_p = 1.97 \cdot 10^{-8} T^2 + 6.78 \cdot 10^{-6} T + 0.239 \quad \frac{BTU}{lbm \cdot °F} \tag{4.16}$$

### 4.3.3.2  Nusselt correlation for convection to wall from air

Due to the high velocities present within the risers, a Nusselt correlation for forced convection is more accurate than a natural circulation correlation. To calculate the temperature on the inner wall of the riser, the Dittus-Boelter correlation is used:

$$Nu = 0.023 * \text{Re}_D{}^{0.8} \text{Pr}^{0.4} = \frac{hD}{k} \quad \Rightarrow \quad h = \frac{0.023 * \text{Re}_D{}^{0.8} \text{Pr}^{0.4} * k}{D} \tag{4.17}$$

at $T_{ave}$

and valid for:

- Re > 10,000
- 0.7 < Pr < 100
- L/D > 60

After performing calculations for the system, the requirements for the correlation (4.17) were found to be valid. This validates the method for calculating inner wall temperature based on the bulk air temperature profile.

### 4.3.3.3 Conduction through wall

$$\frac{\dot{q}}{A} = h\left(T_{outside} - T_{inside}\right)$$  (4.18)

Equation (4.18) is valid for steady state, one dimensional conduction. The heat transfer coefficient, $h$, is approximated with a quadratic fit of table date [27], in equation (4.19), and is valid over 80°F-1000°F.

$$h_{steel} = -1.05 \cdot 10^{-5} T^2 + 2.93 \cdot 10^{-3} T + 24.6 \quad \frac{BTU}{hr \cdot ft \cdot °F}$$  (4.19)

### 4.3.3.4 Radiative heat transfer from vessel to riser

The following assumptions were made pertaining to radiative heat transfer between the vessel and riser.

- Vessel area is determined by the riser height and the vessel diameter
- Riser surface area is used as heat transfer area
- Both are grey bodies with emmisivity ($\varepsilon$) = 0.8

Because of reflectors within the reactor cavity, the flux is considered constant for the full height of riser and the entire riser area encloses the reactor, for viewing window purposes. For grey bodies, where one encloses the other, the viewing window is calculated as follows:

$$\Im = \frac{1}{\varepsilon_{rx}} + \frac{A_{rx}}{A_{riser}}\left(\frac{1}{\varepsilon_{riser}} - 1\right)$$  (4.20)

Maximum riser temperature is used to be conservative. Applying these assumptions and rearranging the heat transfer equation for radiation, the vessel wall temperature is calculated with equation (4.21).

$$T_{rx} = \left[ \frac{0.9 \cdot \dot{Q}}{A_{riser} \sigma \mathcal{S}} + T_{riser}^{\ 4} \right]^{1/4} \quad in \ {}^\circ R \tag{4.21}$$

## 4.3.4 Calculation of Pressure Drops

From above, the pressure drop equation (4.22) becomes:

$$\Delta p_i = \frac{F_i \rho u^2}{2 g_c} \tag{4.22}$$

Evaluation requires the velocity within each section, where the continuity equation is used to find velocity for each section. Density is a function of temperature within the section, and an approximation, derived by regression from table data [27], is valid from 80EF to 1000EF is:

$$\rho = 4.97 \cdot 10^{-08} T^2 - 1.01 \cdot 10^{-04} T + 0.0789 \quad \frac{lbm}{ft^3} \tag{4.23}$$

## 4.3.5 Solution Spreadsheet

To allow for easy simulation of different system configurations, a large spreadsheet was developed in Microsoft Excel, where each row is a different simulation. On one sheet (Figure 15), the system configuration (DPs) are input in one set of columns and the results (FRs) are listed in another set of columns.

| | Uncoded Input | | | | | | | | Output | | | | | | | |
|---|---|---|---|---|---|---|---|---|---|---|---|---|---|---|---|---|
| Driser | Hriser | Wriser | nRisers | Zin | Inlet length (ft) | Inlet flow area (ft^2) | Aout | | Riser inlet pressure >pi | Riser outlet pressure >po | Riser velocity > vmin | Riser air exit temperature > Texit | Average riser wall temperature | Max riser wall temperature | Rx Vessel Wall Temperature > Tv | Lout |
| 10 | 62.5 | 2 | 292 | 109 | 149 | 120 | 80 | | 1.25E-02 | 2.11E-02 | 40.04427 | 259.5651 | 236 | 311 | 411 | 135.5 |
| 9 | 68.75 | 2.2 | 262.8 | 119.9 | 134.1 | 108 | 88 | | 1.29E-02 | 1.60E-02 | 41.59802 | 268.9162 | 251 | 331 | 441 | 114.35 |
| 9 | 68.75 | 2.2 | 321.2 | 119.9 | 163.9 | 108 | 88 | | 1.82E-02 | 2.32E-02 | 40.25633 | 244.4514 | 227 | 295 | 398 | 144.15 |
| 9 | 68.75 | 1.8 | 321.2 | 119.9 | 134.1 | 108 | 88 | | 1.03E-02 | 1.24E-02 | 38.91967 | 287.8783 | 253 | 342 | 435 | 114.35 |
| 9 | 68.75 | 2.2 | 262.8 | 98.1 | 134.1 | 108 | 72 | | 1.11E-02 | 1.84E-02 | 38.60127 | 281.1908 | 262 | 348 | 453 | 114.35 |
| 11 | 68.75 | 2.2 | 321.2 | 98.1 | 163.9 | 132 | 72 | | 1.65E-02 | 3.89E-02 | 35.95175 | 232.2531 | 217 | 278 | 372 | 144.15 |
| 9 | 68.75 | 1.8 | 262.8 | 98.1 | 134.1 | 132 | 72 | | 4.64E-03 | 9.50E-03 | 36.8521 | 339.2351 | 297 | 412 | 502 | 114.35 |
| 9 | 68.75 | 2.2 | 321.2 | 98.1 | 134.1 | 108 | 88 | | 1.62E-02 | 2.06E-02 | 38.16082 | 251.8045 | 234 | 305 | 405 | 114.35 |
| 11 | 68.75 | 2.2 | 321.2 | 119.9 | 163.9 | 108 | 72 | | 2.37E-02 | 4.23E-02 | 37.37469 | 227.6139 | 213 | 272 | 368 | 144.15 |
| 9 | 68.75 | 2.2 | 262.8 | 119.9 | 163.9 | 108 | 72 | | 1.24E-02 | 2.09E-02 | 40.75498 | 272.1878 | 254 | 335 | 444 | 144.15 |
| 9 | 56.25 | 1.8 | 321.2 | 119.9 | 134.1 | 132 | 88 | | 9.03E-03 | 1.48E-02 | 42.07969 | 274.5861 | 242 | 325 | 422 | 126.85 |
| 11 | 68.75 | 1.8 | 321.2 | 98.1 | 134.1 | 108 | 88 | | 1.36E-02 | 1.70E-02 | 36.36096 | 264.6635 | 234 | 311 | 398 | 114.35 |
| 9 | 56.25 | 2.2 | 321.2 | 98.1 | 163.9 | 108 | 88 | | 1.84E-02 | 2.35E-02 | 40.45731 | 243.786 | 227 | 294 | 397 | 156.65 |
| 11 | 68.75 | 2.2 | 321.2 | 98.1 | 163.9 | 108 | 88 | | 2.29E-02 | 2.97E-02 | 36.63027 | 229.9961 | 215 | 275 | 370 | 144.15 |
| 11 | 68.75 | 2.2 | 321.2 | 119.9 | 134.1 | 108 | 88 | | 2.53E-02 | 3.32E-02 | 38.6758 | 223.6697 | 210 | 267 | 364 | 114.35 |
| 11 | 68.75 | 1.8 | 262.8 | 98.1 | 134.1 | 132 | 88 | | 7.28E-03 | 1.16E-02 | 37.42175 | 293.516 | 259 | 351 | 443 | 114.35 |
| 9 | 68.75 | 1.8 | 321.2 | 98.1 | 163.9 | 108 | 88 | | 9.27E-03 | 1.10E-02 | 36.78894 | 298.1218 | 261 | 355 | 444 | 144.15 |

**Figure 15 - RCCS Model Results Spreadsheet**

An additional two sheets contain the model calculations. The first sheet (Figure 16a-16c) contains all of the physical parameters which describe the system, either variable, constrained, or calculated. The second sheet (Figure 17a-17e) contains all of the intermediate and final calculations required for the system, such as physical parameters (hydraulic diameter, perimeter, etc), dimensionless quantities (Re, Pr, etc.), and results (Temperature, velocity, pressure, etc). For each calculation, such as Reynolds number or air velocity, there are six calculations to account for each section of the system.

Two of the parameters, air velocity in the riser ($V_{air}$) and temperature difference between reactor and riser (dT), cannot be solved in closed form because knowledge of their values are required to find intermediate parameters which are used in solving for the desired value. To work around this, an initial value is guessed for each value, the calculations are performed, and results are developed. If the guess and final value are different, the final value is used as the guess and the process is repeated until there is convergence in the values. Microsoft Excel can automate this process through its iterative calculation routine, shown in Figure 18. Iterative calculations are activated through Tools Menu → Options... → Calculations Tab.

| Riser Depth (ft) | Riser Height (ft) | Riser Width (ft) | Number of risers | Inlet delta z (ft) | inlet length (ft) | inlet flow area (ft^2) | Outlet Flow Area (ft^2) | Area_inlet (ft^2) | Area_entrance_to_plenum (ft^2) | Area_entrance_to_riser (ft^2) | Area_inlet_hot_plenum (ft^2) | Area_entrance_to_exaust (ft^2) | Area_exit_from |
|---|---|---|---|---|---|---|---|---|---|---|---|---|---|
| 1 | 0.71875 | 56.25 | 0.1188 | 262 | 169.6 | 149 | 120 | 72 | 120 | 50 | 22.36 | 50 | 72 | 72 |
| 2 | 0.71875 | 56.25 | 0.1188 | 322 | 169.6 | 149 | 120 | 72 | 120 | 50 | 27.48 | 50 | 72 | 72 |
| 3 | 0.71875 | 56.25 | 0.1188 | 262 | 191.4 | 149 | 120 | 72 | 120 | 50 | 22.36 | 50 | 72 | 72 |
| 4 | 0.71875 | 56.25 | 0.1188 | 322 | 191.4 | 149 | 120 | 72 | 120 | 50 | 27.48 | 50 | 72 | 72 |
| 5 | 0.71875 | 68.75 | 0.1188 | 262 | 169.6 | 149 | 120 | 72 | 120 | 50 | 22.36 | 50 | 72 | 72 |
| 6 | 0.71875 | 68.75 | 0.1188 | 322 | 169.6 | 149 | 120 | 72 | 120 | 50 | 27.48 | 50 | 72 | 72 |
| 7 | 0.71875 | 68.75 | 0.1188 | 262 | 191.4 | 149 | 120 | 72 | 120 | 50 | 22.36 | 50 | 72 | 72 |
| 8 | 0.71875 | 68.75 | 0.1188 | 322 | 191.4 | 149 | 120 | 72 | 120 | 50 | 27.48 | 50 | 72 | 72 |
| 9 | 0.88542 | 56.25 | 0.1188 | 262 | 169.6 | 149 | 120 | 72 | 120 | 50 | 27.55 | 50 | 72 | 72 |
| 10 | 0.88542 | 56.25 | 0.1188 | 322 | 169.6 | 149 | 120 | 72 | 120 | 50 | 33.86 | 50 | 72 | 72 |
| 11 | 0.88542 | 56.25 | 0.1188 | 262 | 191.4 | 149 | 120 | 72 | 120 | 50 | 27.55 | 50 | 72 | 72 |
| 12 | 0.88542 | 56.25 | 0.1188 | 322 | 191.4 | 149 | 120 | 72 | 120 | 50 | 33.86 | 50 | 72 | 72 |
| 13 | 0.88542 | 68.75 | 0.1188 | 262 | 169.6 | 149 | 120 | 72 | 120 | 50 | 27.55 | 50 | 72 | 72 |
| 14 | 0.88542 | 68.75 | 0.1188 | 322 | 169.6 | 149 | 120 | 72 | 120 | 50 | 33.86 | 50 | 72 | 72 |
| 15 | 0.88542 | 68.75 | 0.1188 | 262 | 191.4 | 149 | 120 | 72 | 120 | 50 | 27.55 | 50 | 72 | 72 |

**Figure 16a - Calculation Sheet 1**

| ...exaust (ft^2) | Width_inlet (ft) | Width_entrance_to_plenum (ft) | Width_entrance_to_riser_Total (ft) | Width_inlet_hot_plenum (ft) | Width_entrance_to_exaust (ft) | Width_exit_from_exaust (ft) | Depth_inlet (ft) | Depth_entrance_to_plenum (ft) | Depth_entrance_to_riser (ft) | Depth_inlet_hot_plenum (ft) | Depth_entrance_to_exaust (ft) | Depth_exit_from_exaust (ft) | Length_inlet (ft) | Length_entrance_to_plenum (ft) | Length_riser (ft) | Length_plenum (ft) | Length_exaust (ft) | Leng |
|---|---|---|---|---|---|---|---|---|---|---|---|---|---|---|---|---|---|---|
| 9.798 | 0.5 | 31.11 | 0.5 | 6 | 6 | 9.798 | 100 | 0.71875 | 100 | 6 | 6 | 149 | 22.5 | 56.25 | 22.5 | 141.8 | 0 | |
| 9.798 | 0.5 | 38.24 | 0.5 | 6 | 6 | 9.798 | 100 | 0.71875 | 100 | 6 | 6 | 149 | 22.5 | 56.25 | 22.5 | 141.8 | 0 | |
| 9.798 | 0.5 | 31.11 | 0.5 | 6 | 6 | 9.798 | 100 | 0.71875 | 100 | 6 | 6 | 149 | 22.5 | 56.25 | 22.5 | 141.8 | 0 | |
| 9.798 | 0.5 | 38.24 | 0.5 | 6 | 6 | 9.798 | 100 | 0.71875 | 100 | 6 | 6 | 149 | 22.5 | 68.75 | 22.5 | 129.3 | 0 | |
| 9.798 | 0.5 | 31.11 | 0.5 | 6 | 6 | 9.798 | 100 | 0.71875 | 100 | 6 | 6 | 149 | 22.5 | 68.75 | 22.5 | 129.3 | 0 | |
| 9.798 | 0.5 | 38.24 | 0.5 | 6 | 6 | 9.798 | 100 | 0.71875 | 100 | 6 | 6 | 149 | 22.5 | 68.75 | 22.5 | 129.3 | 0 | |
| 9.798 | 0.5 | 31.11 | 0.5 | 6 | 6 | 9.798 | 100 | 0.71875 | 100 | 6 | 6 | 149 | 22.5 | 68.75 | 22.5 | 129.3 | 0 | |
| 9.798 | 0.5 | 38.24 | 0.5 | 6 | 6 | 9.798 | 100 | 0.88542 | 100 | 6 | 6 | 149 | 22.5 | 56.25 | 22.5 | 141.8 | 0 | |
| 9.798 | 0.5 | 31.11 | 0.5 | 6 | 6 | 9.798 | 100 | 0.88542 | 100 | 6 | 6 | 149 | 22.5 | 56.25 | 22.5 | 141.8 | 0 | |
| 9.798 | 0.5 | 38.24 | 0.5 | 6 | 6 | 9.798 | 100 | 0.88542 | 100 | 6 | 6 | 149 | 22.5 | 56.25 | 22.5 | 141.8 | 0 | |
| 9.798 | 0.5 | 31.11 | 0.5 | 6 | 6 | 9.798 | 100 | 0.88542 | 100 | 6 | 6 | 149 | 22.5 | 68.75 | 22.5 | 129.3 | 0 | |
| 9.798 | 0.5 | 38.24 | 0.5 | 6 | 6 | 9.798 | 100 | 0.88542 | 100 | 6 | 6 | 149 | 22.5 | 68.75 | 22.5 | 129.3 | 0 | |
| 9.798 | 0.5 | 31.11 | 0.5 | 6 | 6 | 9.798 | 100 | 0.88542 | 100 | 6 | 6 | 149 | 22.5 | 68.75 | 22.5 | 129.3 | 0 | |

**Figure 16b – Calculation Sheet 1 (cont.)**

| ...exit_from_exaust (ft) | Temperature_Inlet (F) | Number of Inlet Bends | Number of Exit Bends | Area_Cold_Plenum (ft^2) | Area_Hot_Plenum (ft^2) | Thickness_Riser (ft) | Emissivity_Stainless_steel | Emmisivity_Rx_Vessel | Z_exaust-Z_inlet (ft) | Delta_Z_inlet (ft) |
|---|---|---|---|---|---|---|---|---|---|---|
| | 110 | 10 | 9 | 50 | 50 | 1/64 | 4/5 | 4/5 | 71.5 | 98.1 |
| | 110 | 10 | 9 | 50 | 50 | 1/64 | 4/5 | 4/5 | 71.5 | 98.1 |
| | 110 | 10 | 9 | 50 | 50 | 1/64 | 4/5 | 4/5 | 71.5 | 119.9 |
| | 110 | 10 | 9 | 50 | 50 | 1/64 | 4/5 | 4/5 | 71.5 | 119.9 |
| | 110 | 10 | 9 | 50 | 50 | 1/64 | 4/5 | 4/5 | 71.5 | 98.1 |
| | 110 | 10 | 9 | 50 | 50 | 1/64 | 4/5 | 4/5 | 71.5 | 98.1 |
| | 110 | 10 | 9 | 50 | 50 | 1/64 | 4/5 | 4/5 | 71.5 | 119.9 |
| | 110 | 10 | 9 | 50 | 50 | 1/64 | 4/5 | 4/5 | 71.5 | 119.9 |
| | 110 | 10 | 9 | 50 | 50 | 1/64 | 4/5 | 4/5 | 71.5 | 98.1 |
| | 110 | 10 | 9 | 50 | 50 | 1/64 | 4/5 | 4/5 | 71.5 | 98.1 |
| | 110 | 10 | 9 | 50 | 50 | 1/64 | 4/5 | 4/5 | 71.5 | 119.9 |
| | 110 | 10 | 9 | 50 | 50 | 1/64 | 4/5 | 4/5 | 71.5 | 119.9 |
| | 110 | 10 | 9 | 50 | 50 | 1/64 | 4/5 | 4/5 | 71.5 | 98.1 |

**Figure 16c – Calculation Sheet 1 (cont.)**

**Figure 17a - Calculation Sheet 2**

| # | V_riser_guess_iterated | V_Calculated | Pw_inlet (ft) | Pw_plenum (ft) | Pw_riser (ft) | P_whot_plenum (ft) | Pw_exaust (ft) | Pw_exaust (ft) | Db_inlet (ft) | Db_plenum (ft) | Db_riser (ft) | Db_hot_plenum (ft) | Db_exaust (ft) | Db_exaust (ft) | Temperature_inlet (F) | Temperature_plenum (F) | Temperature_riser (F) | Temperature_hot_plenum | Temperature_exaust | Temperature_exaust |
|---|---|---|---|---|---|---|---|---|---|---|---|---|---|---|---|---|---|---|---|---|
| 1 | 39.72 | 39.72 | 126 | 201 | 439 | 201 | 48 | 48 | 3.8 | 1 | 0.2 | 1 | 6 | 6 | 110 | 110 | 323 | 323 | 323 | 323 |
| 2 | 39.03 | 39.03 | 126 | 201 | 539 | 201 | 48 | 48 | 3.8 | 1 | 0.2 | 1 | 6 | 6 | 110 | 110 | 287 | 287 | 287 | 287 |
| 3 | 41.92 | 41.92 | 126 | 201 | 439 | 201 | 48 | 48 | 3.8 | 1 | 0.2 | 1 | 6 | 6 | 110 | 110 | 312 | 312 | 312 | 312 |
| 4 | 41.16 | 41.16 | 126 | 201 | 539 | 201 | 48 | 48 | 3.8 | 1 | 0.2 | 1 | 6 | 6 | 110 | 110 | 278 | 278 | 278 | 278 |
| 5 | 36.77 | 36.77 | 126 | 201 | 439 | 201 | 48 | 48 | 3.8 | 1 | 0.2 | 1 | 6 | 6 | 110 | 110 | 340 | 340 | 340 | 340 |
| 6 | 36.37 | 36.37 | 126 | 201 | 539 | 201 | 48 | 48 | 3.8 | 1 | 0.2 | 1 | 6 | 6 | 110 | 110 | 300 | 300 | 300 | 300 |
| 7 | 38.93 | 38.93 | 126 | 201 | 439 | 201 | 48 | 48 | 3.8 | 1 | 0.2 | 1 | 6 | 6 | 110 | 110 | 328 | 328 | 328 | 328 |
| 8 | 38.46 | 38.46 | 126 | 201 | 539 | 201 | 48 | 48 | 3.8 | 1 | 0.2 | 1 | 6 | 6 | 110 | 110 | 290 | 290 | 290 | 290 |
| 9 | 39.37 | 39.37 | 126 | 201 | 526 | 201 | 48 | 48 | 3.8 | 1 | 0.21 | 1 | 6 | 6 | 110 | 110 | 285 | 285 | 285 | 285 |
| 10 | 38.08 | 38.08 | 126 | 201 | 647 | 201 | 48 | 48 | 3.8 | 1 | 0.21 | 1 | 6 | 6 | 110 | 110 | 257 | 257 | 257 | 257 |
| 11 | 41.51 | 41.51 | 126 | 201 | 526 | 201 | 48 | 48 | 3.8 | 1 | 0.21 | 1 | 6 | 6 | 110 | 110 | 276 | 276 | 276 | 276 |
| 12 | 40.12 | 40.12 | 126 | 201 | 647 | 201 | 48 | 48 | 3.8 | 1 | 0.21 | 1 | 6 | 6 | 110 | 110 | 250 | 250 | 250 | 250 |
| 13 | 36.71 | 36.71 | 126 | 201 | 526 | 201 | 48 | 48 | 3.8 | 1 | 0.21 | 1 | 6 | 6 | 110 | 110 | 298 | 298 | 298 | 298 |
| 14 | 35.76 | 35.76 | 126 | 201 | 647 | 201 | 48 | 48 | 3.8 | 1 | 0.21 | 1 | 6 | 6 | 110 | 110 | 267 | 267 | 267 | 267 |
| 15 | 38.81 | 38.81 | 126 | 201 | 526 | 201 | 48 | 48 | 3.8 | 1 | 0.21 | 1 | 6 | 6 | 110 | 110 | 288 | 288 | 288 | 288 |



**Figure 17b – Calculation Sheet 2 (Cont.)**

| Visc_inlet | Visc_plenum | Visc_riser | Visc_hot_plenum | Visc_exaust | Visc_exaust | Re_d_inlet | Re_d_plenum | Re_d_riser | Re_d_hot_plenum | Re_d_exaust | Re_d_exaust | f_inlet+Bends | f_plenum | f_riser | f_hot_plenum | f_exaust | f_exaust |
|---|---|---|---|---|---|---|---|---|---|---|---|---|---|---|---|---|---|
| 1.86E-04 | 1.86E-04 | 3.23E-04 | 3.23E-04 | 3.23E-04 | 3.23E-04 | 8.09E+05 | 2.12E+05 | 2.51E+04 | 1.22E+05 | 7.38E+05 | 7.38E+05 | 1.33E-02 | 1.74E-02 | 2.75E-02 | 1.87E-02 | 1.30E-02 | 1.30E-02 |
| 1.86E-04 | 1.86E-04 | 2.98E-04 | 2.98E-04 | 2.98E-04 | 2.98E-04 | 7.95E+05 | 2.08E+05 | 2.67E+04 | 1.30E+05 | 7.86E+05 | 7.86E+05 | 1.33E-02 | 1.74E-02 | 2.72E-02 | 1.85E-02 | 1.29E-02 | 1.29E-02 |
| 1.86E-04 | 1.86E-04 | 3.15E-04 | 3.15E-04 | 3.15E-04 | 3.15E-04 | 8.54E+05 | 2.24E+05 | 2.71E+04 | 1.32E+05 | 7.98E+05 | 7.98E+05 | 1.32E-02 | 1.73E-02 | 2.71E-02 | 1.85E-02 | 1.29E-02 | 1.29E-02 |
| 1.86E-04 | 1.86E-04 | 2.92E-04 | 2.92E-04 | 2.92E-04 | 2.92E-04 | 8.39E+05 | 2.20E+05 | 2.87E+04 | 1.40E+05 | 8.46E+05 | 8.46E+05 | 1.32E-02 | 1.73E-02 | 2.69E-02 | 1.83E-02 | 1.28E-02 | 1.28E-02 |
| 1.86E-04 | 1.86E-04 | 3.35E-04 | 3.35E-04 | 3.35E-04 | 3.35E-04 | 7.49E+05 | 1.96E+05 | 2.24E+04 | 1.09E+05 | 6.59E+05 | 6.59E+05 | 1.34E-02 | 1.76E-02 | 2.80E-02 | 1.90E-02 | 1.32E-02 | 1.32E-02 |
| 1.86E-04 | 1.86E-04 | 3.07E-04 | 3.07E-04 | 3.07E-04 | 3.07E-04 | 7.41E+05 | 1.94E+05 | 2.42E+04 | 1.18E+05 | 7.11E+05 | 7.11E+05 | 1.34E-02 | 1.76E-02 | 2.76E-02 | 1.88E-02 | 1.31E-02 | 1.31E-02 |
| 1.86E-04 | 1.86E-04 | 3.26E-04 | 3.26E-04 | 3.26E-04 | 3.26E-04 | 7.93E+05 | 2.08E+05 | 2.43E+04 | 1.19E+05 | 7.17E+05 | 7.17E+05 | 1.33E-02 | 1.75E-02 | 2.76E-02 | 1.87E-02 | 1.30E-02 | 1.30E-02 |
| 1.86E-04 | 1.86E-04 | 3.00E-04 | 3.00E-04 | 3.00E-04 | 3.00E-04 | 7.84E+05 | 2.05E+05 | 2.61E+04 | 1.28E+05 | 7.70E+05 | 7.70E+05 | 1.33E-02 | 1.75E-02 | 2.73E-02 | 1.85E-02 | 1.29E-02 | 1.29E-02 |
| 1.86E-04 | 1.86E-04 | 2.97E-04 | 2.97E-04 | 2.97E-04 | 2.97E-04 | 8.02E+05 | 2.10E+05 | 2.78E+04 | 1.32E+05 | 7.96E+05 | 7.96E+05 | 1.33E-02 | 1.74E-02 | 2.69E-02 | 1.85E-02 | 1.29E-02 | 1.29E-02 |
| 1.86E-04 | 1.86E-04 | 2.78E-04 | 2.78E-04 | 2.78E-04 | 2.78E-04 | 7.76E+05 | 2.03E+05 | 2.87E+04 | 1.36E+05 | 8.21E+05 | 8.21E+05 | 1.32E-02 | 1.73E-02 | 2.68E-02 | 1.84E-02 | 1.28E-02 | 1.28E-02 |
| 1.86E-04 | 1.86E-04 | 2.91E-04 | 2.91E-04 | 2.91E-04 | 2.91E-04 | 8.46E+05 | 2.22E+05 | 2.99E+04 | 1.42E+05 | 8.57E+05 | 8.57E+05 | 1.32E-02 | 1.73E-02 | 2.66E-02 | 1.83E-02 | 1.28E-02 | 1.28E-02 |
| 1.86E-04 | 1.86E-04 | 2.73E-04 | 2.73E-04 | 2.73E-04 | 2.73E-04 | 8.17E+05 | 2.14E+05 | 3.07E+04 | 1.46E+05 | 8.81E+05 | 8.81E+05 | 1.33E-02 | 1.74E-02 | 2.65E-02 | 1.82E-02 | 1.27E-02 | 1.27E-02 |
| 1.86E-04 | 1.86E-04 | 3.05E-04 | 3.05E-04 | 3.05E-04 | 3.05E-04 | 7.48E+05 | 1.96E+05 | 2.52E+04 | 1.20E+05 | 7.22E+05 | 7.22E+05 | 1.34E-02 | 1.76E-02 | 2.74E-02 | 1.87E-02 | 1.30E-02 | 1.30E-02 |



**Figure 17c – Calculation Sheet 2 (Cont.)**

| K_inlet+Bends | K_plenum | K_riser | K_hot_plenum | K_exaust | K_exaust | A_riser/A_inlet | A_riser/A_plenum | A_riser/A_riser | A_riser/A_hot_plenum | A_riser/A_exaust | A_riser/A_exaust | inlet | Plenum | riser | hot_plenum | exaust |
|---|---|---|---|---|---|---|---|---|---|---|---|---|---|---|---|---|
| 1.04E+01 | 3.34E-01 | 4.99E-01 | 9.97E-01 | 9.06E+00 | 1.00E+00 | 1.86E-01 | 4.47E-01 | 1.00E+00 | 4.47E-01 | 3.11E-01 | 3.11E-01 | 3.79E-01 | 1.46E-01 | 8.08E+00 | 2.84E-01 | 9.04E-01 |
| 1.04E+01 | 3.34E-01 | 4.99E-01 | 9.97E-01 | 9.06E+00 | 1.00E+00 | 2.29E-01 | 5.50E-01 | 1.00E+00 | 5.50E-01 | 3.82E-01 | 3.82E-01 | 5.73E-01 | 2.20E-01 | 8.00E+00 | 4.27E-01 | 1.36E+00 |
| 1.04E+01 | 3.34E-01 | 4.99E-01 | 9.97E-01 | 9.06E+00 | 1.00E+00 | 1.86E-01 | 4.47E-01 | 1.00E+00 | 4.47E-01 | 3.11E-01 | 3.11E-01 | 3.79E-01 | 1.45E-01 | 7.99E+00 | 2.83E-01 | 9.03E-01 |
| 1.04E+01 | 3.34E-01 | 4.99E-01 | 9.97E-01 | 9.06E+00 | 1.00E+00 | 2.29E-01 | 5.50E-01 | 1.00E+00 | 5.50E-01 | 3.82E-01 | 3.82E-01 | 5.73E-01 | 2.19E-01 | 7.92E+00 | 4.26E-01 | 1.36E+00 |
| 1.04E+01 | 3.34E-01 | 4.99E-01 | 9.97E-01 | 9.06E+00 | 1.00E+00 | 1.86E-01 | 4.47E-01 | 1.00E+00 | 4.47E-01 | 3.11E-01 | 3.11E-01 | 3.79E-01 | 1.46E-01 | 9.94E+00 | 2.85E-01 | 9.01E-01 |
| 1.04E+01 | 3.34E-01 | 4.99E-01 | 9.97E-01 | 9.06E+00 | 1.00E+00 | 2.29E-01 | 5.50E-01 | 1.00E+00 | 5.50E-01 | 3.82E-01 | 3.82E-01 | 5.73E-01 | 2.21E-01 | 9.82E+00 | 4.29E-01 | 1.36E+00 |
| 1.04E+01 | 3.34E-01 | 4.99E-01 | 9.97E-01 | 9.06E+00 | 1.00E+00 | 1.86E-01 | 4.47E-01 | 1.00E+00 | 4.47E-01 | 3.11E-01 | 3.11E-01 | 3.79E-01 | 1.46E-01 | 9.81E+00 | 2.84E-01 | 9.01E-01 |
| 1.04E+01 | 3.34E-01 | 4.99E-01 | 9.97E-01 | 9.06E+00 | 1.00E+00 | 2.29E-01 | 5.50E-01 | 1.00E+00 | 5.50E-01 | 3.82E-01 | 3.82E-01 | 5.73E-01 | 2.20E-01 | 9.70E+00 | 4.28E-01 | 1.36E+00 |
| 1.04E+01 | 3.34E-01 | 4.99E-01 | 9.96E-01 | 9.06E+00 | 1.00E+00 | 2.30E-01 | 5.51E-01 | 1.00E+00 | 5.51E-01 | 3.83E-01 | 3.83E-01 | 5.76E-01 | 2.21E-01 | 7.74E+00 | 4.29E-01 | 1.37E+00 |
| 1.04E+01 | 3.34E-01 | 4.99E-01 | 9.96E-01 | 9.06E+00 | 1.00E+00 | 2.82E-01 | 6.77E-01 | 1.00E+00 | 6.77E-01 | 4.70E-01 | 4.70E-01 | 8.69E-01 | 3.34E-01 | 7.70E+00 | 6.47E-01 | 2.07E+00 |
| 1.04E+01 | 3.34E-01 | 4.99E-01 | 9.96E-01 | 9.06E+00 | 1.00E+00 | 2.30E-01 | 5.51E-01 | 1.00E+00 | 5.51E-01 | 3.83E-01 | 3.83E-01 | 5.75E-01 | 2.20E-01 | 7.66E+00 | 4.28E-01 | 1.37E+00 |
| 1.04E+01 | 3.34E-01 | 4.99E-01 | 9.96E-01 | 9.06E+00 | 1.00E+00 | 2.82E-01 | 6.77E-01 | 1.00E+00 | 6.77E-01 | 4.70E-01 | 4.70E-01 | 8.69E-01 | 3.33E-01 | 7.63E+00 | 6.45E-01 | 2.07E+00 |
| 1.04E+01 | 3.34E-01 | 4.99E-01 | 9.96E-01 | 9.06E+00 | 1.00E+00 | 2.30E-01 | 5.51E-01 | 1.00E+00 | 5.51E-01 | 3.83E-01 | 3.83E-01 | 5.76E-01 | 2.22E-01 | 9.48E+00 | 4.31E-01 | 1.37E+00 |
| 1.04E+01 | 3.34E-01 | 4.99E-01 | 9.96E-01 | 9.06E+00 | 1.00E+00 | 2.82E-01 | 6.77E-01 | 1.00E+00 | 6.77E-01 | 4.70E-01 | 4.70E-01 | 8.70E-01 | 3.36E-01 | 9.42E+00 | 6.49E-01 | 2.07E+00 |

| P_delta_inlet (psi) | P_delta_plenum (psi) | P_delta_riser ??? (psi) | P_delta_hot_plenum (psi) | P_delta_exhaust (psi) | P_delta_exhaust (psi) | P_total | Q (BTU/SEC) | Q (W) | Cp_base_on_Tave (Btu/lbm/F) | Density_initial (lbm/ft^3) | Density_ave_riser (lbm/ft^3) | Density_outlet (lbm/ft^3) | Gravity_constant (ft/sec^2) | H_center (ft) | beta_air (1/F) |
|---|---|---|---|---|---|---|---|---|---|---|---|---|---|---|---|
| 4.42E-03 | 1.69E-03 | 8.16E-02 | 2.48E-03 | 7.91E-03 | 8.45E-04 | 9.89E+00 | 3.13E+03 | 3.30E+06 | 0.241 | 0.068 | 0.059 | 0.051 | 32.2 | 141.48 | 0.00149 |
| 6.44E-03 | 2.47E-03 | 8.00E-02 | 3.80E-03 | 1.21E-02 | 1.29E-03 | 1.07E+01 | 3.13E+03 | 3.30E+06 | 0.241 | 0.068 | 0.061 | 0.054 | 32.2 | 141.48 | 0.00153 |
| 4.92E-03 | 1.88E-03 | 9.06E-02 | 2.80E-03 | 8.95E-03 | 9.55E-04 | 9.79E+00 | 3.13E+03 | 3.30E+06 | 0.241 | 0.068 | 0.060 | 0.052 | 32.2 | 163.28 | 0.0015 |
| 7.16E-03 | 2.74E-03 | 8.86E-02 | 4.26E-03 | 1.36E-02 | 1.46E-03 | 1.06E+01 | 3.13E+03 | 3.30E+06 | 0.241 | 0.068 | 0.061 | 0.055 | 32.2 | 163.28 | 0.00154 |
| 3.79E-03 | 1.46E-03 | 8.51E-02 | 2.09E-03 | 6.61E-03 | 7.08E-04 | 1.17E+01 | 3.13E+03 | 3.30E+06 | 0.242 | 0.068 | 0.059 | 0.050 | 32.2 | 135.23 | 0.00147 |
| 5.60E-03 | 2.16E-03 | 8.45E-02 | 3.25E-03 | 1.03E-02 | 1.10E-03 | 1.26E+01 | 3.13E+03 | 3.30E+06 | 0.241 | 0.068 | 0.060 | 0.053 | 32.2 | 135.23 | 0.00152 |
| 4.24E-03 | 1.63E-03 | 9.49E-02 | 2.38E-03 | 7.54E-03 | 8.07E-04 | 1.16E+01 | 3.13E+03 | 3.30E+06 | 0.241 | 0.068 | 0.059 | 0.051 | 32.2 | 157.03 | 0.00148 |
| 6.25E-03 | 2.40E-03 | 9.40E-02 | 3.68E-03 | 1.17E-02 | 1.25E-03 | 1.24E+01 | 3.13E+03 | 3.30E+06 | 0.241 | 0.068 | 0.061 | 0.054 | 32.2 | 157.03 | 0.00153 |
| 6.58E-03 | 2.53E-03 | 7.88E-02 | 3.89E-03 | 1.24E-02 | 1.33E-03 | 1.05E+01 | 3.13E+03 | 3.30E+06 | 0.241 | 0.068 | 0.061 | 0.054 | 32.2 | 141.48 | 0.00153 |
| 9.31E-03 | 3.58E-03 | 7.48E-02 | 5.69E-03 | 1.82E-02 | 1.94E-03 | 1.18E+01 | 3.13E+03 | 3.30E+06 | 0.241 | 0.068 | 0.062 | 0.056 | 32.2 | 141.48 | 0.00157 |
| 7.32E-03 | 2.80E-03 | 8.72E-02 | 4.36E-03 | 1.40E-02 | 1.49E-03 | 1.04E+01 | 3.13E+03 | 3.30E+06 | 0.241 | 0.068 | 0.061 | 0.055 | 32.2 | 163.28 | 0.00155 |
| 1.03E-02 | 3.96E-03 | 8.26E-02 | 6.36E-03 | 2.04E-02 | 2.18E-03 | 1.18E+01 | 3.13E+03 | 3.30E+06 | 0.241 | 0.068 | 0.062 | 0.057 | 32.2 | 163.28 | 0.00158 |
| 5.73E-03 | 2.21E-03 | 8.33E-02 | 3.34E-03 | 1.06E-02 | 1.13E-03 | 1.22E+01 | 3.13E+03 | 3.30E+06 | 0.241 | 0.068 | 0.060 | 0.053 | 32.2 | 135.23 | 0.00152 |
| 8.21E-03 | 3.17E-03 | 8.01E-02 | 4.97E-03 | 1.58E-02 | 1.69E-03 | 1.36E+01 | 3.13E+03 | 3.30E+06 | 0.241 | 0.068 | 0.062 | 0.055 | 32.2 | 135.23 | 0.00156 |

**Figure 17d – Calculation Sheet 2 (Cont.)**

| mass_flow_rate (lbm/sec) | dT_Guess_iterated (F) | dT_Calculated (F) | T_inlet_cold (F) | T_outlet_riser_hot (F) | T_ave_riser_section (F) | Pr_based_on_degrees_F | k_heat_transfer_coefficient (Btu/hr/ft/F) | h_riser_air_from_nusselt (Btu/hr/ft^2/F) | Area_wall_heat_transfer (ft^2) | F_delta_air_inner_wall (F) | T_wall_inner (F) | Riser_Thickness (ft) | k_conductivity_wall_steel (Btu/hr/ft/F) | T_Delta_across_wall (F) | T_wall_outer (F) | T_Wall_outer_max | Boltzmans_Constant (Btu/hr/ft^2/R^4) | T_Vessel_Based_on | F_Viewing |
|---|---|---|---|---|---|---|---|---|---|---|---|---|---|---|---|---|---|---|---|
| 60.7 | 213.5 | 213.5 | 110 | 323.5 | 217 | 0.692 | 0.0189 | 1.692E-03 | 24685 | 74.949 | 292 | 1/64 | 24.7 | 0.288 | 292 | 399 | 1.71E-09 | 501 | 0.77 | 858 |
| 73.4 | 176.9 | 176.9 | 110 | 286.9 | 198 | 0.694 | 0.0184 | 1.731E-03 | 30338 | 59.589 | 258 | 1/64 | 24.8 | 0.234 | 258 | 347 | 1.71E-09 | 446 | 0.78 | 806 |
| 64.1 | 202.3 | 202.3 | 110 | 312.3 | 211 | 0.693 | 0.0188 | 1.786E-03 | 30338 | 70.993 | 282 | 1/64 | 24.8 | 0.288 | 282 | 384 | 1.71E-09 | 491 | 0.77 | 843 |
| 77.4 | 167.8 | 167.8 | 110 | 277.8 | 194 | 0.694 | 0.0183 | 1.824E-03 | 30338 | 56.566 | 250 | 1/64 | 24.8 | 0.234 | 251 | 335 | 1.71E-09 | 438 | 0.78 | 794 |
| 56.2 | 230.4 | 230.4 | 110 | 340.4 | 225 | 0.692 | 0.0192 | 1.565E-03 | 24685 | 81.025 | 306 | 1/64 | 24.7 | 0.288 | 307 | 422 | 1.71E-09 | 519 | 0.77 | 881 |
| 68.4 | 189.8 | 189.8 | 110 | 299.8 | 205 | 0.693 | 0.0186 | 1.614E-03 | 30338 | 63.905 | 269 | 1/64 | 24.7 | 0.288 | 269 | 364 | 1.71E-09 | 459 | 0.77 | 824 |
| 59.5 | 217.7 | 217.7 | 110 | 327.7 | 219 | 0.692 | 0.0190 | 1.658E-03 | 24685 | 76.479 | 295 | 1/64 | 24.7 | 0.288 | 296 | 405 | 1.71E-09 | 506 | 0.77 | 864 |
| 72.3 | 179.6 | 179.6 | 110 | 289.6 | 200 | 0.694 | 0.0184 | 1.706E-03 | 30338 | 60.467 | 260 | 1/64 | 24.8 | 0.234 | 260 | 350 | 1.71E-09 | 449 | 0.77 | 810 |
| 74.2 | 175.0 | 175.0 | 110 | 285.0 | 198 | 0.694 | 0.0184 | 1.737E-03 | 29598 | 60.870 | 258 | 1/64 | 24.8 | 0.240 | 259 | 346 | 1.71E-09 | 448 | 0.78 | 806 |
| 88.2 | 147.3 | 147.3 | 110 | 257.3 | 184 | 0.695 | 0.0180 | 1.744E-03 | 36376 | 49.344 | 233 | 1/64 | 24.8 | 0.195 | 233 | 307 | 1.71E-09 | 403 | 0.78 | 767 |
| 78.2 | 166.1 | 166.1 | 110 | 276.1 | 193 | 0.694 | 0.0182 | 1.830E-03 | 29598 | 57.790 | 251 | 1/64 | 24.8 | 0.240 | 251 | 334 | 1.71E-09 | 440 | 0.78 | 794 |
| 92.9 | 139.9 | 139.9 | 110 | 249.9 | 180 | 0.696 | 0.0179 | 1.833E-03 | 36376 | 46.932 | 227 | 1/64 | 24.8 | 0.195 | 227 | 297 | 1.71E-09 | 396 | 0.78 | 757 |
| 69.2 | 187.6 | 187.6 | 110 | 297.6 | 204 | 0.694 | 0.0185 | 1.621E-03 | 29598 | 65.224 | 269 | 1/64 | 24.8 | 0.240 | 269 | 363 | 1.71E-09 | 461 | 0.77 | 823 |
| 82.8 | 156.8 | 156.8 | 110 | 266.8 | 188 | 0.695 | 0.0181 | 1.641E-03 | 36376 | 52.440 | 241 | 1/64 | 24.8 | 0.195 | 241 | 319 | 1.71E-09 | 412 | 0.78 | 779 |

**Figure 17e – Calculation Sheet 2 (Cont.)**
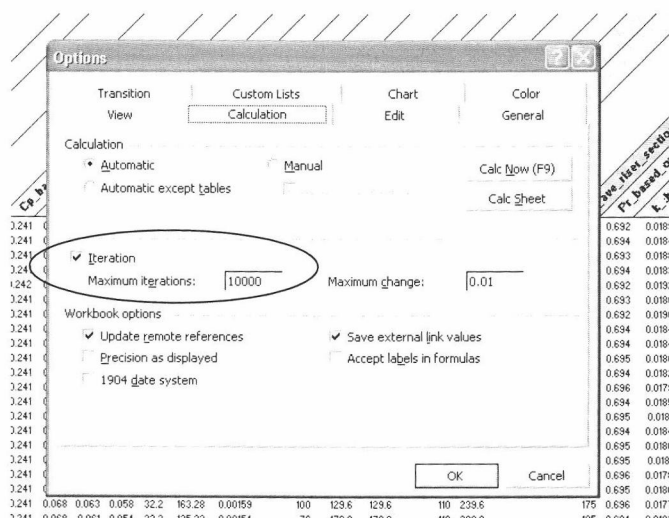


**Figure 18 - MS Excel Iterative Calculations**

## 4.3.6 Comparison to Published Data

General Atomics has published data with the Nuclear Regulatory Commission in applying for licensing [11]. The data developed in the one-dimensional model described above achieves similar results, as shown in Table 2. Even though the air velocity in the riser is slightly higher than that published, it is within 10% and considered sufficient for the remainder of this work.

|  | Quoted from GA | Predicted by model |
|---|---|---|
| Velocity Riser | 11 m/ Sec | 12.2 m/sec |
| Max Riser Air Temp | 300-400 F | 322 F |
| Max outer wall Temp | N/A | 397 F |
| Vessel Max Temp | N/A | 500 F |

**Table 2- Comparison of GA and Modeled Data**

There are several possible causes for the differences that do exist, including the method used in calculating wetted perimeter, the estimated values of relative roughness, the estimated values of emissivity, and other assumptions listed above. Additionally, the selection of elapsed time after a casualty can significantly affect the calculated values.

## 4.4 POPULATE DESIGN MATRICES

Once models are developed that characterize the system, the design matrices, developed in section 4.2 and shown in Figure 13, can be populated with actual values using equations (3.1) and (3.2). Unfortunately, due to the nature of thermal-fluid systems, the required partial derivatives are not easily carried out. In order to populate the design matrices, adequate surrogate models must first be developed. In this study, a sequential DOE and response surface modeling method is adopted and quadratic surrogate models are built due to their better accuracy in predicting non-linear system

behavior. The process used to develop surrogate models and populate the design
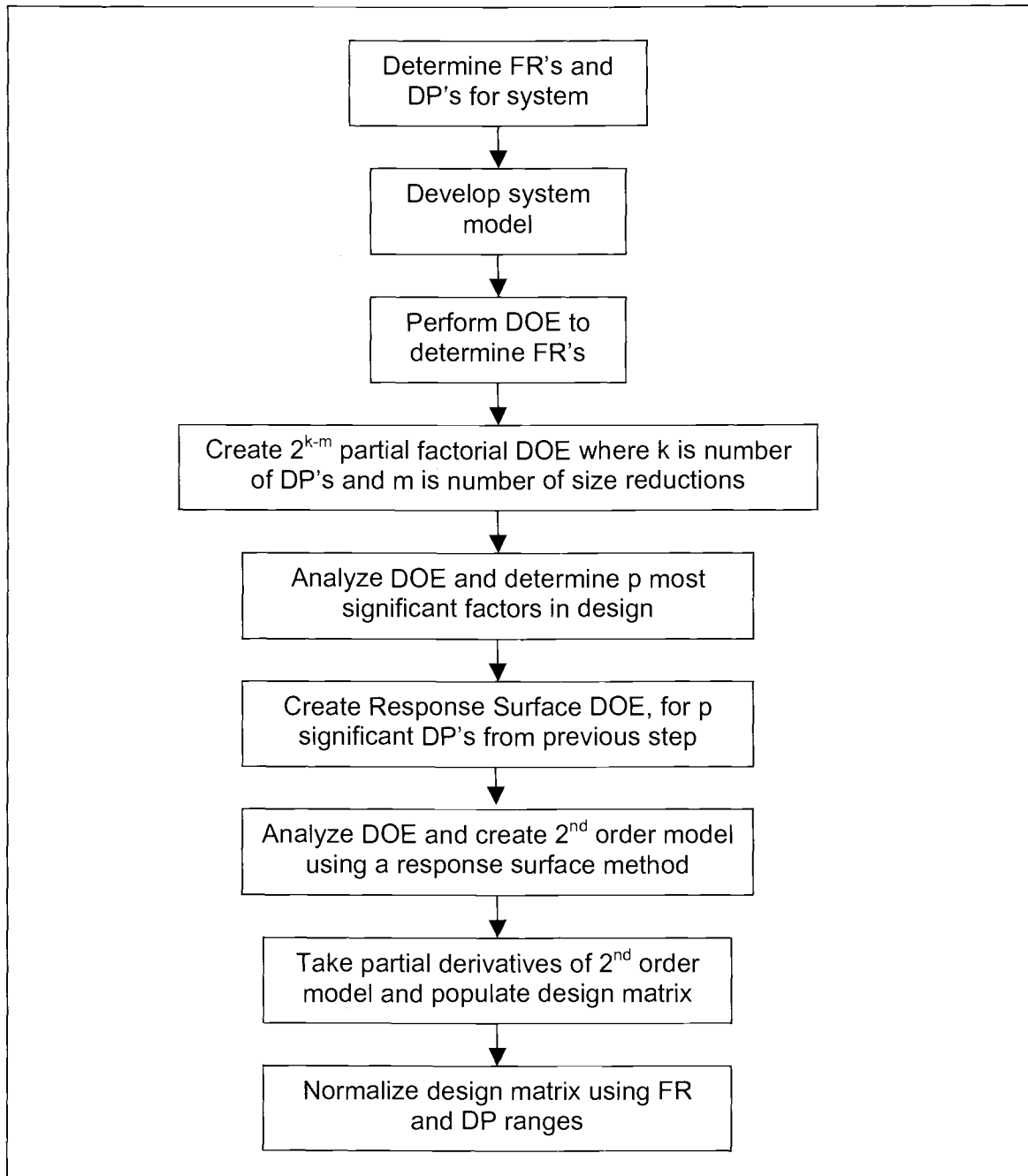
matrices is outlined in Figure 19.



Figure 19 - Sequential DOE and response surface modeling process for
quadratic surrogate model development

## 4.4.1 Surrogate model development

As a first step, a 2-level statistics based DOE is performed to determine which variables are significant. The results are presented in Figure 20 by the order of significance for each factor. The experiment was only analyzed for significance of 1st order terms. The most significant terms overall were carried into the 2nd DOE test. The terms carried forward were $W_r$, $H_r$, $D_r$, $n_r$, $Z_{in}$, and $A_{out}$. $A_{in}$ and $L_{in}$ showed very low or no significance in all cases, indicating that they are not key design variables.

Statistically Significant Variables

| Riser inlet pressure >pi | Riser outlet pressure >po | Riser velocity > vmin | Riser air exit temperature > Texit | Average riser wall temperature | Max riser wall temperature | Rx Vessel Wall Temperature > Tv |
|---|---|---|---|---|---|---|
| Wriser | Wriser | Hriser | Wriser | Wriser | Wriser | nRisers |
| Driser | Driser | Zin | Driser | nRisers | Driser | Driser |
| nRisers | nRisers | nRisers | nRisers | Driser | nRisers | Wriser |
| Ain | Aout | Wriser | Hriser | Hriser | Hriser | Hriser |
| Hriser | Hriser | Aout | Zin | Zin | Zin | Zin |
| Zin | Zin | Driser | Aout | Aout | Aout | Aout |
| Aout | Ain | Ain | Ain | Ain | Ain | Ain |
| Lin | Lin | Lin | Lin | Lin | Lin | Lin |

Extremely statistically significant (t>10)
Statistically significant (2<t<10)
Not statistically significant (p>0.05)

**Figure 20 - 2 factor DOE Results**

Following the 2-level DOE test, a more detailed DOE is performed on the remaining variables. For the purpose of this study, a Box-Behnken design was selected, due to software constraints in Minitab for performing a seven factor DOE. Minitab is used to analyze the data, and any terms with significance p<0.05 are kept in the quadratic model.

Model Coefficients

| | Pout | Vriser | Tair,exit | Triser,max | Trx,max | Lout |
|---|---|---|---|---|---|---|
| Constant | 0.08956 | -23.48 | 2111 | 2535 | 2346 | 49 |
| D | -0.007468 | 3.812 | -92.99 | -122.7 | -109.3 | 0 |
| H | 0.0001959 | -0.7466 | 4.854 | 6.427 | 4.967 | -1 |
| W | -0.04307 | 46.2 | -728.4 | -806.5 | -615.4 | 0 |
| n | -0.000255 | 0.1027 | -2.864 | -3.966 | -3.371 | 0 |
| Zin | -0.0005979 | 0.1768 | -2.066 | -1.521 | -1.805 | 0 |
| Lin | 0 | 0 | 0 | 0 | 0 | 1 |
| Aout | 0.0004754 | -0.03008 | -0.8885 | -0.9345 | -0.9379 | 0 |
| D^2 | 0.00008463 | -0.0681 | 1.74 | 2.315 | 2.169 | 0 |
| H^2 | 0.000002166 | 0.001108 | 0 | 0 | 0 | 0 |
| W^2 | 0.005084 | -7.126 | 91.63 | 101.6 | 76.1 | 0 |
| n^2 | 9.192E-08 | -0.00003711 | 0.001687 | 0.002569 | 0.002544 | 0 |
| Zin^2 | 0 | -0.0002189 | 0.001872 | 0 | 0.002474 | 0 |
| Lin^2 | 0 | 0 | 0 | 0 | 0 | 0 |
| Aout^2 | 0.000005912 | -0.001007 | 0.004215 | 0.006882 | 0.004592 | 0 |
| D*H | -0.00003 | 0.01479 | -0.1175 | -0.14 | -0.12 | 0 |
| D*W | 0.004313 | -1.388 | 14.82 | 18.12 | 14.38 | 0 |
| D*n | 0.00001926 | -0.005133 | 0.06041 | 0.0899 | 0.06849 | 0 |
| D*Zin | 0.00002179 | -0.002012 | 0.03838 | 0.0344 | 0.0344 | 0 |
| D*Lin | 0 | 0 | 0 | 0 | 0 | 0 |
| D*Aout | -0.00005938 | 0.007922 | 0 | 0 | 0 | 0 |
| H*W | -0.0002 | 0.09596 | -0.9292 | -1 | -0.9 | 0 |
| H*n | -8.904E-07 | 0.0004778 | -0.003608 | -0.004795 | -0.00411 | 0 |
| H*Zin | 0 | 0 | 0 | -0.005505 | 0 | 0 |
| H*Lin | 0 | 0 | 0 | 0 | 0 | 0 |
| H*Aout | 0.00000325 | -0.000903 | 0 | 0 | 0 | 0 |
| W*n | 0.000137 | -0.04519 | 0.4674 | 0.5351 | 0.3639 | 0 |
| W*Zin | 0.0001548 | 0 | 0.2842 | 0.2867 | 0.2867 | 0 |
| W*Lin | 0 | 0 | 0 | 0 | 0 | 0 |
| W*Aout | -0.0004219 | 0.07306 | 0 | -0.2344 | 0 | 0 |
| n*Zin | 6.284E-07 | -0.00007899 | 0.001145 | 0.001571 | 0 | 0 |
| n*Lin | 0 | 0 | 0 | 0 | 0 | 0 |
| n*Aout | -0.000001819 | 0.000218 | 0 | 0 | 0 | 0 |
| Zin*Lin | 0 | 0 | 0 | 0 | 0 | 0 |
| Zin*Aout | 0 | 0.000148 | 0 | 0 | 0 | 0 |
| Lin*Aout | 0 | 0 | 0 | 0 | 0 | 0 |

**Figure 21 - 3 factor DOE Results**

Figure 21 presents the results for the $2^{nd}$ DOE that was performed. The DOE was performed in two steps. First, it was run with all terms to determine which terms are significant. Those that were not significant ($p > 0.05$) were not included in the $2^{nd}$ analysis, giving the results shown above, which are quadratic model coefficients.

Once the DOE results are analyzed using response surface methods, surrogate models can be developed for the various performance parameters. Equation (4.24) is an example of the surrogate model developed for maximum riser wall temperature. Equations for the remainder of the system are included as Appendix A.

$$
\begin{aligned}
T_{riser,max} = {} & 2535 - 122.7D_r + 6.427H_r - 806.5W_r - 3.966n_r - 3.966Z_{in} - 0.9345A_{out} \\
& + 2.315D_r^2 + 101.6W_r^2 + 0.002569n_r^2 + 0.006882A_{out}^2 - 0.140D_rH_r + 18.12D_rW_r \quad (4.24) \\
& + 0.0899D_rn_r + 0.0344D_rZ_{in} - 1.00H_rW_r - 0.004795H_rn_r - 0.005505H_rZ_{in} \\
& + 0.5351W_rn_r + 0.2867W_rZ_{in} - 0.2344W_rA_{out} + 0.001571n_rZ_{in}
\end{aligned}
$$

## 4.4.2 Validation of surrogate models

Looking at equation 4.24, it becomes obvious that the terms do not have a physical basis, but are just an approximation for the system. Validation of the assumptions used in creating these equations and the accuracy of the model predictions come from a normal residual plot and residual vs. fitted value plot.
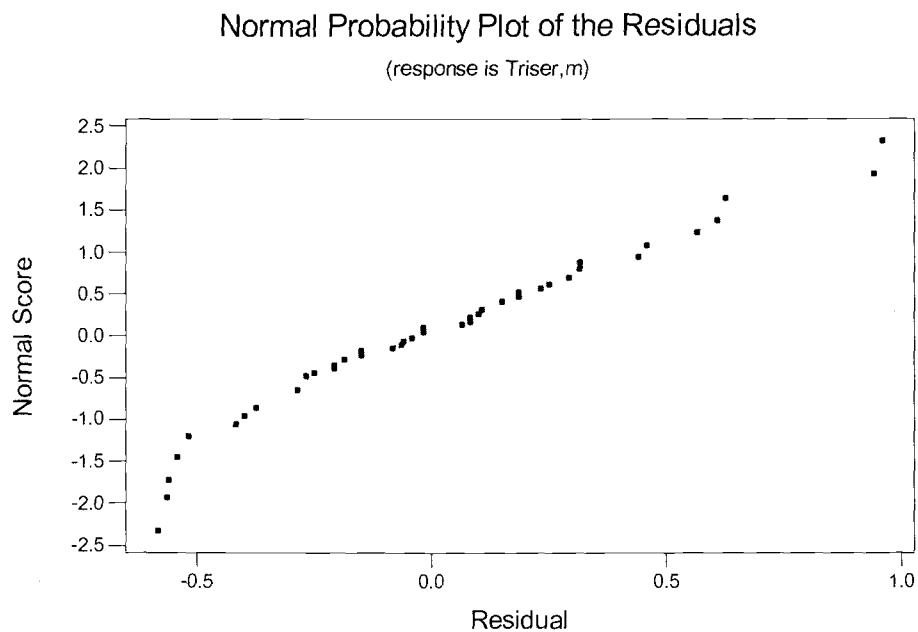


**Normal Probability Plot of the Residuals**
(response is Triser,m)

Figure 22 - Residual Normal Plot - $T_{riser,max}$

## Residuals Versus the Fitted Values
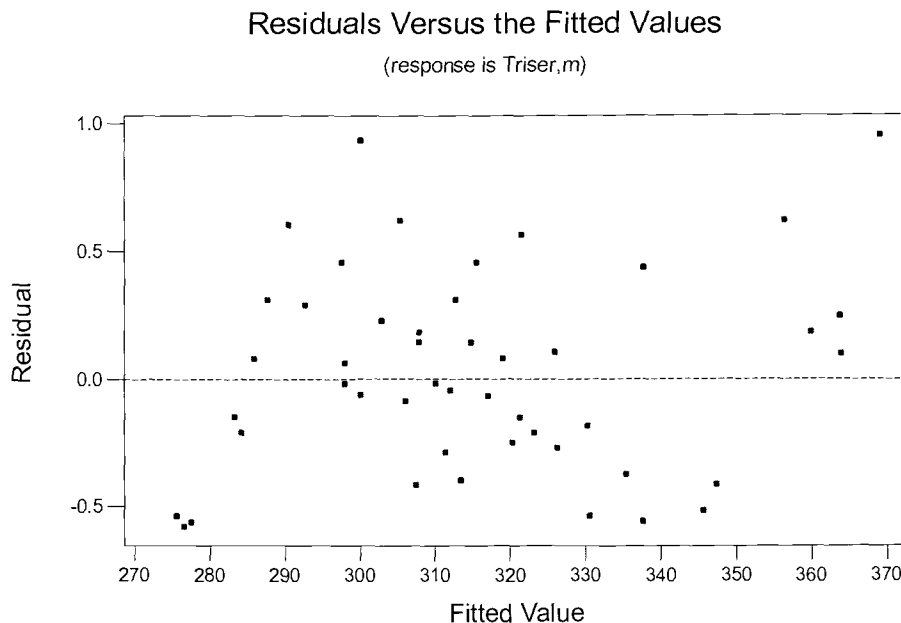
(response is Triser,m)



**Figure 23 - Residuals vs. Fitted Values for $T_{riser,max}$**

As seen in Figure 22 the residuals are normally distributed, indicating that response surface methods should work well. Also, from Figure 23 we see that the surrogate model has a good ability to predict, with the largest error less than 1°F (<0.5%). The same validations exist with the other surrogate models and are shown in Appendix A.

Based on the validation tests, the following variables are selected:

| Variable | Description | UNIT | Current Value |
|---|---|---|---|
| $T_{air,exit}$ | Maximum air temperature (riser exit) | EF | 260 |
| $T_{rx,max}$ | Maximum reactor vessel temperature | EF | 317 |
| $\Delta p_0$ | Outlet pressure drop | psi | 0.0211 |
| $V_{air}$ | Air velocity at riser exit | ft/sec | 40.0 |
| $Z_{in}-Z_{out}$ | delta Z between inlet and outlet | ft | 71.5 |
| $T_{wall,max}$ | Maximum riser wall temperature | EF | 425 |
| $L_{out}$ | Outlet length of cooling system | ft | 135.5 |

**Table 3 - Selected Performance Parameters**

| Variable | Description | UNIT | Design Range |
|---|---|---|---|
| $W_r$ | Riser width | in | 1.8-2.2 |
| $D_r$ | Riser depth | in | 9-11 |
| $n_r$ | Number of risers | - | 262-322 |
| $H_r$ | Riser height | ft | 56-69 |
| $Z_{in}$ | Inlet delta z | ft | 98-120 |
| $A_{out}$ | Outlet flow area | $ft^2$ | 72-88 |
| $L_{in}$ | Inlet length | FT | 134-164 |

**Table 4 - Selected Design Parameters**

## 4.4.3 Using design axioms to populate matrices

Using the surrogate models developed in section 4.4.1 and equation (3.1), the design matrix for Level 3.2.2 and master matrix can be populated with numerical values. Since the surrogate models are all quadratic, the process for taking partial derivatives is trivial. The resulting design matrix is:

$$
\begin{Bmatrix} FR_{3221} \\ FR_{3222} \\ FR_{3223} \\ FR_{3224} \\ FR_{3225} \\ FR_{3226} \\ FR_{3227} \end{Bmatrix} = \begin{bmatrix} -0.805 & -0.543 & -0.496 & 0.185 & -0.156 & -0.066 & 0 \\ -0.418 & -0.509 & -0.518 & 0.117 & -0.092 & -0.040 & 0 \\ 2.971 & 2.023 & 1.855 & -0.717 & 0.590 & -1.319 & 0 \\ 0.123 & -0.121 & -0.160 & -0.314 & 0.266 & 0.115 & 0 \\ 0 & 0 & 0 & 0.833 & -1.453 & 0 & 0 \\ -0.723 & -0.607 & -0.586 & 0.206 & -0.171 & -0.078 & 0 \\ 0 & 0 & 0 & 0 & -1.652 & 0 & 2.258 \end{bmatrix} \cdot \begin{Bmatrix} DP_{3221} \\ DP_{3222} \\ DP_{3223} \\ DP_{3224} \\ DP_{3225} \\ DP_{3226} \\ DP_{3227} \end{Bmatrix}
$$

(Level 3.2.2)

A cursory look at the populated design matrix shows that this is neither a diagonal nor triangular matrix. A closer look reveals that the elements to the right of the diagonal are the same order of magnitude of smaller than the corresponding diagonal element, which indicates that it may be possible to make the matrix more triangular by adjusting the values of the design parameters.

This gives the master design matrix in Figure 24. Cells which are considered "problem" cells have been highlighted. These are cells which are preventing the system from being decoupled. It is noted that even though the outlet area values for air exit temperature and maximum reactor temperature are not zero, they are much smaller than their corresponding diagonal element and are approximately zero.

| | | | | | | | DP3: Reactor cavity cooling system | | | | | | | | |
|---|---|---|---|---|---|---|---|---|---|---|---|---|---|---|---|
| | | | | | | | | | | | DP3.2 | | | | |
| | | | | | DP3.1 | | | | | | | DP3.2.2 | | | |
| | | | Four inlets and oulets for natural circulation | Orientation of inlets and outlets | Completely passive system | Conductive Hx through core | Riser Width | Riser Depth | Number of Risers | Riser Height | Inlet Delta z | Outlet Area | Inlet Length |
| FR3: Maintain temp during emergency | FR3.1 | | Allow operation when inlets or outlets are partially blocked | 1 | 0 | 0 | 0 | 0 | 0 | 0 | 0 | 0 | 0 | 0 |
| | | | Insensitive to wind direction | 0 | 1 | 0 | 0 | 0 | 0 | 0 | 0 | 0 | 0 | 0 |
| | | | Work without outside power | 0 | 0 | 1 | 0 | 0 | 0 | 0 | 0 | 0 | 0 | 0 |
| | FR3.2 | FR3.2.2 | Maximum Fuel temperature < 1450C | 0 | 0 | 0 | X | 0 | 0 | 0 | 0 | 0 | 0 | 0 |
| | | | Air exit temperature | 0 | X | 0 | 0 | -0.805 | -0.543 | -0.496 | 0.1849 | -0.156 | -0.066 | 0 |
| | | | Maximum Reactor Temperature | 0 | X | 0 | 0 | -0.418 | -0.509 | -0.518 | 0.1166 | -0.092 | -0.04 | 0 |
| | | | Outlet pressure drop | 0 | X | 0 | 0 | 2.9715 | 2.0232 | 1.8545 | -0.717 | 0.5904 | -1.319 | 0 |
| | | | Air velocity in riser | 0 | X | 0 | 0 | 0.123 | -0.121 | -0.16 | -0.314 | 0.266 | 0.1149 | 0 |
| | | | Delta z between inlet and outlet | 0 | 0 | 0 | 0 | 0 | 0 | 0 | 0.8333 | -1.453 | 0 | 0 |
| | | | Maximum riser wall temperature | 0 | X | 0 | 0 | -0.723 | -0.607 | -0.586 | 0.2061 | -0.171 | -0.078 | 0 |
| | | | Outlet Length | 0 | 0 | 0 | 0 | 0 | 0 | 0 | 0 | -1.652 | 0 | 2.2576 |

**Figure 24 - Populated RCCS Master Matrix**

The calculation of the partial derivatives was automated using Microsoft Excel. As an example, the calculation of Riser Temperature is shown in Figure 25. A square matrix is created, where the cell value is the coefficient corresponding to the two

parameters shown. The coefficients on the diagonal are doubled. For example, the cell circled, is the intersection of D and W and has a value of 18.12. In evaluating Triser, one term of the equation is 18.12*D*W. The bottom row (sums) is the sum of the product of that column times the design parameter values (not shown). Adding all of these sums together, and dividing by 2 gives the value at that set of design parameters. To find the partial derivative (far right columns) a simple matrix multiplication is required. The row is multiplied by the design parameter column (not shown) using the Excel function *MMULT*.

**Matrix Coefficients**                                                                                   **Partial Derivatives**

| Triser,max = | 308.4015 | | | | | | | | | |
|---|---|---|---|---|---|---|---|---|---|---|
| | Const | W | D | H | Zin | Aout | Lin | nR | | dTriser,max |
| Const | 5070 | -806.5 | -122.7 | 6.427 | -1.521 | -0.9345 | 0 | -3.966 | dW | -109.8658 |
| W | -806.5 | 203.2 | 18.12 | -1 | 0.2867 | -0.2344 | 0 | 0.5351 | dD | -18.5252 |
| D | -122.7 | 18.12 | 4.63 | -0.14 | 0.0344 | 0 | 0 | 0.0899 | dH | 1.02131 |
| H | 6.427 | -1 | -0.14 | 0 | -0.005505 | 0 | 0 | -0.004795 | dZin | -0.475168 |
| Zin | -1.521 | 0.2867 | 0.0344 | -0.005505 | 0 | 0 | 0 | 0.001571 | dAout | -0.30218 |
| Aout | -0.9345 | -0.2344 | 0 | 0 | 0 | 0.013764 | 0 | 0 | dLin | 0 |
| Lin | 0 | 0 | 0 | 0 | 0 | 0 | 0 | 0 | dnR | -0.611394 |
| nR | -3.966 | 0.5351 | 0.0899 | -0.004795 | 0.001571 | 0 | 0 | 0.005138 | | |
| sums | 607.739 | -109.8658 | -92.626 | 30.6393 | -26.13424 | -12.0872 | 0 | -89.263524 | | |

**Figure 25 - Calculation of partial derivativess**

## 4.5 R/S ANALYSIS

Once the design matrix is populated with actual values, values for R and S can be calculated. First the design matrix needs to be organized so it most closely resembles a decoupled, or triangular, matrix. Once the design matrix is in the best possible arrangement, R and S can be evaluated.

### 4.5.1 Arranging the design matrices

Unfortunately, no automated tool exists for creating the best arrangement of a design matrix. They can be arranged manually by switching either rows or columns. Before arranging the design matrix, it needs to be normalized so that the arrangement

occurs with cells of similar magnitude. Equation (3.2) can be used for the normalization.

Many of the improvements can be achieved through some simple rules of thumb.

a) Highlight the diagonal, so it is visually obvious

b) Attempt to put the largest element for each FR (row) on the diagonal

c) Attempt to put all zeros (0) to the right/above the diagonal elements

d) If numbers other than zero must be right/above the diagonal, attempt to arrange the cells so the number is smaller than the diagonal in its row.

Once the arrangement of the design matrix is visually as close to a decoupled matrix as possible, further improvements can be made by comparing the values of R and S from competing arrangements to each other. The process is iterative, and for a highly coupled design, can be very time intensive.

## 4.5.2 Calculation of R and S

The calculation of R and S was also automated using a Microsoft Excel spreadsheet. The design matrix was automatically loaded using the values calculated in section 4.4.3, and a sample is shown in Figure 26. As shown, a matrix [A] is developed using the partial derivatives calculated previously. The a matrix [B] is calculated using the normalization described above. These matrices are then arranged using the techniques described above. The diagonal is highlighted in matrix [B]. For the most part, the cells to the right of the diagonal element are smaller than the diagonal element. At the bottom of the spreadsheet various intermediate calculations are made, which are used in the calculation of R and S.

| "A" Matrix | 292 | 2 | 10 | 60 | 110 | 80 | 150 |
|---|---|---|---|---|---|---|---|
| | nR | W | D | H | Zin | Aout | Lin |
| Tair,exit | -0.430422 | -101.6892 | -13.73848 | 0.767064 | -0.36762 | -0.2141 | 0 |
| Trx,max | -0.719204 | -83.4042 | -20.57692 | 0.76688 | -0.34332 | -0.20318 | 0 |
| Δz | 0 | 0 | 0 | 1 | -1 | 0 | 0 |
| Pout | 0.000135 | 0.031676 | 0.004321 | -0.00025018 | 0.0001131 | -0.0003524 | 0 |
| Triser,max | -0.611394 | -109.8658 | -18.5252 | 1.02131 | -0.475168 | -0.30218 | 0 |
| Vriser | -0.023263 | 2.22292 | -0.524996 | -0.2065424 | 0.0972969 | 0.059896 | 0 |
| Lout | 0 | 0 | 0 | 0 | -1 | 0 | 1 |

**"B" Matrix = "A" * DP / FR**

| | W | D | nR | H | Zin | Aout | Lin |
|---|---|---|---|---|---|---|---|
| Tair,exit | -0.791 | -0.535 | -0.489 | 0.179 | -0.157 | 0 | 0 |
| Trx,max | -0.408 | -0.503 | -0.514 | 0.113 | -0.092 | -0.040 | 0 |
| Pout | 2.932 | 2.000 | 1.831 | -0.695 | 0.576 | -1.305 | 0 |
| Vriser | 0.109 | -0.129 | -0.167 | -0.305 | 0.263 | 0.118 | 0 |
| Dz | 0 | 0 | 0 | 0.839 | -1.538 | 0 | 0 |
| Triser,max | -0.712 | -0.601 | -0.579 | 0.199 | -0.169 | -0.078 | 0 |
| Lout | 0 | 0 | 0 | 0 | -1.667 | 0 | 2.273 |

| | | | | | | | |
|---|---|---|---|---|---|---|---|
| |Aii| | 0.791474 | 0.503279 | 1.8308436 | 0.30486398 | 1.5384615 | 0.07838612 | 2.2727273 |
| column rss | 3.148185 | 2.21739 | 2.0537957 | 1.167941404 | 2.3680256 | 1.31495725 | 2.2727273 |
| |Aii|/rss | 0.251406 | 0.226969 | 0.8914439 | 0.261026776 | 0.6496811 | 0.05961116 | 1 |

**"R" Calculations**

| i | 1 | 2 | 3 | 4 | 5 | 6 | 7 |
|---|---|---|---|---|---|---|---|
| Ak,i*Ak,i+1 | 47.70866 | 20.71237 | 2.1949372 | 3.398892537 | 0.4801895 | 0 | |
| (Ak,i)^2 | 9.911069 | 4.916819 | 4.218077 | 1.364087124 | 5.6075454 | 1.72911257 | 5.1652893 |
| 1-Σ/(Σ*Σ) | 0.144838 | 0.036179 | 0.7864639 | 0.74542117 | 0.9749235 | 1 | |

**Figure 26 - R and S Calculations**

Applying the R and S equations (3.3 and 3.4) results in the following:

| R | S |
|---|---|
| 0.002896 | 0.000498 |

**Table 5 - Current Design R&S Results**

## 4.5.3 Discussion of preoptimized design

As seen in the design matrix (Figure 24) and the results of the R/S analysis (Table 5), this part of the system has a fairly high degree of coupling at the parametric level. The design matrix shows coupling through the examination of the off diagonal elements. As a reminder, in an ideal (uncoupled) system R and S are each equal to 1

and in a good (decoupled) system they are equal to each other, but not equal to 1. Also, the closer the values are to 1, the better the system is. In the case of this system, R and S are not equal indicating that the system is coupled. Also, since they are not close to 1 at all, the system is highly influenced by the off-diagonal elements.

While this is not ideal it does not come as a surprise, since the equations defining such a thermal/fluid system are somewhat coupled to start with. As mentioned previously, the remainder of the system is a good decoupled design. Outside of level 3.2.2, the matrix in Figure 24 shows no elements above the diagonal with influence on the system.

## 4.6 OPTIMIZATION

Even though the major pieces and subsystems of the RCCS are highly decoupled, it would be good to further improve the system by reducing the coupling within actual cooling portion of the system. Different methods could be used to do this, including trial-and-error, optimization, and others. Trial and error can work very well for some types of problems, but it is difficult to tell, especially with a complex system, if you have the "best" solution. Since design optimization is an analytical method which attempts to find the "best" solution, it will be used to find a solution.

### 4.6.1 Development of optimization spreadsheet

To determine an optimized set of design parameters (**DP\***), an optimization routine is developed in Microsoft Excel. The automated routines developed for populating the design matrices (section 4.4.3) and calculating R and S (section 4.5.2) are used as the base for the optimization routine. The objective function [equation (3.7)] and equality constraints [equation (3.8)] are added, resulting in the spreadsheet shown in Figure 27.

| Objective Function |
|---|
| Minimize (R+S)/RS |
| f = 2279 |

| Optimization Variables | | | |
|---|---|---|---|
| Minimum | Maximum | Var | Actual |
| 1.8 | 2.2 | W | 2 |
| 9 | 11 | D | 10 |
| 56.25 | 68.75 | H | 60 |
| 98.1 | 119.9 | Zin | 110 |
| 72 | 88 | Aout | 80 |
| 134.1 | 163.9 | Lin | 150 |
| 262 | 322 | nR | 292 |

| R = | 0.002995 |
|---|---|
| S = | 0.000514 |

| Inequality Constraints (gi<=0) | | |
|---|---|---|
| g1 | -0.2 | W Minimum |
| g2 | -1.0 | D Minimum |
| g3 | -3.8 | H Minimum |
| g4 | -11.9 | Zin Minimum |
| g5 | -8.0 | Aout Minimum |
| g6 | -15.9 | Lin Minimum |
| g7 | -30.0 | nR Minimum |
| g8 | -0.2 | W Maximum |
| g9 | -1.0 | D Maximum |
| g10 | -8.8 | H Maximum |
| g11 | -9.9 | Zin Maximum |
| g12 | -8.0 | Aout Maximum |
| g13 | -13.9 | Lin Maximum |
| g14 | -30.0 | nR Maximum |

| Design Matrix | | | | | | | |
|---|---|---|---|---|---|---|---|
| | W | D | nR | H | Zin | Aout | Lin |
| Tair,exit | -0.791 | -0.535 | -0.489 | 0.179 | -0.157 | -0.067 | 0 |
| Trx,max | -0.408 | -0.503 | -0.514 | 0.113 | -0.092 | -0.040 | 0 |
| Pout | 2.932 | 2.000 | 1.831 | -0.695 | 0.576 | -1.305 | 0 |
| Vriser | 0.109 | -0.129 | -0.167 | -0.305 | 0.263 | 0.118 | 0 |
| Dz | 0 | 0 | 0 | 0.839 | -1.538 | 0 | 0 |
| Triser,max | -0.712 | -0.601 | -0.579 | 0.199 | -0.169 | -0.078 | 0 |
| Lout | 0 | 0 | 0 | 0 | -1.667 | 0 | 2.273 |

**Figure 27 - Optimization Spreadsheet**

The optimization model described above was put into Excel, and the Excel Add-In "Solver Add-In" was used to find a solution to the optimization problem. To start with, the initial conditions were the current values for the design parameters. Further runs used initial conditions at various extreme values to ensure that a global minimum was found. The ensure a robust and efficient solution, the settings in Figure 28 were used for all runs. With these settings, a typical run takes less than one second to execute.
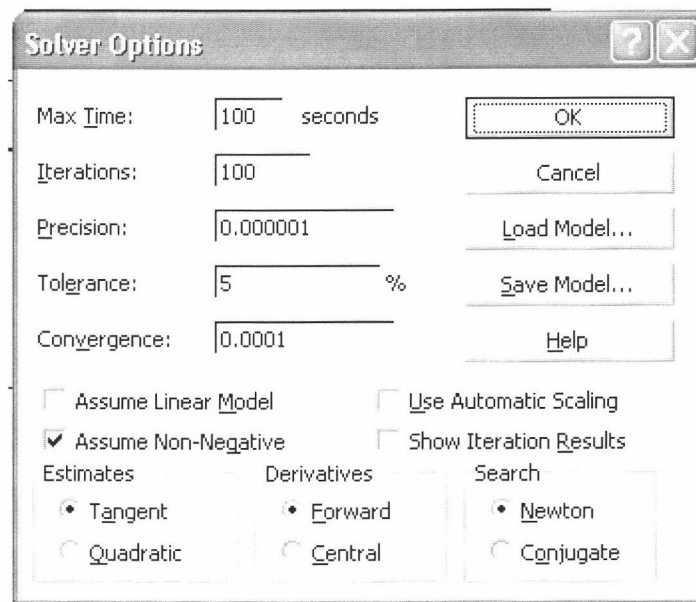
**Figure 28 - Excel Solver Settings**

## 4.6.2 Results of optimization

When the optimization procedure is performed on the RCCS, a new set of optimized design parameters and a new design matrix are developed. A comparison of the design parameters is contained in Table 6.

|  | Units | Current (x) | Improved (x*) |
|---|---|---|---|
| Riser Width | inches | 2 | 2.12 |
| Riser Depth | inches | 10 | 10.55 |
| Riser Height | feet | 62.5 | 56.25 |
| Inlet delta z | feet | 109 | 103.9 |
| Outlet Area | ft$^2$ | 80 | 72 |
| Inlet Length | feet | 149 | 163.9 |
| Number of Risers | - | 292 | 287 |

**Table 6 - Pre- and Post-optimization design parameters**

This leads to a new optimized design matrix for level 3.2.2. and a new master matrix (Figure 29). Examining this new design matrix shows that it is still a coupled design, although upon close examination there are a number of significant changes.

| | | | | DP3: Reactor cavity cooling system | | | | | | | | | | |
| | | | | DP3.1 | | | DP3.2 | | | | | | | |
| | | | | | | | | DP3.2.2 | | | | | | |
| | | | | Four inlets and oulets for natural circulation | Orientation of inlets and outlets | Completely passive system | Conductive Hx through core | Riser Width | Riser Depth | Number of Risers | Riser Height | Inlet Delta z | Outlet Area | Inlet Length |
|---|---|---|---|---|---|---|---|---|---|---|---|---|---|---|
| FR3: Maintain temp during emergency | FR3.2 | FR3.1 | Allow operation when inlets or outlets are partially blocked | 1 | 0 | 0 | 0 | 0 | 0 | 0 | 0 | 0 | 0 | 0 |
| | | | Insensitive to wind direction | 0 | 1 | 0 | 0 | 0 | 0 | 0 | 0 | 0 | 0 | 0 |
| | | | Work without outside power | 0 | 0 | 1 | 0 | 0 | 0 | 0 | 0 | 0 | 0 | 0 |
| | | FR3.2.2 | Maximum Fuel temperature < 1450C | 0 | 0 | 0 | X | 0 | 0 | 0 | 0 | 0 | 0 | 0 |
| | | | Air exit temperature | 0 | X | 0 | 0 | -0.625 | -0.437 | -0.412 | 0.1401 | -0.145 | -0.083 | 0 |
| | | | Maximum Reactor Temperature | 0 | X | 0 | 0 | -0.307 | -0.441 | -0.469 | 0.0869 | -0.084 | -0.051 | 0 |
| | | | Outlet pressure drop | 0 | X | 0 | 0 | 2.5374 | 1.7688 | 1.599 | -0.584 | 0.4631 | -1.217 | 0 |
| | | | Air velocity in riser | 0 | X | 0 | 0 | -0.054 | -0.225 | -0.247 | -0.267 | 0.2545 | 0.1633 | 0 |
| | | | Delta z between inlet and outlet | 0 | 0 | 0 | 0 | 0 | 0 | 0 | 0.7617 | -1.407 | 0 | 0 |
| | | | Maximum riser wall temperature | 0 | X | 0 | 0 | -0.534 | -0.499 | -0.501 | 0.1685 | -0.145 | -0.108 | 0 |
| | | | Outlet Length | 0 | 0 | 0 | 0 | 0 | 0 | 0 | 0 | -1.208 | 0 | 1.9058 |

**Figure 29 - Optimized Master Matrix**

## 4.6.3 Comparison of original and optimized design

The goal of the optimization is to bring the current RCCS design matrix in Figure 24 as close as possible to a decoupled DM in the given design space. In the optimized design matrix, it is noticed that all of the above diagonal elements except one have decreased considerably (see Table 7). This shows that these elements have been

brought closer to zero through the optimization. The elements below the diagonal have decreased in value as well, showing that the objective function is attempting to create an uncoupled matrix. As a result of the optimization, the improved design has a less coupled design matrix, and is much closer to a decoupled, or better, design.

| Element Above the Diagonal | Pre-optimized | Optimized | Decrease in Coupling (%) |
|---|---|---|---|
| $A_{1,2}$ | -0.543 | -0.437 | 19.52 |
| $A_{1,3}$ | -0.498 | -0.412 | 17.2 |
| $A_{1,4}$ | 0.1549 | 0.1401 | 9.55 |
| $A_{1,5}$ | -0.158 | -0.145 | 8.23 |
| $A_{2,3}$ | -0.518 | -0.469 | 9.5 |
| $A_{2,4}$ | 0.1166 | 0.0869 | 25.47 |
| $A_{2,5}$ | -0.092 | -0.084 | 8.7 |
| $A_{3,4}$ | -0.717 | -0.584 | 18.55 |
| $A_{3,5}$ | 0.5904 | 0.4631 | 21.56 |
| $A_{3,6}$ | -1.319 | -1.217 | 7.73 |
| $A_{4,5}$ | 0.266 | 0.2545 | 4.32 |
| $A_{4,6}$ | 0.1149 | 0.1633 | -42.12 |

Table 7 - Improvement in Functional Independence

The only one that has an increased in coupling may be the price that is paid to decrease the others. From a physical point of view, the Outlet Area now has a larger affect on the Air velocity in the riser due to changes than the other design parameters.

Table 8 has a comparison of values of R, S and the objective function for the original and improved designs. As seen, the objective function has decreased significantly, which was brought on by a significant increase in both R and S.

| Level 3.3.2 | $\frac{R+S}{RS}$ | R | S |
|---|---|---|---|
| Preoptimized | 2353 | 0.002896 | 0.000498 |
| Optimized | 1521 | 0.004443 | 0.000771 |

**Table 8 - Comparison of R, S, and objective function values**

## 4.7 SUMMARY OF RESULTS

### 4.7.1 Conceptual level design matrices

The qualitative design matrices developed for the high level, abstract portions of the RCCS, show that the overall system is well designed and is functionally independent at a conceptual level. The individual decompositions at levels 3, 3.1, and 3.2 all show uncoupled design matrices. When combined into a master design matrix for the entire system, some additional interactions between FRs and DPs are shown, but the system is still a decoupled, or good, system.

### 4.7.2 Parametric level design matrices

Once the system models are developed and the quantitative design matrices are populated at a parametric level, an evaluation of the systems functional independence can be made. With the RCCS, the system has a high degree of functional coupling, due largely to the nature of thermal-fluid systems. In particular, the system exhibits coupling with the air temperature at the riser exit, the maximum riser wall temperature, the outlet pressure drop, and air velocity within the risers. It makes sense that these exhibit functional coupling, since as riser wall temperature increases, the heat transfer to air within the riser will increase, leading to higher air temperature, air velocity, and pressure drop. The issue with this coupling is that if a change in one performance parameter is required, such as riser wall temperature needs to be decrease by 10EF, there is not a

single design variable that can be changed to achieve that. Instead a number of design variables will be changed, and then other performance parameters will be changed by it. To accomplish a change in a single performance parameter, without affected others, will require extensive work. Likewise, if a system design variable changes over time, a number of performance parameters will change with it, and identifying the source and correcting the problem could be difficult.

## 4.7.3 Optimized design

The design suggested by the optimization routine has significantly better functional independence, as measured by R and S, than the original system design has. The only exception is the effect of outlet area on air velocity, which has an increased level of coupling, as noted in section 4.6.3.

The parameters leading to the largest changes in coupling are riser height, inlet delta Z, riser depth, and number of risers. The decrease in riser height and inlet delta Z led to reduced coupling with outlet pressure drop. This makes physical sense, because the system is shorter, it will have smaller overall pressure drops. The decrease in number of risers and increase in riser depth leads to less coupling on the outlet air temperature. Likewise the decrease in riser height led to reduced coupling with reactor temperature.

# 5. CONCLUSIONS

According to Axiomatic Design principles, the current Reactor Cavity Cooling System is a relatively well designed system. Because the original design is simple and modular, it meets the goals of functional independence (Axiom 1) at a conceptual level. Looking at the subsystems within the RCCS, there is little improvement that Axiomatic Design could recommend at the conceptual level.

At a parametric level, the design is naturally coupled due to characteristics of thermal-fluid systems. Even though parts of the system are naturally coupled, it is possible to reduce the degree of coupling through an integrated use of several different design tools. First, DOE was used to develop numerically simpler, but comparable surrogate models of the system. Next, an optimization model was developed in Excel, which attempts to minimize the degree of coupling through the evaluation of R&S values. It was shown that even though the system is still coupled, the degree of coupling for the overall system (measured through R&S) was significantly reduced through the optimization procedure.

From the perspective of axiomatic design, the above results imply that the changed system is better than the original system. Most importantly, the system is less sensitive to variations that could occur. These could include manufacturing errors, environmental conditions, maintenance changes, site-to-site variations, and material changes with time. Comparatively speaking, a system with less susceptibility to variations is an inherently safer system, has more robust performance, and results in lower cost..

## 5.1 CONTRIBUTION TO KNOWLEDGE

This work contributes to the knowledge base of engineering design and related areas in the following aspects:

a) A number of new techniques for applying Axiomatic Design Theory to real product design, at both the functional and parametric levels, have been pursued.

b) A new approach to enhance system robustness using R and S is demonstrated.

c) The concept of modularity has been explored and quantified through the "functional independence" in Axiomatic Design Theory.

d) The surrogate modeling approach demonstrates a way that the designer can develop a simplified, yet statistically accurate system model, that can be used in the Axiomatic Design processes of design matrix population and R/S analysis.

## 5.2 CONTRIBUTION TO DESIGN PRACTICE

This work contributes to design practice in the following aspects:

a) A new method has been developed, which can be utilized by designers in the evaluation and improvement of large, mechanical system designs.

b) A process of decomposition and mapping is demonstrated that a designer can apply to any system.

c) A surrogate modeling technique method for system model development and design matrix population is demonstrated.

d) An optimization routine for developing system improvements based on axiomatic design is developed and demonstrated.

e)  The entire process demonstrates a strategy to systematically use computer supported problem formulation at early design stages, rather than just heuristics based approaches.

By following this process, a designer can develop a system that demonstrates more functional independence than would be achieved through just heuristics based approaches. The improvements suggested by the optimization routines, lead to improved function independence for the entire system, which in turn can lead to higher reliability, reduced development cost, and ultimately higher profitability.

## 5.3 RECOMMENDATIONS FOR FURTHER IMPROVEMENTS

Further improvements to the surrogate models and optimization model could by made by:

- improvements in the quality of the 1-d models described and used for this study
- inclusion of fuel and concrete temperatures in the models
- basing the surrogate models off of the more accurate Sinda/Fluint or CFD models
- increasing the range of the DOE variables beyond $\forall 10\%$ of nominal
- trying different arrangements for the rows and columns within the design matrix
- developing an automated approach to arranging the rows and columns

If some of these improvements are pursued, it is probable that a new set of recommended design parameters would be developed by the optimization model that would reduce the coupling even further, and thus lead to a further improvement in the system.

With additional investigations, the proposed approach could be applied to an entire nuclear reactor system design. Another interesting area of study could be the development of a shared ontology between design teams and management to establish

a common basis for mapping, decomposition, and R/S analysis to allow the comparison of multiple, competing design alternatives.

# BIBLIOGRAPHY

[1]   Ullman, D., 2003. *The Mechanical Design Process* (New York: McGraw-Hill).

[2]   Taguchi, G., Chowdhury, S, and Taguchi, S., 2000. *Robust Engineering* (New York: McGraw-Hill).

[3]   Wu, Y. and Wu, A., 2000. *Taguchi Methods for Robust Design* (New York: American Society of Mechanical Engineers).

[4]   Suh, N. P., 1990. *The Principles of Design* (New York: Oxford University Press).

[5]   Suh, N. P., 2001. *Axiomatic Design: Advances and Applications* (New York: Oxford University Press).

[6]   United States, 26 October, 2003. *Generation IV Nuclear Energy Systems.* (Washington D.C.: Department of Energy) <http://gen-iv.ne.doe.gov>.

[7]   ANS Winter Meeting, 13 November, 2001. "Technology Goals for Generation IV Nuclear Energy Systems". (Reno, Nevada: American Nuclear Society) <http://gen-iv.ne.doe.gov/pdf /finalgenivgoals_may01.pdf>.

[8]   ANS Winter Meeting, 13 November, 2001. "Generation IV Gas-cooled Reactor Concepts". (Reno, Nevada: American Nuclear Society) <http://gen-iv.ne.doe.gov/pdf /Reno_ANS_Presentation_RS041-00_6_TWG_2_Gas_-_Southworth.pdf >

[9]   ANS Winter Meeting, 13 November, 2001. "Report on Generation IV Working Group 3: Liquid Metal Reactors". (Reno, Nevada: American Nuclear Society) <http://gen-iv.ne.doe. gov/pdf/Reno_ANS_Presentation_RS042-00_7_TWG_3_Liquid_Metal_-_Lineberry.pdf>.

[10]  Labar, M. P., April 2002. "The Gas Turbine – Modular Helium Reactor: A Promising Option for Near Term Deployment". (San Diego: General Atomics) < http://www.ga.com/gtmhr/images/ANS.pdf>.

[11]  General Atomics, 6 Aug. 2002. "GT-MHR Conceptual Design Description Report - Part 1". (Nuclear Regulatory Commission) <http://www.nrc.gov/reactors/new-licensing/new-licensing-files/gtmhr-preapp1.pdf>.

[12]  Rantanen, K. and Domb, E., 2002. *Simplified TRIZ* (Boca Raton, FL : St. Lucie Press).

[13]  Ideation International, 2003. "Yield/Reliability Problem – Analog Integrated Circuit: Inventive Problem Solving Case Study" <http://www.ideationtriz.com/Yield_Reliability_Case_Study.asp>.

[14] Mann, D., June 1999. "Axiomatic Design and TRIZ: Compatibilities and Contradictions". <http://www.triz-journal.com/archives/1999/06/a>.

[15] Royzen, Z., Nov. 1998. "Case Study: TRIZ Solves a Hard Drive Reliability Problem". <http://www.triz-journal.com/archives/1998/11/a>.

[16] Yang, K. and Zhang, H., August 2000. "Compatibility Analysis and Case Studies of Axiomatic Design and TRIZ." <http://www.triz-journal.com/archives/2000/08/index.htm>.

[17] Taguchi, G., 1993. *Taguchi Methods: Design of Experiments* (Dearborn, MI: ASI Press).

[18] Simpson, T. W., Peplinski, J., Koch, P. N. and Allen, J. K., 1997. "On the use of statistics in design and the implications for deterministic computer experiments." *Proceedings of 1997 ASME Design Engineering Technical Conferences* (New York: American Society of Mechanical Engineers), DETC97/DTM3881.

[19] Sekimoto, S. and Ukai, M., 1994. "A Study of Creative Design Based on the Axiomatic Design Theory." *ASME Proceedings on Design Theory and Methodology.* (New York: American Society of Mechanical Engineers).

[20] Chan, L.W. and Leung, T.P., 1997. "Optimization of an Electrical Interconnect System Using Axiomatics and Fuzzy Sets." *Journal of Engineering Design*, Vol. 8, No. 4. (Abingdon, England : Carfax Pub. Co)

[21] Montgomery, D.C., 1991. *Design and Analysis of Experiments* (New York: John Wiley and Sons).

[22] Box, G. E. P. and Draper, N. R., 1987, *Empirical Model-Building and Response Surfaces* (New York: John Wiley & Sons).

[23] Meyers, R.H., and Montgomery, D.C., 2002. *Response Surface Methodology : Process and Product Optimization Using Designed Experiments* (New York: John Wiley and Sons).

[24] Papalambros, P. Y. and Wilde, D. J., 2000. *Principles of Optimal Design* (New York: Cambridge University Press).

[25] Bloomer, J. L., 2000. *Practical Fluid Mechanics for Engineering Applications* (New York: Marcel Dekker).

[26] Todreas, N. E. and Kazimi, M. S., 1990. *Nuclear Systems II: Elements of Thermal Hydraulic Design* (New York: Hemisphere Publishing Corporation).

[27] Welty, J. R., Wicks, C. E., and Wilson, R. E., 1984. *Fundamentals of Momentum, Heat, and Mass Transfer,* 3rd Ed (New York: John Wiley and Sons).

# APPENDICES

## APPENDIX A – SURROGATE MODELS AND VALIDATION

$$p_{out} = 0.08956 - 0.007468D_r - 0.04307W_r - 0.000255n_r - 0.0005979Z_{in} + 0.0004754A_{out}$$
$$+ 3.221 \cdot 10^{-5} D_r{}^2 + 2.166 \cdot 10^{-6} H_r{}^2 + 0.005084W_r{}^2 + 9.192 \cdot 10^{-8} n_r{}^2 + 5.912 \cdot 10^{-6} A_{out}{}^2 \qquad \text{(A.1)}$$
$$- 3.0 \cdot 10^{-6} D_r H_r + 0.004313 D_r W_r + 1.926 \cdot 10^{-5} D_r n_r + 2.179 \cdot 10^{-5} D_r Z_{in}$$
$$- 5.938 \cdot 10^{-5} D_r A_{out} - 0.00020 H_r W_r - 8.904 \cdot 10^{-7} H_r n_r + 3.25 \cdot 10^{-6} H_r A_{out} + 0.000137 W_r n_r$$
$$+ 0.0001548 W_r Z_{in} - 0.0004219 W_r A_{out} + 6.284 \cdot 10^{-7} n_r Z_{in} - 1.819 \cdot 10^{-6} n_r A_{out}$$
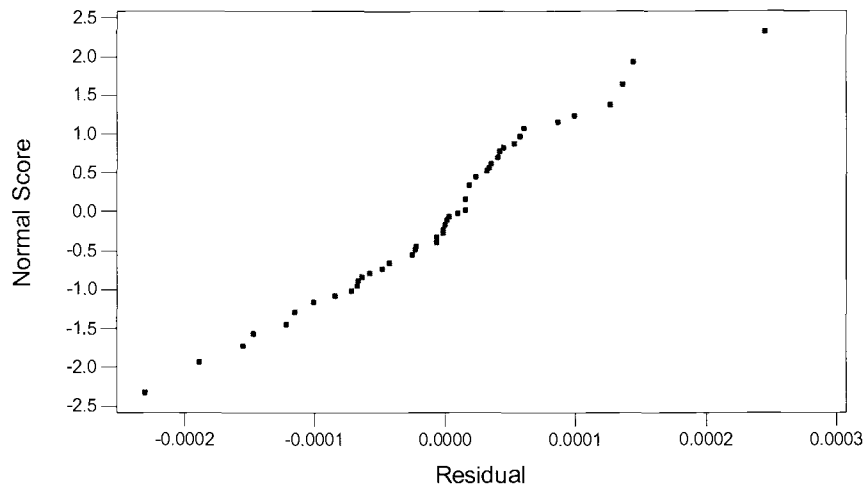


**Figure A.1 - Normal Plot of pout**
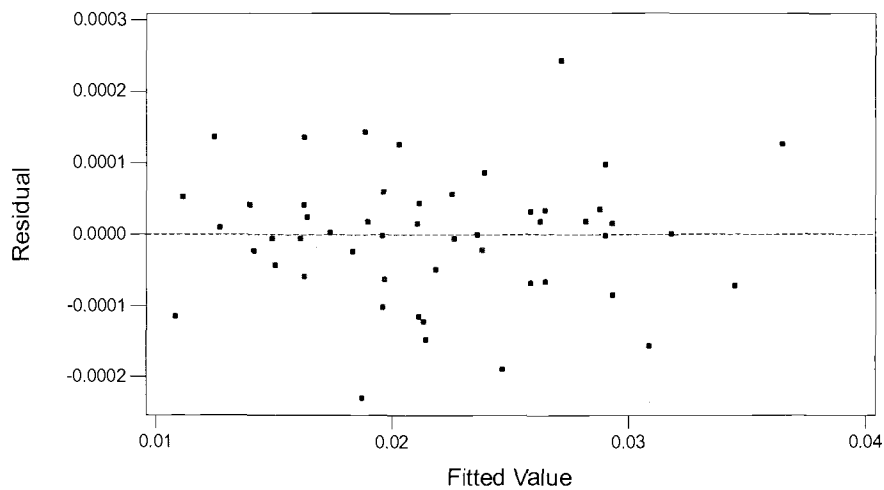


**Figure A.2 - Residuals of pout**

$$v_{riser} = -23.48 + 3.812D_r - 0.7466H_r + 46.2W_r + 0.1027n_r + 0.1768Z_{in} - 0.03008A_{out}$$
$$- 0.0681D_r^2 + 0.001108H_r^2 - 7.126W_r^2 - 3.711 \cdot 10^{-5}n_r^2 - 0.002189Z_{in}^2$$
$$- 0.001007A_{out}^2 + 0.01479D_rH_r - 1.388D_rW_r - 0.005133D_rn_r - 0.002012D_rZ_{in} \quad (A.2)$$
$$+ 0.007922D_rA_{out} + 0.09596H_rW_r + 0.0004778H_rn_r - 0.000903H_rA_{out} - 0.04519W_rn_r$$
$$+ 0.07306W_rA_{out} - 7.899 \cdot 10^{-5}n_rZ_{in} + 0.000218n_rA_{out} + 0.000148Z_{in}A_{out}$$

## Normal Probability Plot of the Residuals

(response is Vriser)
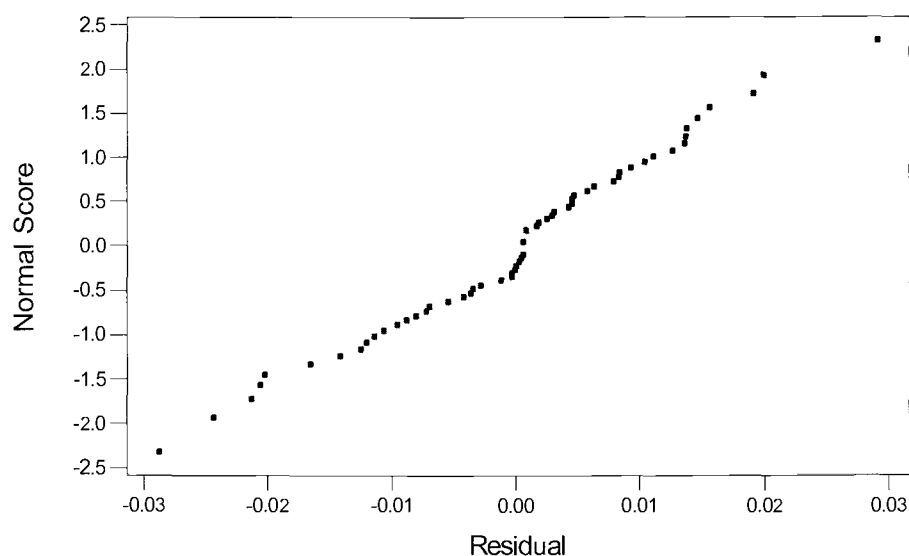


**Figure A.3 - Normal Plot of Vriser**

## Residuals Versus the Fitted Values

(response is Vriser)
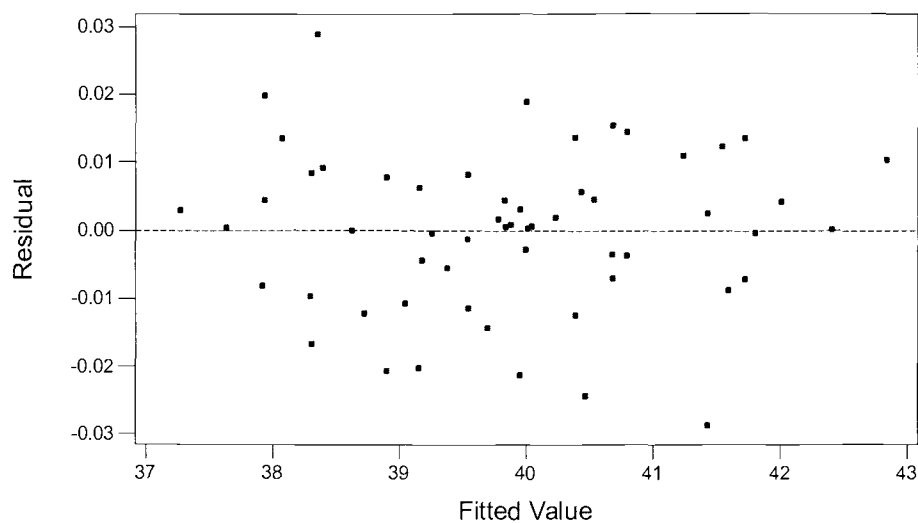


**Figure A.4 - Residuals of Vriser**

$$T_{air,exit} = 2111 - 92.99D_r + 4.854H_r - 728.4W_r - 2.864n_r - 2.066Z_{in} - 0.8885A_{out}$$
$$+ 1.740D_r{}^2 + 91.63W_r{}^2 - 0.001687n_r{}^2 - 0.001872Z_{in}{}^2 + 0.004215A_{out}{}^2 \qquad (A.3)$$
$$- 0.1175D_rH_r + 14.82D_rW_r + 0.06041D_rn_r + 0.03838D_rZ_{in} - 0.9292H_rW_r$$
$$- 0.003608H_rn_r + 0.4674W_rn_r + 0.2842W_rZ_{in} + 0.001145n_rZ_{in}$$

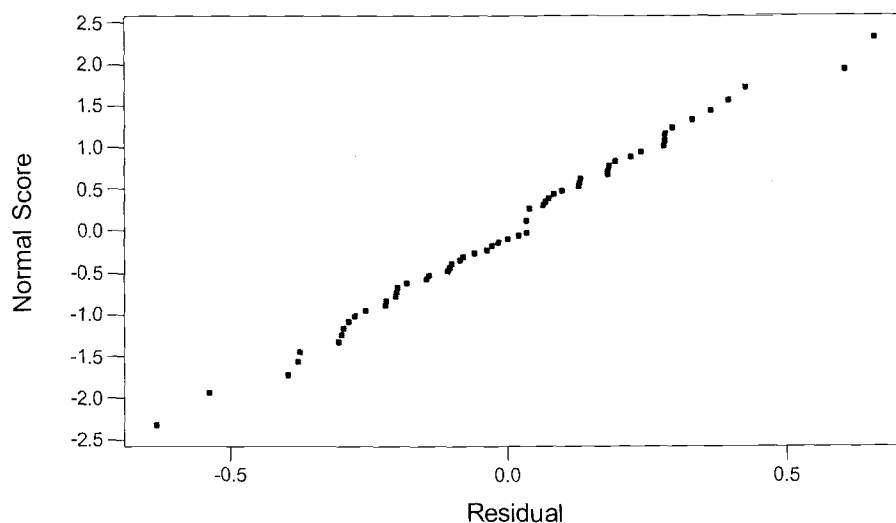## Normal Probability Plot of the Residuals

(response is Tair,exi)



**Figure A.5 - Normal Plot of Tair,exit**

## Residuals Versus the Fitted Values

(response is Tair,exi)
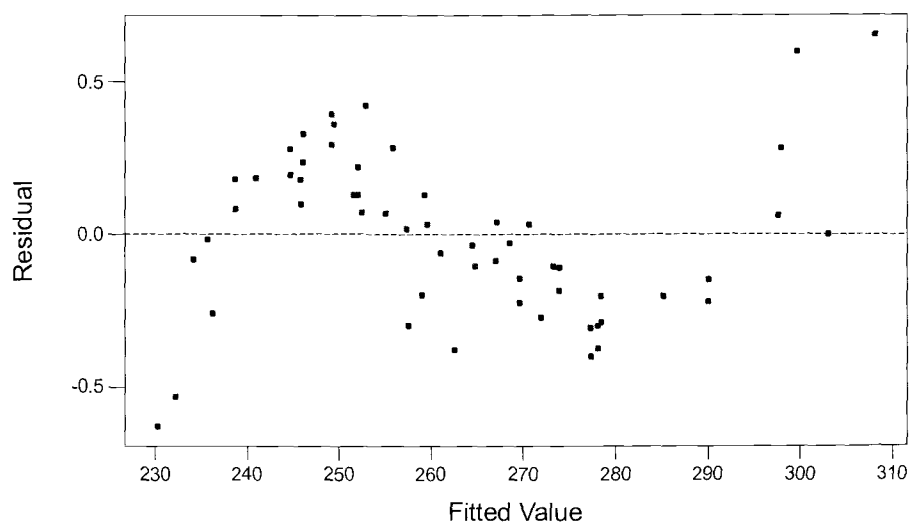


**Figure A.6 - Residuals of Tair,exit**

$$T_{riser,max} = 2535 - 122.7D_r + 6.427H_r - 806.5W_r - 3.966n_r - 3.966Z_{in} - 0.9345A_{out}$$
$$+ 2.315D_r{}^2 + 101.6W_r{}^2 + 0.002569n_r{}^2 + 0.006882A_{out}{}^2 - 0.140D_rH_r + 18.12D_rW_r \quad \text{(A.4)}$$
$$+ 0.0899D_rn_r + 0.0344D_rZ_{in} - 1.00H_rW_r - 0.004795H_rn_r - 0.005505H_rZ_{in}$$
$$+ 0.5351W_rn_r + 0.2867W_rZ_{in} - 0.2344W_rA_{out} + 0.001571n_rZ_{in}$$

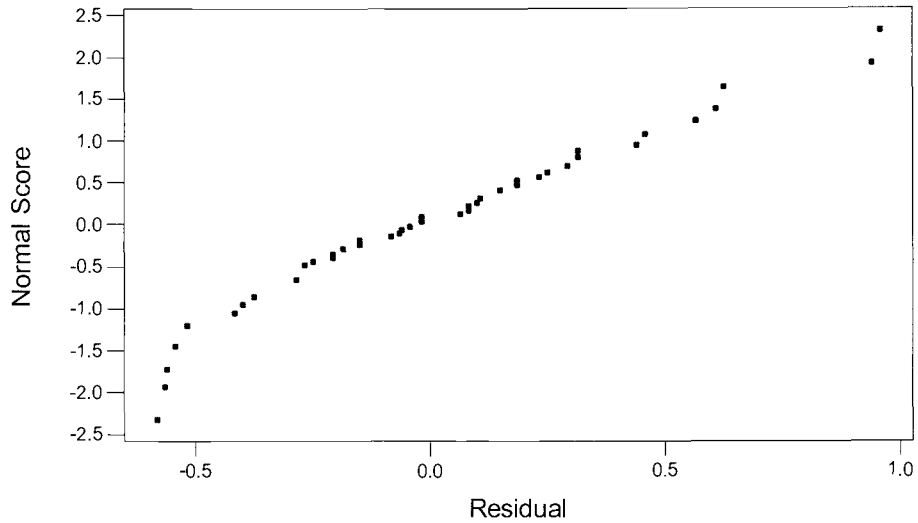## Normal Probability Plot of the Residuals

(response is Triser,m)



**Figure A.7 - Normal Plot of Triser,max**

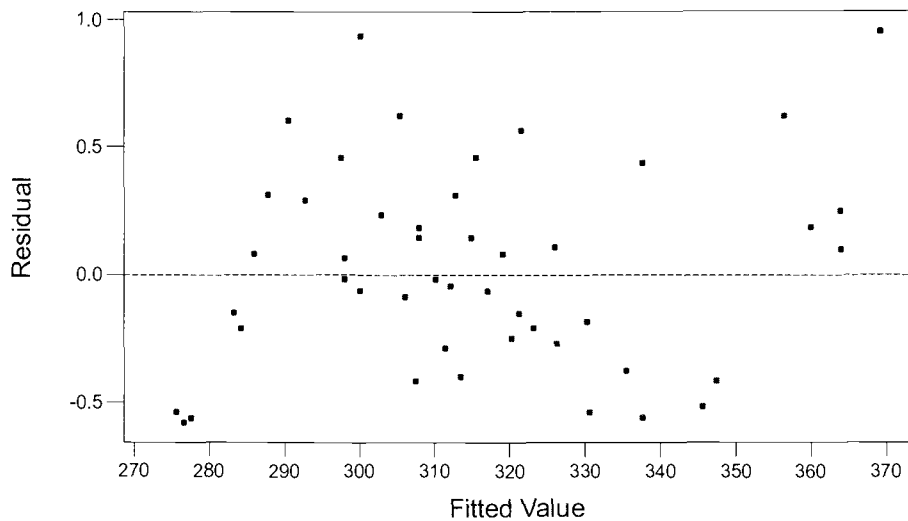## Residuals Versus the Fitted Values

(response is Triser,m)



**Figure A.8 - Residuals of Triser,max**

$$T_{rx,max} = 2346 - 109.3D_r + 4.967H_r - 615.4W_r - 3.371n_r - 1.805Z_{in} - 0.9379A_{out}$$
$$+ 2.169D_r{}^2 + 76.1W_r{}^2 + 0.002544n_r{}^2 + 0.002474Z_{in}{}^2 + 0.004592A_{out}{}^2 \qquad (A.5)$$
$$- 0.120D_rH_r + 14.38D_rW_r + 0.06849D_rn_r + 0.0344D_rZ_{in} - 0.900H_rW_r$$
$$- 0.00411H_rn_r + 0.3639W_rn_r + 0.2867W_rZ_{in}$$

## Normal Probability Plot of the Residuals
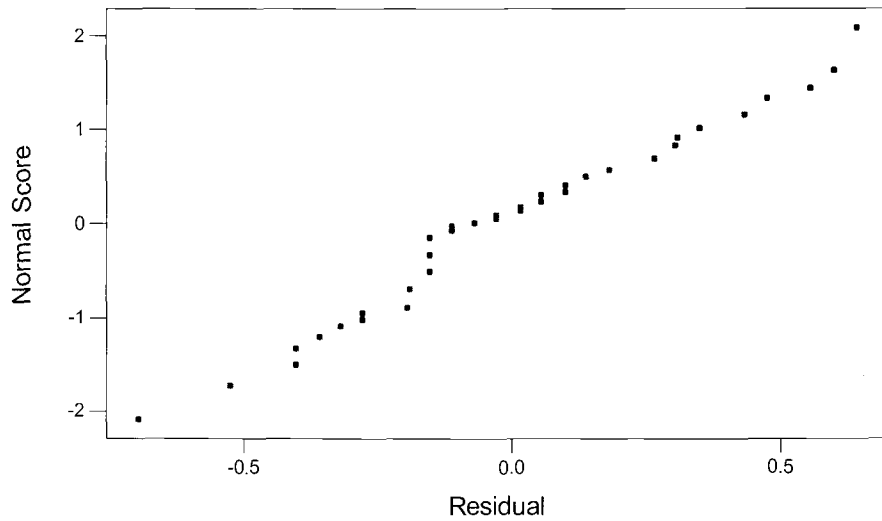
(response is Trx,max)



Figure A.9 - Normal Plot of Trx,max

## Residuals Versus the Fitted Values
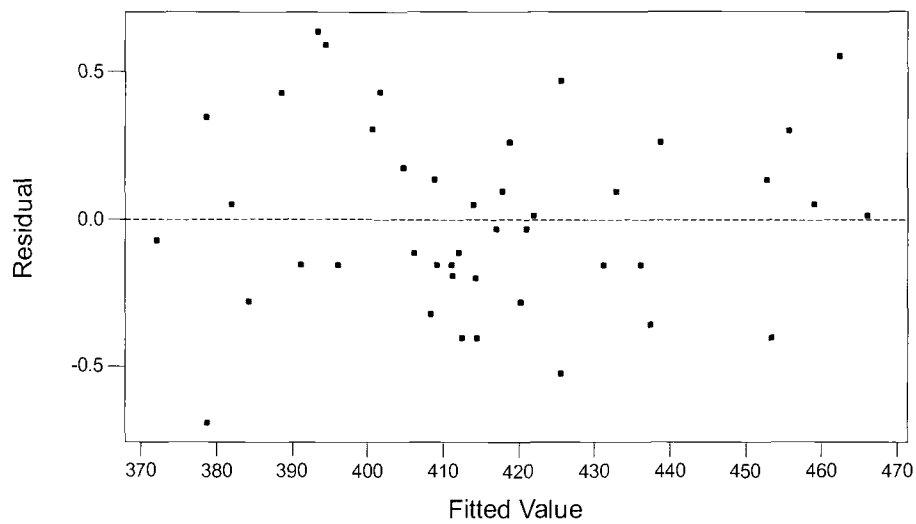
(response is Trx,max)



**Figure A.10 - Residuals of Triser,max**

$$L_{out} = 49 - H_r + L_{in}$$ (A.6)

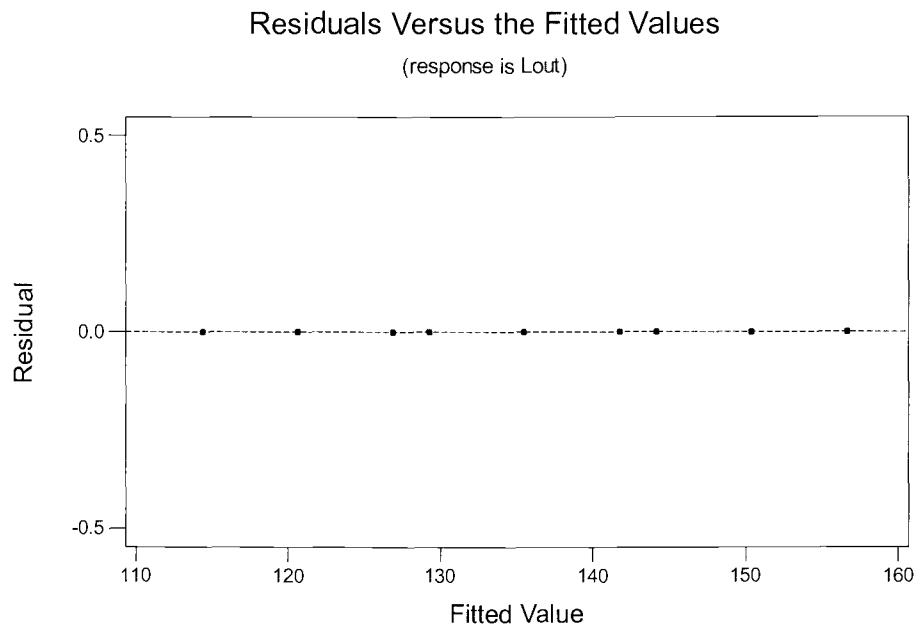## Residuals Versus the Fitted Values
(response is Lout)



**Figure A.11 - Residuals of Lout**

Since there is zero residual on all values, it is not possible to create a normal probability plot.

# APPENDIX B – LIST OF COURSES FOR MASTER DEGREE

| Course | Description | Credits |
|---|---|---|
| BA-562 | Managing Projects | 3 |
| BIOE-550 | Biomechanical Engineering | 4 |
| CE-588 | Probability Based Analysis and Design | 4 |
| ME-501 | Research | 2 |
| ME-502 | Independent Study (Advanced Optimization) | 3 |
| ME-503 | Thesis | 12 |
| ME-507 | Seminar | 1 |
| ME-513 | Computer Aided Design II | 3 |
| ME-517 | Design Optimization | 3 |
| ME-518 | Concurrent Design | 3 |
| ME-520 | Applied Stress Analysis I | 3 |
| ME-521 | Applied Stress Analysis II | 3 |
| ME-523 | Advanced Stress Analysis | 3 |
| ME-552 | Instrumentation | 3 |
| ME-553 | Experimental Mechanics | 3 |
| MTH-581 | Mathematical Methods for Engineers | 3 |
|  |  |  |